Wong Wing Yan Barbara Publications

DPhil in Primary Health Care
The University of Oxford

Z Ashkir, A H A Samat, R Ariga, L E M Finnigan, S Jermy, M A Akhtar, G Sarto, P Murthy, **B W Y Wong**, M P Cassar, N Beyhoff, E C Wicks, K Thomson, M Mahmod, E M Tunnicliffe, S Neubauer, H Watkins, B Raman. Myocardial Disarray and Fibrosis across Hypertrophic Cardiomyopathy Stages Associate with ECG Markers of Arrhythmic Risk. **Eur Heart J Cardiovasc Imaging**. 2024 Oct 17, DOI: 10.1093/ehjci/jeae260 (Impact factor: 6.7)

Tng T*, **Wong WY***, Sim E, Tan EK, Goh W, Lim KL. Systematic analysis of multi-omics data reveals component-specific blood-based biomarkers for Parkinson's disease. Translational Medicine Communications. 2024 Apr 23, DOI: 10.1186/s41231-024-00169-9 (Impact factor 4.5)

Pang SY, Lo RCN, Ho PW, Liu HF, Chang EES, Leung CT, Malki Y, Choi ZY, **Wong WY**, Kung MH, Ramsden DB, Ho SL. LRRK2, GBA and their interaction in the regulation of autophagy: implications on therapeutics in Parkinson's disease. Translational Neurodegeneration. 2022 Jan 31, DOI: 10.1186/s40035-022-00281-6 (Impact factor 9.89)

Ren Mengda, **Wong WY**. A programme to detect contour and measure lengths of sonicated PFF (α-syn preformed fibril) on TEM images (https://github.com/rmd13/PFFdetection)

Tng *et al.*
Translational Medicine Communications (2024) 9:12
https://doi.org/10.1186/s41231-024-00169-9

Translational Medicine Communications

REVIEW

Open Access

Systematic analysis of multi-omics data reveals component-specific blood-based biomarkers for Parkinson's disease

Teddy J. W. Tng[1,2,3†], Barbara Wing Yan Wong[4†], Esther H. Y. Sim[5], Eng King Tan[6], Wilson W. B. Goh[1,2,7*] and Kah-Leong Lim[1,6*]

Abstract

Parkinson's disease (PD) is a prevalent neurodegenerative disorder affecting millions of elderly individuals worldwide. Clinically, PD is diagnosed based on the presentation of motoric symptoms. Other methods such as F-DOPA PET scan or α-Synuclein detection from the cerebral spinal fluid are either too expensive or invasive for routine use. Omics platforms such as transcriptomics, proteomics, and metabolomics may identify PD biomarkers from blood, which can reduce cost and increase efficiency. However, there are many biological moieties being measured and issues with false positives/negatives. It is also unknown which omics platform offers most useful information. Therefore, it is important to assess the reliability of these omics studies. Here, we shortlisted and analysed nearly 80 published reports across transcriptomics, proteomics and metabolomics in search of overlapping blood-based biomarkers for PD. The top biomarkers were reported across 29%, 42% and 12.5% of shortlisted papers in transcriptomics, proteomics and metabolomics respectively. These percentages increased to 42%, 60% and 50% accordingly when studies were grouped by specific blood subtypes for analysis, demonstrating the need for test kits to be blood-subtype specific. Following systematic analyses, we propose six novel PD biomarkers: two mRNAs (Whole blood, WB) – Arg1 and SNCA, two proteins (Plasma EV) – SNCA and APOA1, and two metabolites (WB) – 8-OHdG and uric acid for further validation. While these proposed biomarkers are useful, they are also snapshots, representing subsets of larger pathways of origin where the different omics levels corroborate. Indeed, identifying the interconnections across different biological layers can strengthen contextual reasoning, which in turn, would give rise to better quality biomarkers. Knowledge integration across the omics spectrum revealed consistent aberrations on the same neuroinflammation pathway, showcasing the value of integrative (i)-omics agreements for increasing confidence of biomarker selection. We believe that our findings could pave the way for identifying reproducible PD biomarkers, with potential for clinical deployment.

Keywords Multi-omics, Parkinson's, Biomarker, Blood-subtype

†Teddy J. W. Tng and Barbara Wing Yan Wong contributed equally to this work.

*Correspondence:
Wilson W. B. Goh
wilsongoh@ntu.edu.sg
Kah-Leong Lim
kahleong.lim@ntu.edu.sg
Full list of author information is available at the end of the article

Graphical Abstract

Six Proposed blood-based biomarkers. Seventy-nine publications across transcriptomics, proteomics and metabolomics were shortlisted and analysed for reported biomarkers. The proposed biomarkers are SNCA, APOA1, Arg1, 8-OHdG and Uric acid.

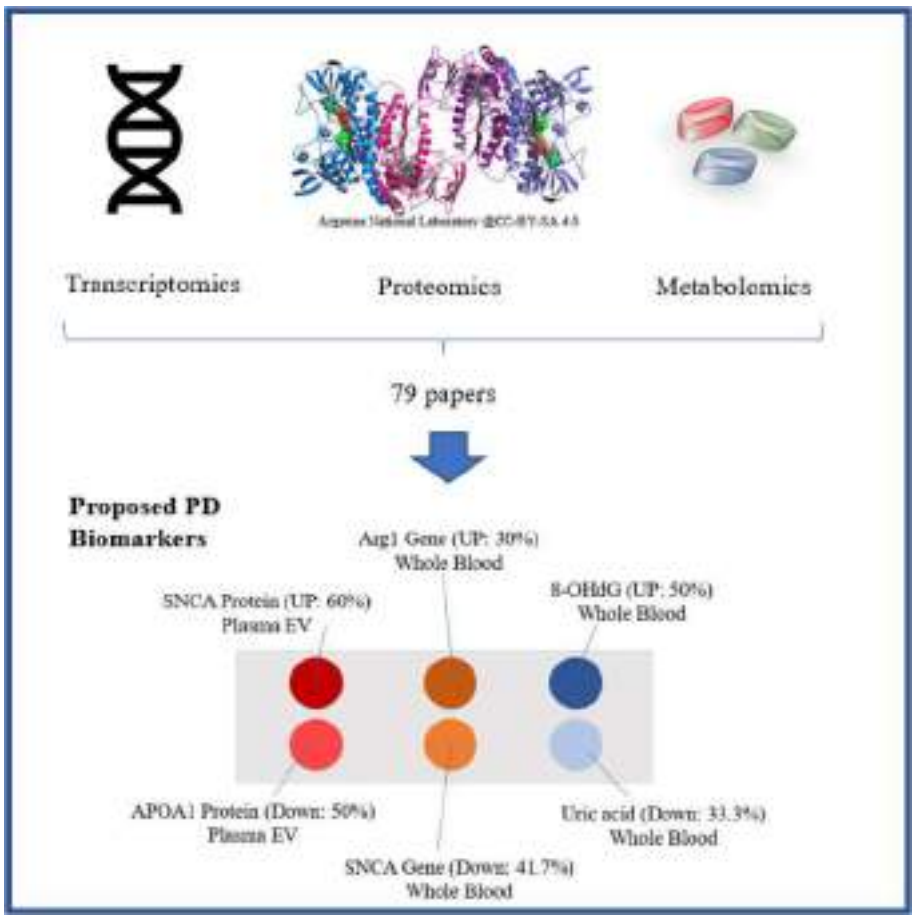

Background: Parkinson's Disease and Current Diagnostic Tools

Parkinson's disease (PD) is a prevalent neurological disorder [1] characterized by the loss of dopaminergic neurons in the substantia nigra pars compacta of the midbrain [2]. Since its discovery in 1817, the incidence rates of PD have increased by 10 times over the past nine decades [3]. PD prevalence is strongly associated with the elderly, a phenomenon that aligns with the notion that age is a major risk factor for the development of PD [4]. As the global population continues to age rapidly, PD poses a significant threat in deteriorating the quality of life for many afflicted individuals as well as their caregivers.

PD is a progressive neurodegenerative disease typically diagnosed via neurological examination for classical motor symptoms such as bradykinesia and resting tremors [5]. Clinically, PD diagnosis is usually conducted using the Unified Parkinson's Disease Rating Scale (UPDRS), which assesses an individuals' PD-related motor and non-motor deficits such as rigidity and olfactory dysfunction [6]. Additionally, the UPDRS score is used to track disease progression, with increasing score indicating worsening of PD disability [7]. However, even with clinical markers, the misdiagnosis rate for PD remains high at 42% [8, 9]. Clearly, less subjective phenotypic biomarkers would be helpful to improve PD diagnosis. To reduce subjectivity in PD diagnosis, brain imaging tools such as Magnetic resonance imaging (MRI) and Positron Emission Tomography (PET) have been used as a supplement and have shown potential to achieve a reliable diagnosis for parkinsonism. In particular, the

123I-ioflupane DaTSCAN was approved by the US FDA in 2011 for doctors to confirm a PD diagnosis [10]. However, these imaging tools are expensive to conduct, and a negative result does not absolutely rule out PD [11, 12]. Therefore, a cheaper but feasible alternative is needed for PD diagnosis.

Recently, mounting evidence suggested that biofluids can reflect the pathophysiology of PD [13–15]. This, in part, is fuelled by the Braak's hypothesis that sporadic PD begins via the olfactory or gastrointestinal system before affecting the central nervous system, suggesting that PD is not confined to the brain [16]. Biofluids such as urine, blood, cerebrospinal fluid (CSF) and tear fluid have been studied for the metabolites of dopamine since PD is driven by the loss of dopaminergic neurons. CSF analysis could be a reliable prognostic tool as it better mirrors pathological changes of the brain [13, 17]. However, collecting CSFs is invasive and is not practically suitable in clinical settings for suspected cases of PD [13]. Hence, this had led to the investigations of using non-invasive blood-based biomarkers such as serum, whole blood, and exosomes to facilitate PD diagnosis. With the rise of sequencing technologies, many studies have used omics to analyse diverse biological modalities of the genome, transcriptome, proteome, and metabolome in the blood of PD patients, with the view that they may provide valuable insights into the etiology of PD. However, current studies tend to be within the respective omics field and lacks cross-platform corroborations. This was demonstrated by Redenšek et al. where only 4% (5 out of 107 papers examined) of PD-related omics study from 2005 to 2017 were integrative [18]. The lack of corroboration represents an important research gap. The overall contributory value of each individual study can be greatly enhanced by careful data mining and knowledge integration, to demonstrate how functionally coherent (or discordant) the targets reported across the omics spectrum are. Integrating multi-layered studies and identifying corroborations could reduce false-positive and false-negative results. It could also strengthen our contextual reasoning and understanding of the interconnections across different biological layers, thus deepening our insights into PD prognosis. To achieve this, we examined a total of 79 papers spanning transcriptomics, proteomics, and metabolomics, which revealed six blood-based biomarkers suitable for PD diagnosis.

Individual omics platform demonstrate diagnostic potential with improved agreement on biomarkers across studies for specific blood components

Advances in high-throughput "omics" technologies provides new ways of studying diseases. Omics refers to a field of biological study that has the suffix -omics, which include genomics, transcriptomics, proteomics, metabolomics and more recently microbiomics [19, 20]. Omics technologies provide insight not only at single biological moieties, but also at higher order functional structures such as biological mechanisms or pathways critical for initiating various diseases. For example, genome-wide association studies (GWAS) have identified common PD risk loci consisting of *PARK16*, *ITPKB*, *MCCC1*, *SNCA*, *FAM47E-SCARB2*, *DLG2*, *LRRK2*, *RIT2* and *FYN* [21]. Common risk loci like *SNCA* provides a handle for researchers to investigate the pathology of PD, for instance alternative splicing of SNCA risk loci can result in a SNCA112 transcript that results in SNCA proteins that are structurally more prone to aggregation [22]. The aggregation of α-synuclein protein into Lewy bodies is the histopathological hallmark of PD [23]. Through omics studies, we also now know that LRRK2 interacts with many other important proteins and play a central role in pathways underlying PD [24].

To exploit omics for potential blood-based biomarkers, we gathered papers about PD spanning transcriptomics, proteomics and metabolomics studies via PubMed or Google Scholar between 2015 to 2021. The screening criteria is summarised by the PRISMA flow diagram (Fig. 1). Briefly, in our predefined timeframe, the search engine pairings of "Parkinson" and "Metabolomics" in PubMed yielded 260 results, while "Parkinson" and "Proteomics" yielded 568 results, whereas "Parkinson" with "Transcriptomics" yielded 104 results. The search results suggest that proteins are most popularly studied in the field of PD, which reflects the widely accepted role of misfolded protein aggregates in PD pathogenesis. As our focus is on blood-based biomarkers, we finetuned our search terms accordingly. The following final combinations of search terms were used: "PD", "Parkinson's Disease", "Blood" / "Blood-based biomarkers", "Plasma EV", "Serum EV" with "Transcriptomics" or "mRNA", "Proteomics" or "Proteins", "Metabolomics" or "Metabolites" for the respective omics. Only original research articles were selected. Review papers were examined for the original research articles that were cited so as to avoid double counting, thus resulting in some of the older original research articles being included in this analysis. This resulted in 18 transcriptomics- [25–42], 34 proteomics- [14, 43–74] and 27 metabolomics-related papers [46, 59, 72, 75–99], with a total of 6 different blood subtypes covered across the 79 papers. These included whole blood (24.0%), peripheral blood mononuclear cell (6.3%), serum (16.5%), plasma (26.6%), plasma extracellular vesicle (EV) (15.2%) and serum EV (11.1%). Interestingly, transcriptomic studies tend to focus on whole blood samples (66.7%), while

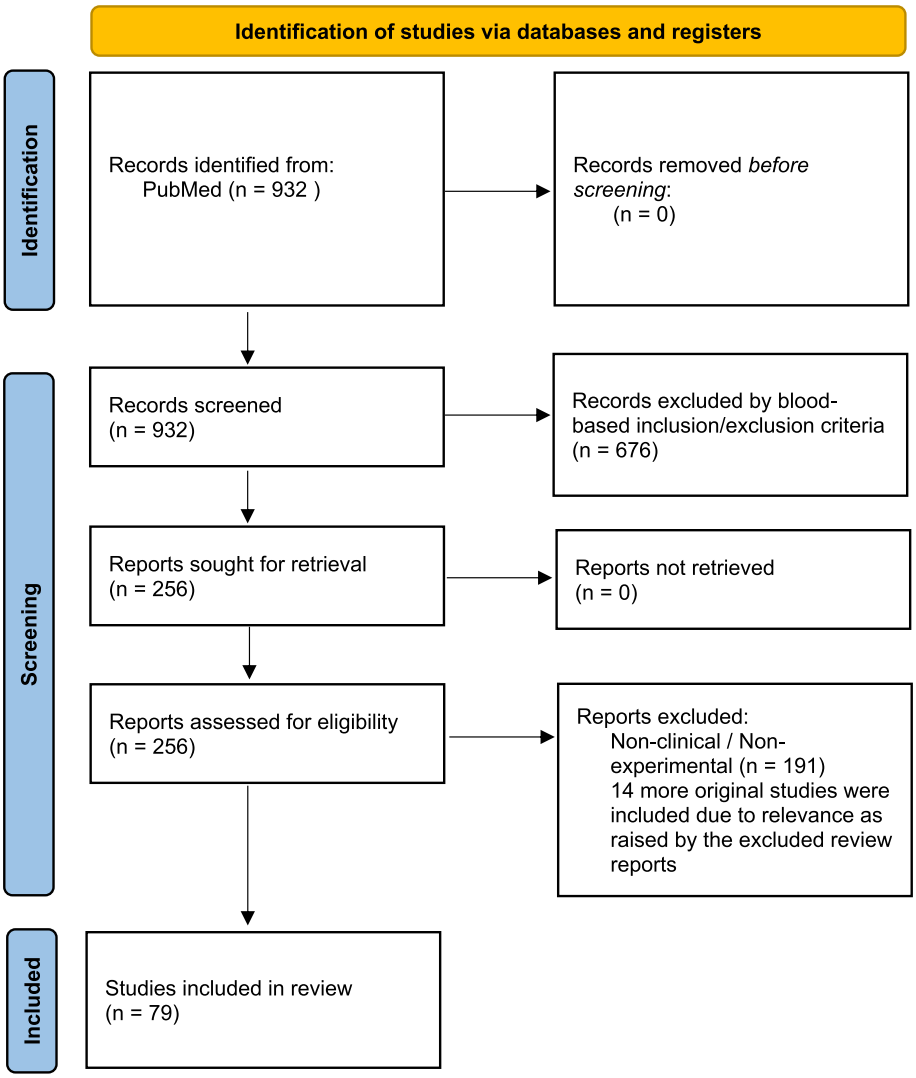

Fig. 1 PRISMA 2020 flow diagram for new systematic reviews. The screening process of 932 papers on PubMed related to Parkinson, Transcriptomics, Proteomics and Metabolomics to a final 79 papers for review that are blood-based specific

proteomic studies focused on EVs (55.9%) and metabolomic studies on plasma (44.4%).

Individually, omics technology reveals some potential for identifying risk factors, diagnostic biomarkers and therapeutic targets for PD as summarized in Supplementary Table 1, 2, 3 and 4 across the 79 papers we examined. For each of the 18 transcriptomics-, 34 proteomics-, 27 metabolomics-related papers, we noted the list of reported targets and examined the agreement rate of reported targets across papers within each omics field. For each transcript, protein or metabolite, agreement rate is defined as the number of papers that reported it as biomarker divided by the total number of papers examined in the corresponding omics field. The highest agreement rate was 29% amongst papers publishing transcriptome signatures between 2007–2021, 42% amongst papers publishing proteome signatures between 2009–2021 and 12.5% amongst papers publishing metabolite signatures between 2009–2021 (Table 1). For each omic field, we further subdivided the transcript, protein or metabolite into the blood

Table 1 Comparison of highest agreement rates across all papers within transcriptomics, proteomics and metabolomics. Percentage agreement increased with specificity of blood component

	Transcriptomics	Proteomics	Metabolomics
ALL Blood types	29%	42%	12.5%
Blood Type-Specific	42%	60%	50%

subtypes (ie. Serum, plasma, EV etc.) that they were reported in and calculated the agreement rate within the blood subtypes. Importantly, the highest agreement rates increased to 42%, 60% and 50% for transcriptomics, proteomics and metabolomics respectively, when we grouped the papers by specific blood subtypes. This suggests that different blood subtypes reflect varying differential changes to PD that can be used as biomarkers and future studies should be specific about the component of blood being examined.

Multi-omics analysis suggests 6 blood component specific parkinson's disease biomarkers

Genetic analysis of biomarkers suggests the use of Arg1 and SNCA gene in whole blood as potential blood-based mRNA biomarkers of PD

We included 15 studies that looked at gene upregulation and 17 studies that looked at gene downregulation across distinct blood subgroups (Table 2). Across all studies, commonly reported upregulated genes include Arginase 1 (ARG1) (26.67%) and Thrombomodulin (THBD) (26.7%). These genes were also reported in papers specific for whole blood. Interestingly, Arg1, an anti-inflammatory marker for anti-inflammatory microglia polarisation, is reported to be supressed in MPP + PD model [100] and affected by micro-RNA miR-155 in AAV2-SYN PD model [101]. Given the role of neuroinflammation and microglia polarisation [102] in PD, we selected Arg1 as a candidate biomarker. On the other hand, the most downregulated gene across all papers is SNCA (29.4%). SNCA is also the most reported downregulated gene in papers on whole blood (42%).

Protein analysis of the various blood subtypes suggest use of SNCA and APOA1 in plasma EV as potential protein biomarkers of PD

We identified 31 papers studying protein upregulation across various blood subtypes and 18 papers studying protein downregulation suitable for our intersection analysis (Table 3). The more commonly reported upregulated proteins across all blood subtypes in these papers are SNCA (42%), MAPT (10%), TTR (10%) and VWF (10%) (Table 3). When examining the specific blood subtypes, SNCA is still the most reported upregulated protein in plasma EV (60%), serum EV (57%) and plasma (25%). The more commonly reported downregulated proteins across all blood subtypes in the 18 papers are APOA1 (16.7%), FGG (16.7%), IGKV3-20 (16.7%) and SNCA (16.7%). Surprisingly, SNCA protein that is most reported as upregulated is also reported to be downregulated by other studies [53, 55, 73]. Although it seems puzzling to observe downregulation in αSYN gene expression and upregulation in SNCA protein, various explanations have been proposed. For example, a downregulation in αSYN gene could be induced by upregulation in DNA methylation in the CpG sites that lead to the exhibition of PD phenotypes [103]. Contrastingly, an upregulation of SNCA protein could be observed after autophagy-lysosomal pathway failure, where low-aggregated SNCA will predominantly be released via exosomes, in line with our observations of increased SNCA reported in plasma EVs

Table 2 Analysis of top transcriptomic hits categorised by blood subtypes

ALL UP (15)			WB UP (10)			PBMC UP (3)			Serum UP (2)		
Name	**Freq**	**percentage**	**Name**	**Freq**	**percentage**	**Name**	**Freq**	**percentage**	**Name**	**Freq**	**percentage**
ARG1	4	26.66667	THBD	4	40	ALAS2	1	33.33333	ADAP2	2	100
THBD	4	26.66667	ADARB2	3	30	AP1S2	1	33.33333	ATAT1	2	100
ADARB2	3	20	ALOX5A	3	30	ARG1	1	33.33333	CCL19	2	100
ALOX5A	3	20	ARG1	3	30	ARSB	1	33.33333	IL20	2	100
ARHGAP	3	20	ARHGAP	3	30	ASAH1	1	33.33333	MAPKAP	2	100
ATP6V0D	3	20	BASP1	3	30	Atg7	1	33.33333	MOB3C	2	100
BASP1	3	20	CLIC3	3	30	ATP6V0D	1	33.33333	MRPL19	2	100
CLIC3	3	20	GPX3	3	30	CD68	1	33.33333	RPS18	2	100
GPX3	3	20	GSTM3	3	30	CLTCL1	1	33.33333	BRSK1	1	50
GSTM3	3	20	IDS	3	30	CTSA	1	33.33333	BUD31	1	50

ALL Down (17)			WB Down (12)			PBMC Down (5)		
Name	**Freq**	**percentage**	**Name**	**Freq**	**percentage**	**Name**	**Freq**	**percentage**
SNCA	5	29.41176	SNCA	5	41.66667	NURR1	2	40
LRRN3	4	23.52941	LRRN3	4	33.33333	ALAS2	1	20
ALAS2	3	17.64706	CNTNAP	3	25	AMBRA1	1	20
CNTNAP	3	17.64706	CTSE	3	25	APAF1	1	20
CTSE	3	17.64706	FCER2	3	25	ARHGAP	1	20
FCER2	3	17.64706	FCRL2	3	25	ARPC5L	1	20
FCRL2	3	17.64706	HBG1	3	25	ATG12	1	20
HBD	3	17.64706	IGFBP2	3	25	ATG16L1	1	20
HBG1	3	17.64706	ITLN1	3	25	ATG2	1	20
HBM	3	17.64706	KCNH8	3	25	ATG4B	1	20

Table 3 Analysis of top proteomic hits categorised by blood subtypes

ALL UP (31)

Name	Freq	percentage
SNCA	13	41.93548
MAPT	3	9.677419
TTR	3	9.677419
VWF	3	9.677419
AGT	2	6.451613
APCS	2	6.451613
Aß1–42	2	6.451613
CALM3	2	6.451613
CLU	2	6.451613
CRP	2	6.451613
F2	2	6.451613

Plasma EV UP (10)

Name	Freq	percentage
SNCA	6	60
CALM3	2	20
HLA-B	1	10
HLA-C	1	10
ABCA7	1	10
ABCB6	1	10
ACTN1	1	10
ACTN2	1	10
ACTN3	1	10
ACTN4	1	10
ADD1	1	10

Serum EV UP (7)

Name	Freq	percentage
SNCA	4	57.14286
AGT	2	28.57143
CRP	2	28.57143
FGB	2	28.57143
IGKV3-2(	2	28.57143
VWF	2	28.57143
COL1A2	1	14.28571
ACTB	1	14.28571
AHSG	1	14.28571
APCS	1	14.28571
APOA1	1	14.28571

Plasma UP (8)

Name	Freq	percentage
SNCA	2	25
APCS	1	12.5
APOE	1	12.5
Aß1–42	1	12.5
C3	1	12.5
CHI3L	1	12.5
CHL1	1	12.5
DEFA1	1	12.5
F2	1	12.5
FN1	1	12.5
FN1-10	1	12.5

Serum UP (5)

Name	Freq	percentage
TTR	2	40
APOA4	1	20
APOH	1	20
AZGP1	1	20
C4B	1	20
CF1	1	20
CFH	1	20
CLU	1	20
FGG	1	20
FIGNL1	1	20
FIGNL2	1	20

WB UP (1)

Name	Freq
Aβ1–42	1
MAPT	1

ALL DOWN (18)

Name	Freq	percentage
APOA1	3	16.66667
FGG	3	16.66667
IGKV3-2(	3	16.66667
SNCA	3	16.66667
C1R	2	11.11111
C4B	2	11.11111
CRLF3	2	11.11111
EPB41	2	11.11111
F2	2	11.11111
IGHG1	2	11.11111

Plasma EV DOWN (2)

Name	Freq	percentage
CRLF3	2	100
EPB41	2	100
FGG	2	100
PDIA3	2	100
RAD23A	2	100
ABCC1	1	50
ABCC4	1	50
ABCG2	1	50
ABHD14I	1	50
ACAT2	1	50

Serum EV DOWN (5)

Name	Freq	percentage
IGKV3-2(	3	60
IGHG1	2	40
A2M	1	20
ADIPOQ	1	20
ANPEP	1	20
ATP5A	1	20
C1QB	1	20
C1QC	1	20
C1R	1	20
C1S	1	20

Plasma DOWN (6)

Name	Freq	percentage
ACY1	1	16.66667
ANTXR2	1	16.66667
APOA1	1	16.66667
B2M	1	16.66667
BAG2	1	16.66667
CFH	1	16.66667
CR2	1	16.66667
CTSD	1	16.66667
F8	1	16.66667
FGG	1	16.66667

Serum DOWN (4)

Name	Freq	percentage
ALB	1	25
AMBP	1	25
APOA1	1	25
APOA4	1	25
APOE	1	25
DYNC1H	1	25
F2	1	25
HP	1	25
HPR	1	25
HSA	1	25

WB DOWN (1)

Name	Freq
SNCA	1

ALL Pathway UP (31)

Name	Freq	percentage
Parkinson	15	48.3871
Pathways	15	48.3871
Alzheimer	14	45.16129
Compleme	5	16.12903
ECM-rece	5	16.12903
Coronavir	4	12.90323
Nil	4	12.90323
Staphyloc	4	12.90323
MAPK sig	3	9.677419
Neutrophi	3	9.677419

ALL Pathway Down (18)

Name	Freq	percentage
Compleme	6	33.33333
African try	4	22.22222
Parkinson	4	22.22222
Pertussis	4	22.22222
Staphyloc	4	22.22222
Cholesterc	3	16.66667
Coronavir	3	16.66667
Fat digesti	3	16.66667
Nil	3	16.66667
Pathways	3	16.66667

[104]. Nonetheless, we selected SNCA as our biomarker of choice since its expression is reported by most as being affected in PD. We have also chosen APOA1 alongside SNCA as a downregulated biomarker for ease of testing using a common plasma EV blood subtype and also due to its relation to PD such as risk of having mild cognitive impairment as reported by other literatures [105–107].

Metabolites analysis of various blood subtypes suggests 8-OhDG markers for PD patients

We studied 26 and 24 papers on metabolites upregulation and downregulation in PD patients, respectively. The more commonly reported downregulated metabolites in PD patients are Uric acid (12.5%), Catechol sulfate (8.33%) and Cis-aconitic acid (8.33%) (Table 4). When examining the specific blood subtypes, the percentage for uric acid increased from 12.5% to 33% in whole blood. On the other hand, the more frequently reported upregulated metabolites across all studies are Proline (11.5%), 8-OhDG (7.69%) and Alanine (7.69%) (Table 4). 8-OhDG was chosen as our choice of upregulated biomarker for ease of testing using a common whole blood subtype and also due to its relation to PD via oxidative stress as reported by others [108, 109].

Table 4 Analysis of top metabolomic hits categorised by blood subtypes

Up Whole blood - 4 papers

Name	Freq	percentage
8-OHdG	2	50
13-hydro	1	25
Arachido	1	25
Cholester	1	25
Ferritin	1	25
Glutathio	1	25
MDA	1	25
Nitrite	1	25
Stearic ac	1	25

Serum - 7 papers

Name	Freq	percentage
Ornithin	2	28.6
Phosphoe	2	28.6
Proline	2	28.6
Tyrosine	2	28.6
1-methyll	1	14.3
3-hydroxy	1	14.3
3-hydroxy	1	14.3
3-hydroxy	1	14.3
Aliphatic	1	14.3
Biliverdir	1	14.3

Blood plasma - 11 papers

Name	Freq	percentage
Bile acid	2	18.2
Carnitine	2	18.2
LysoPC(1	2	18.2
Succinate	2	18.2
Alanine	2	18.2
1,3-Dime	1	9.09
2-Octenoi	1	9.09
2-oxoisoc	1	9.09
3-carboxy	1	9.09
3-ketosph	1	9.09

Plasma EV -1 paper

Name	Freq	percentage
ex-miR-3	1	100
miR-125a	1	100
miR-137	1	100
miR-181c	1	100
miR-193a	1	100
miR-331-	1	100
miR-454	1	100
miR196-p	1	100

Serum EV -1 paper

Name	Freq	percentage
ex-let-7d	1	100
ex-miR-2	1	100
ex-miR-2	1	100
miR-29a	1	100
ex-miR-2	1	100
ex-miR-1	1	100
ex-miR-2	1	100
ex-miR-1	1	100

ALL - Total 26 papers

Name	Freq	percentage
Proline	3	11.5
8-OHdG	2	7.69
Alanine	2	7.69
Bile acid	2	7.69
Carnitine	2	7.69
LysoPC(1	2	7.69
Ornithin	2	7.69
Phosphoe	2	7.69
Succinate	2	7.69
Tyrosine	2	7.69

Down Whole blood - 6 papers

Name	Freq	percentage
Uric acid	2	33.3
12-hydro	1	16.7
17,18-dih	1	16.7
Acetate	1	16.7
Amino m	1	16.7
Ascorbate	1	16.7
Br-GSH	1	16.7
Butanoic	1	16.7
Catalase	1	16.7
Cholester	1	16.7

Serum - 6 papers

Name	Freq	percentage
Catechol	2	33.3
Citrulline	2	33.3
1-myristo	1	16.7
1,3-dimet	1	16.7
2-myristo	1	16.7
3-methyl-	1	16.7
Arg/3-AA	1	16.7
Bilirubin	1	16.7
Caffeine	1	16.7
Ergothior	1	16.7

Blood plasma- 10 papers

Name	Freq	percentage
Cis-aconi	2	20
FFA 11:1	2	20
Formic ac	2	20
Kynureni	2	20
Linoleic a	2	20
Oleic acid	2	20
Palmitole	2	20
Trigonelli	2	20
1,5-anhyd	1	10
186.1189	1	10

Plasma EV- 1 paper

Name	Freq	percentage
ex-miR-5	1	100
miR-626	1	100
miR-505	1	100

Serum EV- 1 paper

Name	Freq	percentage
ex-miR-1	1	100

All - total 24 papers

Name	Freq	percentage
Uric acid	3	12.5
Catechol	2	8.33
Cis-aconi	2	8.33
Citrulline	2	8.33
Ethanola	2	8.33
FFA 11:1	2	8.33
Formic ac	2	8.33
Hypoxant	2	8.33
Kynureni	2	8.33
Linoleic a	2	8.33

Overlap of biomarkers from multi-omics integration likely to be true signal amongst false positives or false negatives artefact from omics methodologies

Given that there are usually more expressed genes relative to acquired samples, transcriptomic analyses typically suffer from a lack of statistical power (curse-of-dimensionality) or produce many false positives/negatives due to erroneous assumptions on data distribution [110]. To counter such issues, more appropriate bioinformatics algorithms were developed such as DESeq2 [111] or limma-voom [112]. In addition, fluid-based proteomics also face many challenges and complexities. High abundance proteins such as albumin can mask low abundance proteins and must be removed to facilitate observation of lower abundance proteins. However, the removal of albumin might result in unintended removal of non-targeted low abundance proteins [113, 114]. Many peptides in serum also give highly intense signals that makes identification of endogenous peptides difficult. In addition, there is a wide array of technical variables that can influence the proteomic results [115]. Variables such as blood withdrawal site or simply letting serum samples sit beyond 60 min can lead to detection of false targets arising from hemolysis caused by residual disinfecting alcohol [116] or unwanted cell lysis [117] respectively.

The current way transcriptomics and proteomics are conducted and analyzed, may produce many false positives and false negatives. Multi-omics integration

can value add by reducing the extent of false positives and false negatives presented. With the large amount of transcriptomics, proteomics, and metabolomics data available, targets that are repeatedly reported as common across the different omics layers are more likely to be true signals rather than technical artefacts. We define a cross-omics agreement rate as the intersection of transcriptomics and proteomics set of targets divided by the minimum number of targets of the 2 sets [ie. $A \cap B/\min(A, B)$]. Analysis between the lists of compiled upregulated mRNAs and proteins identified 53 overlaps (13.7%) amongst the 2515 mRNAs and 386 proteins reported by the various studies. Similarly, between the lists of compiled downregulated mRNAs and proteins, there were 66 overlaps (12.9%) amongst the 1504 mRNAs and 508 proteins reported by the various studies. However, not all mRNA expression is positively correlated with protein expression [118]. Hence, we examined cross-omics agreement regardless of direction of expression as well. There was an increase in percentage overlap with a total of 211 overlaps (23%) between the 4019 mRNAs and 894 proteins reported by the various studies. The Hypergeometric test is an important statistical instrument used to estimate the probability of chance occurrences of overlapping genes between 2 genes sets [119]. Using the phyper() function in R and the assumption of 19,950 protein coding genes in the GRCh38 human genome [120], cross-omics biomarker overlap between all mRNAs and proteins reported is significant ($p\text{-}val = 0.005339753$). This suggests that overlapping biomarkers via multi-omics integration are likely true signals and should be further validated, including our proposed biomarkers SNCA and Arg1.

Both transcriptomics and proteomics point to common theme of neuroinflammation and metabolic processes despite seemingly different list of biomarkers

Omics technologies can easily produce a large number of differentially expressed targets which is often overwhelming for researchers to look at individually. Hence, a common strategy is to identify the higher-order functional perspective by summarizing observed differential genes in light of their parent pathway (for instance, via DAVID) [121]. Pathway analysis can improve experiment credibility by locating the most important pathways. For instance, when the protein list from each study was ran through EnrichR to obtain pathways affected for each study (Table 5), 33% reported downregulation of Complement and coagulation cascades for proteomics (vs 17% overlap in protein targets). Pathway analysis may also reduce the study's scope to a few hundred pathways rather than thousands of DEGs. Hence, in addition to intersections analysis, we exploited popular public repositories like Gene Ontology (GO) to study the pathways associated with PD.

We observed unifying themes for GO pathways derived from the compiled list of transcripts and proteins (Fig. 2). We pooled together upregulated differentially expressed genes from all the literature analysed and ran a pathway analysis using enrichGO function from clusterProfiler package in R (v4.0.5). The same was done for downregulated DEGs, upregulated proteins and downregulated proteins. Significant GO pathways from upregulated DEGs point towards IL6 and immune system changes, which were also observed in significant GO pathways from upregulated proteins. A study by Fielding et al. reported that IL6 is the key signal for neutrophil trafficking during inflammation, chemokine production and leukocyte apoptosis [122]. Similarly, we observed significant pathways of IL6 production, regulation of IL6 production and positive regulation of IL6 production from upregulated DEGs, which were supported by significant pathways of neutrophil degranulation, neutrophil activation involved in immune response, cell killing and other inflammatory pathways involving MHC I from upregulated proteins. Despite seemingly modest overlap in the list of upregulated DEGs and proteins, PD is associated with neuroinflammation when evaluated collectively across omics layers as illustrated in the upset plot (Fig. 3A). The upset plot shows that different pathways were upregulated predominantly across the different omics, with neuroinflammation dominating transcriptomics; amino acid metabolism dominating metabolomics and blood related changes dominating proteomics (Fig. 3A).

Many significant pathways from downregulated DEGs and proteins are inflammation-related (eg. T-cell activation, lymphocyte proliferation and antigen processing / presentation). Other than neuroinflammation, the significant pathways from both downregulated DEGs and proteins converged on downregulated metabolic pathways such as cellular response to toxic substance, hydrogen peroxide catabolic process, ubiquitin-dependent protein catabolic process and regulation of cellular amino acid metabolic process. This reaffirms the proposition that PD is a metabolic disease [123] and also demonstrated in the upset plot, where the top hits other than neuroinflammation are protein and lipid metabolism (Fig. 3B).

Inter i-omics agreement on pathways can deepen confidence in selected biomarkers

The importance of integrating multi-layered studies is demonstrated when we observe how pathways across transcriptomics, proteomics and metabolomics corroborate. Pathways for the list of compiled metabolites

Table 5 Related pathways across transcriptomics, proteomics and metabolomics

S No.	Blood Component	Top 10 pathways affected	Level in PD (compared to healthy controls)
Transcriptomics			
1	Whole blood	Nil	Downregulated
		Dilated cardiomyopathy, Hypertrophic cardiomyopathy, Cardiac muscle contraction, ECM-receptor interation, Platelet activation, Arrhythmogenic righ ventricular cardiomyopathy, Antigen processing and presentation, Adrenergic signaling in cardiomyocytes, Focal adhesion,	Upregulated
2	Whole blood	Nil	Downregulated
		Staphylococcus aureus infection, Complement and coagulation cascades	Upregulated
3	Whole blood	Nil	Downregulated
		Osteoclast differentiation, Leishmaniasis, Tuberculosis,	Upregulated
4	Whole blood	Parkinson disease, Alzheimer disease, Pathways of neurodegeneration	Downregulated
5	Whole blood	Nil	Downregulated
		Osteoclast differenciation, Natural killer cell mediated cytotoxicity, Antigent processing and presentation, B cell receptor signalling pathway, Graft-versus-host disease, Lysosome, Phagosome, Chemokine signaling pathway, Fc gamma R-mediated phagocytosis, Tuberculosis	Upregulated
6	Whole blood	Parkinson Disease, Perussis, Prion Disease, Huntington disease,	Downregulated
		Nil	Upregulated
7	peripheral blood mononuclear cells (PBMCs)	Th1 and Th2 cell differentiation, Th17 cell differentiation, Epstein-Barr virus infection, Toxoplasmosis, Leukocyte transendothelial migration, Human immunodeficiency virus 1 infection, Tuberculosis, Leishmaniasis, Pathways in cancer, Human cytomegalovirus infection	Downregulated
		Porphyrin and chlorophyll metabolism, Amoebiasis	Upregulated
8	peripheral blood mononuclear cells (PBMCs)	Sulfur metabolism, Collecting duct acid secretion, Glycine, serine and threonine metabolism, Porphyrin and chlorophyll metabolism, Malaria	Downregulated
9	Whole blood	Nil	Downregulated
		Endocrine and other factor-regulated calcium reabsorption, Nitrogen metabolism,	Upregulated
10	Whole blood / leukocytes	Citrate cycle (TCA cycle), Pyruvate metabolism, Cocaine addiction, Aminoacyl-tRNA biosynthesis, Amphetamine addiction, Salmonella infection, Parkinson disease, Prion disease, Huntington Disease, Amyotrophic lateral sclerosis	Downregulated
		Nil	Upregulated
11	peripheral blood mononuclear cell (PBMC)	Autophagy, Mitophagy, RIG-I-like receptor signaling pathway, NOD-like recptor signaling pathway, Shigellosis	Downregulated
		Lysosome, Glycosaminoglycan degradation, Other glycan degradation, Glycosphingolipid biosynthesis, Phagosome, Sphinagolipid metabolism, Collecting duct acid secretion, Apoptosis, Tuberculosis, Synaptic vesicle cycle	Upregulated
12	Whole blood	Nil	Downregulated
		Nil	Upregulated

Table 5 (continued)

S No.	Blood Component	Top 10 pathways affected	Level in PD (compared to healthy controls)
13	peripheral blood mononuclear cells (PBMCs)	Nil	Downregulated
		Inflammatory bowel disease, Cytokine-cytokin receptor interaction, African trypanosomiasis, Malaria, Perussis, Leishmaniasis, Asthma, IL-17 signaling pathway, Hematopoietic cell lineage, Amoebiasis	Upregulated
14	Whole blood	Nil	Downregulated
15	Whole blood	Ubiquitin mediated proteolysis, Protein processing in endoplasmis reticulum, Parkinson disease	Downregulated
		Fructose and mannose metabolism, Inflammatory bwel disease	Upregulated
16	Whole blood	Nil	Downregulated
		Arachidonic acid metabolism	Upregulated
17	Peripheral blood	Nil	Downregulated
18	Blood Serum	Nil	Upregulated
	Blood Serum	Viral protein interaction with cytokine and cytokine receptor,	Upregulated
Proteomics			
1	Plasma EV	Parkinson disease, MAPK signaling pathway, Alzheimer disease, Pathways of neurodegeneration	Upregulated
2	Plasma EV	Parkinson disease, Alzheimer disease, Pathways of neurodegeneration	Upregulated
3	Plasma EV	Parkinson disease, Alzheimer disease, Pathways of neurodegeneration	Upregulated
4	Plasma EV	Parkinson disease, Alzheimer disease, Pathways of neurodegeneration	Upregulated
5	Plasma EV	Parkinson disease, Alzheimer disease, Pathways of neurodegeneration	Upregulated
6	Plasma EV	Parkinson disease, Alzheimer disease, Pathways of neurodegeneration	Upregulated
7	Plasma EV	Parkinson disease, Alzheimer disease, Pathways of neurodegeneration,	Upregulated
8	Plasma EV	Ferroptosis, Prion disease, Pathways of neurodegeneration,	Upregulated
9	Plasma EV	Nil	Upregulated
10	Plasma EV	Complement and coagulation cascades, Staphylococcus aureus infection, Coronavirus disease, Vitamin digestion and absorption, African trypanosomiasis, Fat digestion and absorption, Cholesterol metabolism, PPAR signaling pathway, Pertussis, Platelet activation,	Downregulated
11	Plasma EV	Proteasome, Gastric acid secretion, Endocytosis, Parkinson disease, Phagosome, Aldosterone-regulated sodium reabsorption, Salivary secretion, Adrenergic signaling in cardiomyocytes, Aldosterone synthesis and secretion, Glycolysis / Gluconeogenesis, Endocrine and other factor-regulated calcium reabsorption,	Upregulated
		Proteasome, Pentose phosphate pathway, Spinocerebellar ataxia, Prion disease, Parkinson disease, Amyotrophic lateral sclerosis, Huntington disease, Pathways of neurodegeneration, Glycolysis / Gluconeogenesis, Cysteine and methionine metabolism,	Downregulated
12	Serum EV	Parkinson disease, Alzheimer disease, Pathways of neurodegeneration	Upregulated
		Nil	Downregulated

Table 5 (continued)

S No.	Blood Component	Top 10 pathways affected	Level in PD (compared to healthy controls)
13	Serum EV	Parkinson disease, Alzheimer disease, Pathways of neurodegeneration	Downregulated
14	Serum EV	Asthma, African trypanosomiasis, Allograft rejection, Graft-versus-host disease, Type I diabetes mellitus, Type II diabetes mellitus, Malaria, Legionellosis, Inflammatory bowel disease, Fc epsilon RI signaling pathway,	Upregulated
		Thermogenesis, Citrate cycle (TCA cycle), Asthma, Oxidative phosphorylation, Non-alcoholic fatty liver disease, Diabetic cardiomyopathy, Parkinson disease, Melanoma, Prion disease, Huntington disease,	Downregulated
15	Serum EV	Parkinson disease, Alzheimer disease, Pathways of neurodegeneration	Upregulated
16	Serum EV	Parkinson disease, Alzheimer disease, Pathways of neurodegeneration	Upregulated
17	Serum EV	Parkinson disease, Alzheimer disease, Pathways of neurodegeneration	Upregulated
18	Serum EV	Complement and coagulation cascades, Platelet activation, Pertussis, Systemic lupus erythematosus, Neutrophil extracellular trap formation, ECM-receptor interaction, Hypertrophic cardiomyopathy, Coronavirus disease, Staphylococcus aureus infection, Dilated cardiomyopathy,	Upregulated
		Complement and coagulation cascades, Pertussis, Staphylococcus aureus infection, Systemic lupus erythematosus, Coronavirus disease, Renin-angiotensin system, Ferroptosis, Porphyrin and chlorophyll metabolism, Type II diabetes mellitus, Glutathione metabolism,	Downregulated
19	Serum EV	Complement and coagulation cascades, Platelet activation, Coronavirus disease, ECM-receptor interaction, Staphylococcus aureus infection, Neutrophil extracellular trap formation, Focal adhesion, , , ,	Upregulated
		Allograft rejection, Staphylococcus aureus infection, Autoimmune thyroid disease, Viral myocarditis, Systemic lupus erythematosus, Pertussis, Complement and coagulation cascades, Dilated cardiomyopathy, Chagas disease, Coronavirus disease,	Downregulated
20	Blood Plasma	Complement and coagulation cascades, Coronavirus disease, Neuroactive ligand-receptor interaction	Upregulated
		Complement and coagulation cascades, Staphylococcus aureus infection, Vitamin digestion and absorption, African trypanosomiasis, Fat digestion and absorption, Cholesterol metabolism, PPAR signaling pathway, Platelet activation, Neutrophil extracellular trap formation, Lipid and atherosclerosis,	Downregulated
21	Blood Plasma	Nil	Upregulated
		Nil	Downregulated
22	Blood Plasma	PI3K-Akt signaling pathway, ECM-receptor interaction, Growth hormone synthesis, secretion and action, JAK-STAT signaling pathway, Focal adhesion, Cytokine-cytokine receptor interaction, Human papillomavirus infection, Neuroactive ligand-receptor interaction,	Upregulated
		Arginine biosynthesis	Downregulated

Table 5 (continued)

S No.	Blood Component	Top 10 pathways affected	Level in PD (compared to healthy controls)
23	Blood Plasma	ECM-receptor interaction, Staphylococcus aureus infection	Upregulated
		Pantothenate and CoA biosynthesis, Complement and coagulation cascades,	Downregulated
24	Blood Plasma	African trypanosomiasis, Malaria, AGE-RAGE signaling pathway in diabetic complications, NF-kappa B signaling pathway, TNF signaling pathway, Leukocyte transendothelial migration, Fluid shear stress and atherosclerosis, Cell adhesion molecules, Lipid and atherosclerosis,	Upregulated
		African trypanosomiasis, Graft-versus-host disease, Malaria, Legionellosis, Inflammatory bowel disease, Pertussis, Antigen processing and presentation, Epstein-Barr virus infection, Human T-cell leukemia virus 1 infection, Human cytomegalovirus infection,	Downregulated
25	Blood Plasma	Sphingolipid signaling pathway, Lysosome, Estrogen signaling pathway, Autophagy, Apoptosis, Protein processing in endoplasmic reticulum, Tuberculosis, Diabetic cardiomyopathy	Downregulated
26	Blood Plasma	ECM-receptor interaction	Upregulated
27	Blood Plasma	Parkinson disease, Alzheimer disease, Pathways of neurodegeneration, MAPK signaling pathway	Upregulated
28	Blood Plasma	Parkinson disease, Alzheimer disease, Pathways of neurodegeneration	Upregulated
29	Blood Serum	Nil	Upregulated
		Nil	Downregulated
30	Blood Serum	Cholesterol metabolism, Thyroid hormone synthesis, Complement and coagulation cascades	Upregulated
		Vasopressin-regulated water reabsorption	Downregulated
31	Blood Serum	Complement and coagulation cascades, Staphylococcus aureus infection, Platelet activation, Neutrophil extracellular trap formation, Coronavirus disease	Upregulated
		Vitamin digestion and absorption, Fat digestion and absorption, Cholesterol metabolism, African trypanosomiasis, Lipid and atherosclerosis, PPAR signaling pathway, Complement and coagulation cascades, Platelet activation, Phospholipase D signaling pathway,	Downregulated
32	Blood Serum	Nil	Upregulated
		Asthma, JAK-STAT signaling pathway, Cytokine-cytokine receptor interaction	Downregulated
33	Blood Serum	Parkinson disease, Alzheimer disease, Pathways of neurodegeneration	Upregulated
34	Whole Blood	Parkinson disease, MAPK signaling pathway, Alzheimer disease, Pathways of neurodegeneration	Upregulated
		Parkinson disease, Alzheimer disease, Pathways of neurodegeneration	Downregulated
Metabolomics			
1	Blood plasma	Sphingolipid metabolism	Upregulated
		names not identified	Downregulated
2	Blood plasma	names not identified	Upregulated
3	Blood plasma	Citrate cycle (TCA cycle), Arginine biosynthesis	Upregulated
		NIL	Downregulated

Table 5 (continued)

S No.	Blood Component	Top 10 pathways affected	Level in PD (compared to healthy controls)
4	Blood plasma	Nicotinate and nicotinamide metabolism, Tyrosine metabolism	Upregulated
		Tryptophan metabolism	Downregulated
5	Blood Plasma	Steroid hormone biosynthesis	Upregulated
		NIL	Downregulated
6	Blood Serum	Arginine biosynthesis, Aminoacyl-tRNA biosynthesis, Pantothenate and CoA biosynthesis, beta-Alanine metabolism, Glutathione metabolism, Alanine, aspartate and glutamate metabolism ,Pyrimidine metabolism Phenylalanine, tyrosine and tryptophan biosynthesis, Tyrosine metabolism, D-Glutamine and D-glutamate metabolism, Nitrogen metabolism	Upregulated
		Thiamine metabolism ,Taurine and hypotaurine metabolism, Pantothenate and Co biosynthesis, Glutathione metabolism, Glycine, serine and threonine metabolism, Cysteine and methionine metabolism	Downregulated
7	Blood Plasma	Arginine biosynthesis, Butanoate metabolism	Upregulated
		Taurine and hypotaurine metabolism, Biotin metabolism, Lysine degradation	Downregulated
8	Blood Plasma	Linoleic acid metabolism, alpha-Linolenic acid metabolism	Upregulated
		Glycerophospholipid metabolism, Glycosylphosphatidylinositol (GPI)-anchor biosynthesis	Downregulated
9	Blood Plasma	Valine, leucine and isoleucine biosynthesis, Aminoacyl-tRNA biosynthesis	Upregulated
		Biosynthesis of unsaturated fatty acids, Linoleic acid metabolism	Downregulated
10	Blood Plasma	Phenylalanine, tyrosine and tryptophan biosynthesis, Phenylalanine metabolism	Upregulated
		NIL	Downregulated
11	Plasma EV	names not identified	Upregulated
		names not identified	Downregulated
12	Serum EV	names not identified	Upregulated
		names not identified	Downregulated
13	Whole blood	Glutathione metabolism	Upregulated
		Purine metabolism	Downregulated
14	Whole blood	names not identified	Downregulated
15	Whole blood	NIL	Upregulated
		NIL	Downregulated
16	Blood Plasma	Glycerophospholipid metabolism	Upregulated
		Biosynthesis of unsaturated fatty acids, Linoleic acid metabolism, Arachidonic acid metabolism, Synthesis and degradation of ketone bodies, Tryptophan metabolism	Downregulated
17	Whole blood	Biosynthesis of unsaturated fatty acids, Arachidonic acid metabolism	Upregulated
		Biosynthesis of unsaturated fatty acids	Downregulated
18	Blood Plasma	Purine metabolism	Downregulated
19	Blood Plasma	NIL	Upregulated
20	Blood Serum	D-Glutamine and D-glutamate metabolism, Nitrogen metabolism, Arginine biosynthesis	Upregulated
		Arginine and proline metabolism	Downregulated

Table 5 (continued)

S No.	Blood Component	Top 10 pathways affected	Level in PD (compared to healthy controls)
21	Blood Serum	Arginine and proline metabolism, Arginine biosynthesis	Upregulated
		Arginine biosynthesis	Downregulated
22	Blood Serum	Histidine metabolism	Upregulated
		NIL	Downregulated
23	Blood Serum	Sphingolipid metabolism, Glycerophospholipid metabolism, Arginine and proline metabolism	Upregulated
		Arginine biosynthesis	Downregulated
24	Whole blood	Biosynthesis of unsaturated fatty acids	Upregulated
		Butanoate metabolism, Alanine, aspartate and glutamate metabolism, Arginine and proline metabolism, Nitrogen metabolism, D-Glutamine and D-glutamate metabolism	Downregulated
25	Blood Serum	Tyrosine metabolism, Phenylalanine, tyrosine and tryptophan biosynthesis, Ubiquinone and other terpenoid-quinone biosynthesis, Phenylalanine metabolism, Arginine biosynthesis	Upregulated
		Tryptophan metabolism, caffeine metabolism	Downregulated
26	Whole blood	Citrate cycle (TCA cycle), Glyoxylate and dicarboxylate metabolism, Pyruvate metabolism, Galactose metabolism,Alanine, aspartate and glutamate metabolism	Downregulated
27	Blood Serum	NIL	Upregulated

(Table 5) were obtained using MetaboAnalyst 5.0 [124]. Arginine biosynthesis was the most frequent pathway, followed by biosynthesis of unsaturated fatty acids and ROS related pathways like aspartate and glutamate metabolism and glutathione metabolism. The metabolomic pathways exhibit great relevance to the transcriptomic and proteomic pathways identified. Arginine has been shown to inhibit acute microglia-mediated inflammation [125] while fatty acids can serve as inflammatory response signalling molecules [126]. Additionally, glutathione metabolism is related to hydrogen peroxide catabolic process [127] that was picked up by proteomics. The interconnectedness across different biological layers comes to light with metabolomic pathways supporting the major neuroinflammation and metabolic themes highlighted by both transcriptomics and proteomics. Integration of cross omics findings can also result in greater confidence in differentiating targets with clinical value amongst a pool of false positives. For instance, knowledge integration of our proposed biomarkers SNCA, ARG1 and 8-OhDG reveals complex biological relationships. SNCA (α-syn) was shown to increase ARG1 in bone marrow derived macrophages [128], suggesting that SNCA may be responsible for triggering inflammation and immune response. In turn, there is observable increase in 8-OhDG, as interestingly, ARG1 also showed positive correlation with 8-OhDG levels [129]. Hence, via i-omics agreement, there is increased confidence in our proposed biomarkers.

Pathway changes with age, motor severity and medication status agrees with disease progression

Information on the age range, UPDRS III assessment and medication status were used to subset the cohort into younger or older (>67yrs.old for transcriptomics and proteomics, >65 for metabolomics), less or more severe (>UPDRS mean) and not medicated or medicated for further pathway analysis.

When segregated by age, transcriptomics of younger patient cohorts exhibited downregulation in detox and oxidative stress response pathways and upregulation of movement related pathways. Older patient cohorts subsequently exhibited upregulation of *IL6* and inflammation pathways. In terms of proteomics, both young and old cohorts experienced dysregulation of various immune response. Younger cohorts also experienced downregulation of TCA cycle related metabolites.

We divided the cohorts obtained from studies that reported UPDRS III values based on their UPDRS scores (into low: <22 for transcriptomics and proteomics, <18 for metabolomics and high). At low UPDRS III scores, transcriptomic changes mainly involved downregulation of autophagy and upregulation of lipid metabolism related processes which was supported by metabolomic

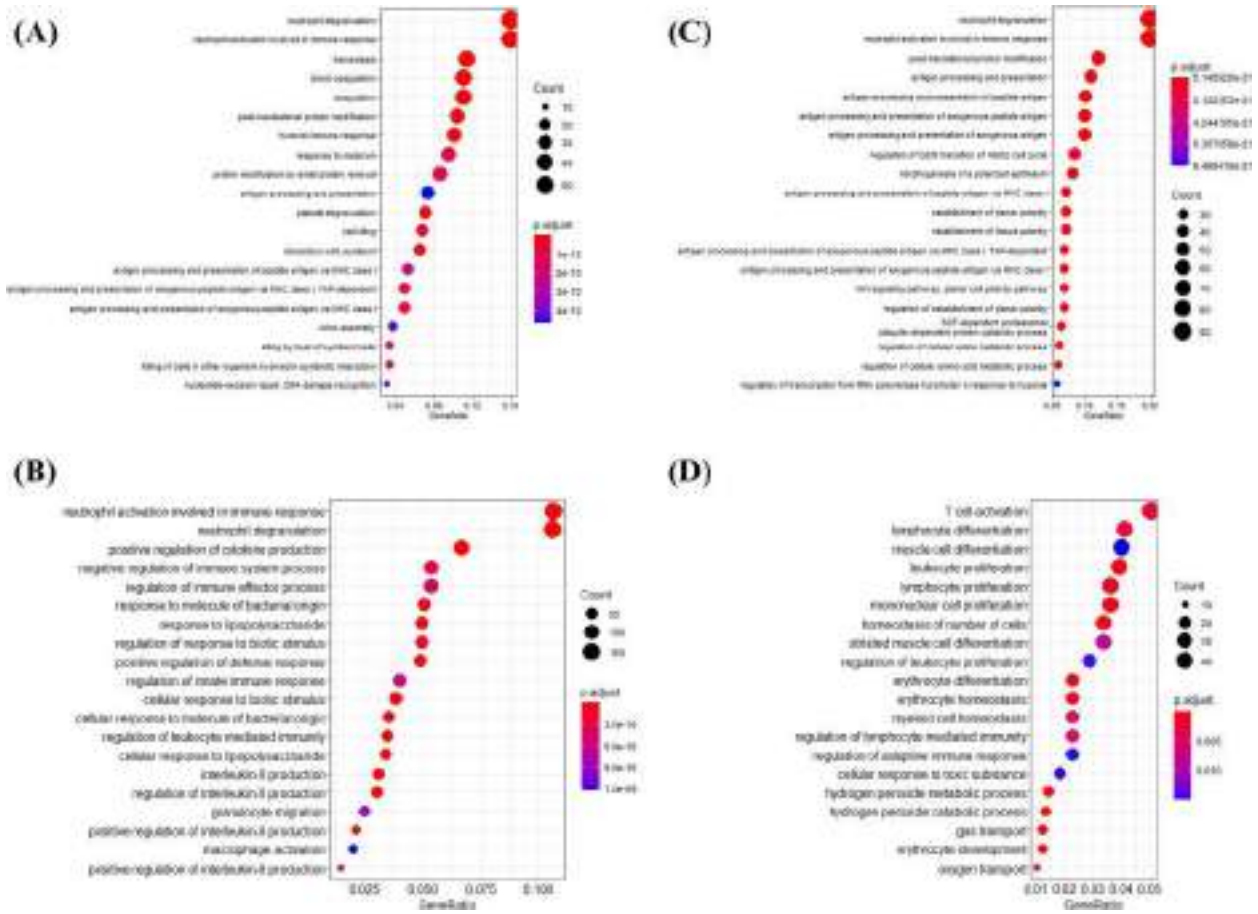

Fig. 2 Gene Ontology (GO) Biological Processes (BP) Pathway Analysis indicates immunological and metabolic implications. **A** GO—BP pathways for compiled upregulated protein list. **B** GO – BP pathways for compiled upregulated transcript list. **C** GO—BP pathways for compiled downregulated protein list. **D** GO – BP pathways for compiled downregulated transcript list

changes involving steroid hormone and fatty acid metabolism. Interestingly, proteomic changes at low UPDRS highlighted downregulation of many pathways involving dopamine uptake and biosynthesis as well as protein stability suggestive that changes start at low UPDRS status which leads to disease progression.

Lastly, the transcriptomics of drug-naïve patient cohorts generally exhibited downregulated ROS processing and upregulated *IL-6* production and inflammation. Downregulated phagocytosis but upregulated defence response to bacterium, killing of symbiont cells and immune responses were observed in proteomics. Metabolically, drug-naïve patient cohorts had downregulated energy production related to citrate cycle and pyruvate, but upregulated arginine and tryptophan metabolism related to inflammation as previously discussed. Interestingly, the drug treated patient cohorts showed some counteracting pathways. When treated, the transcriptomics of medicated patient cohorts had downregulated T cell activation and upregulated regulation of immune responses. Downregulated post translational protein modification and upregulated antigen processing, response to stress and protein removal were observed in proteomics. Metabolically, medicated patients had downregulated biosynthesis of unsaturated fatty acid and upregulated arginine biosynthesis. Taken together, medication had a positive effect on reducing inflammation and regulating protein stress. These pathway changes should however be taken with caution as they were not derived from paired studies of before and after treatment of the same patient but instead via comparison of different cohorts.

Taken together, by comparing age, motor severity and medication status, we observed that older, more severe and unmedicated patient cohorts exhibit dysregulation in energy [130], inflammation [131], lipid [132] and dopamine related pathways [133] which are in agreement with disease progression. A further examination of our 6 proposed biomarkers revealed preferences for different age, motor severity and medication status (Table 6),

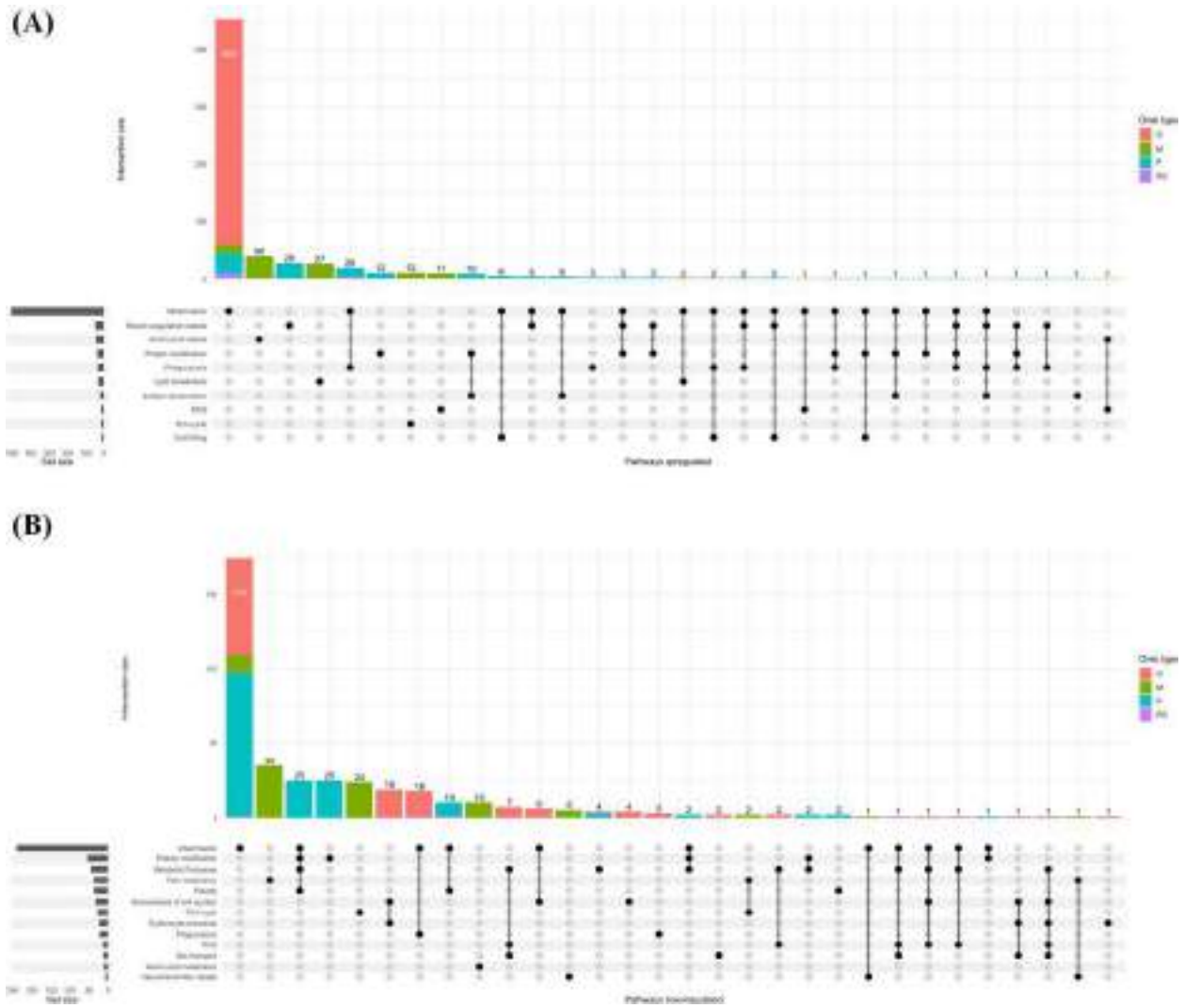

Fig. 3 Upset Plots Reveal Different Pathway Changes Dominated Different Source of Omics Analysis. **A** Upset plot for all pathways upregulated. Inflammation, amino acid metabolism and blood related changes dominated transcriptomics, metabolomics and proteomics respectively. **B** Upset plot for all pathways downregulated. Inflammation, Lipid metabolism and combination of Inflammation, Protein modification, Metabolic processes and polarity dominated transcriptomics, metabolomics and proteomics respectively

with the majority of the biomarkers favouring detection of younger PD patients. In agreement with our findings, previous studies have also identified reduced levels of APOA1 [134, 135] and uric acid [136] to be associated with greater motor severity.

Standardisation of analysis and UPDRS patient staging can improve reproducibility and accuracy of biomarker identification

We observe modest overlap in agreement of targets across studies. However, this is unsurprising since the statistical thresholds, and multiple test corrections used in each independent study differed. We demonstrate this point by comparing the results produced via publicly available database and analytical tools on Gene Expression Omnibus (GEO)

Table 6 Preference for age, UPDRS scoring and medication status of our proposed biomarkers. (-) indicates no information or no preference

UP	***Arg1***	**SNCA**	**8-OHdG**
Age	Younger	Younger	-
UPDRS	-	High	-
Medication	-	No medication	Medication
Down	***SNCA***	**APOA1**	**Uric Acid**
Age	Younger	Older	Younger
UPDRS	-	High [134, 135]	High [136]
Medication	-	Medication	Medication

repository and those reported by the original literature. We analyzed five microarray datasets to detect DEGs in PD patients, including GSE62283, GSE165083, GSE22491, GSE100054, GSE99039 datasets. Using the inbuilt GEO2R function on GEO repository and an intersection analysis (adjpvalue < 0.05, logFC > 1|logFC < -1) for the 5 datasets coded using R, we found that the most upregulated DEGs are CLTCL1, COMMD6, GNS, HGSNAT, LAMP2, LSM 3.00, LSMEM1, MANBA, SCARB2, SDPR, TCIRG1, and TPP1 as appeared twice in those microarray datasets (Table 7), while a lack of overlapping upregulated DEG is detected from the corresponding literature papers (Table 7). The full table of analysis from GEO2R can be found in Supplementary Table 5. Furthermore, the corresponding literature papers suggested BCL2 (using GSE6613 and GSE22491 datasets) [31, 33] and TRAF6 (using GSE99039 and GSE22491 datasets) [30, 31] are the most downregulated DEGs in PD patients, while a lack of overlapping downregulated DEG is identified using GEO2R analysis (Table 7). Interestingly, we found that XIST is more upregulated, and EIF1AY and KDM5D are more downregulated in females than in male PD patients using GSE7475 and GSE100054 datasets (Table 7), but this phenomenon has not been documented thus far. The lack of consistent overlapping DEGs between GEO2R analysis and the corresponding literature papers may be due to non-obvious confounding or batch factors that were known and corrected by the authors but not available in the inbuilt GEO2R function on GEO repository or due to our strict foldchange cut-off. In addition, the lack of overlapping genes seen in RNA sequencing data can also be attributed to the different analysis packages used (ie DESeq2 and edgeR). Dealing with these issues requires good quality meta-data. We therefore propose for more transparency in batch effects and standardisation of analysis pipelines by various studies to enhance reproducibility of results.

Another observation was that studies do not properly synchronize and stage patient severity (or not published) via the universal UPDRS scale (~ 30% among our reviewed papers did not use UPDRS), which makes it difficult to properly find early diagnostic markers. In addition, some papers classified early PD as Hoehn and Yahr stage ≤ 2 [46], while other papers used Hoehn and Yahr stage 1 to 3 [14]. This means that they are not comparing patients at the same time point and given how PD is a progressive disease, it is thus expected that different targets will be reported. Clearly, there is a need for better alignment between researchers and their clinician partners on how patient samples should be categorized and stored. A community-wide standardized framework for characterizing patient's PD status and disease severity using the UPDRS scale with a defined range of scores that distinguishes early PD from advanced PD patients would be useful. We also recommend that researchers use samples from the same PD staging and treatment to minimise confounding factors. This will aid in better comparisons and understanding of omics changes in PD progression.

Future directions: human-microbe i-omics

The gut microbiome is an exciting area to explore for PD given the emerging acceptance of a gut-brain axis in the pathogenesis of sporadic PD [16, 137]. Supporting the hypothesis, gut microbiome alterations have been reported by Toh et al., namely increased *Akkermansia* and reduced *Roseburia* in PD patients [138]. In addition, Sampson et al. also demonstrated that gut microbiome from PD patients can induce enhanced motor deficits when introduced into germ-free mice [139]. With the average 70 kg adult male hosting a total of 39 trillion bacteria in the body, humans are thus considered as supra-organisms and subjected to mutualistic microbiota-host interactions [140]. Microbiomics hence hold great potential to identify new ways to screen risk factors, diagnostic factors and therapeutics to various human diseases [141] such as PD. Future research can focus on studying human-microbe interactions by integrating genomic, proteomic and metabolic analysis, which can lead to some novel and interesting insights.

Concluding remarks

We analysed 79 papers related to transcriptomics, proteomics and metabolomics profile of PD. Individual omics platforms revealed potential in identifying PD blood-based biomarkers with increased reporting rates when grouped by blood subtypes, suggesting that different blood subtypes reflect different expression changes. Our study integrating the different omics datasets have validated SNCA as a potential useful biomarker and suggest

Table 7 GEO2Ranalysis of top transcriptomic hits categorised by blood subtypes

GEO2R Up adjpvalue<0.05 - 5 datasets			GEO2R Up Sex Female VS Male - 2 datasets			GEO2R DOWN adjpvalue<0.05 - 6 datasets			GEO2R DOWN Sex Female VS		
Name	Freq	percentage	Name	Freq	percentage	Name	Freq	percentage	Name	Freq	percentage
CLTCL1	2	40	XIST	2	100	AARD	1	16.7	EIF1AY	2	100
COMMD	2	40	RPL36A-	1	50	ABHD17	1	16.7	KDM5D	2	100
GNS	2	40				ACADL	1	16.7	RPS4Y1	2	100
HGSNAT	2	40				ACBD4	1	16.7	DDX3Y	1	50
LAMP2	2	40				ACTL6B	1	16.7	MALAT1	1	50
LSM 3.00	2	40				ACVRL1	1	16.7	PRKY	1	50
LSMEM	2	40				ADAM2	1	16.7	TXLNGY	1	50
MANBA	2	40				AGAP3	1	16.7	USP9Y	1	50
SCARB2	2	40				AGBL3	1	16.7			
SDPR	2	40				AGTPBP	1	16.7			

Arg1 expression, APOA1 protein level and two metabolites (WB) – 8-OHdG and uric acid could add further value as additional biomarkers. It is also possible that some of these potential biomarkers are more sensitive or specific for certain PD subtypes (tremor dominant, gait disorder etc.) and these should be further validated in future studies. Corroboration of targets from different omics platforms can help overcome the false positives / negatives artefacts from current omics methodologies. Interestingly, when we pool all the genes and proteins together, there is indication of immunological and metabolic implications for pathways associated with PD. Neuroinflammation and metabolic disruption are common themes around the pathogenesis of PD, suggesting that despite the seemingly different biomarkers, i-omics agree in terms of overarching pathways. We also demonstrated how knowledge integration of cross omics findings show that our proposed targets SNCA, ARG1 and 8-OhDG work in the same pathway and increase our confidence in the proposed biomarkers. While current methodologies can yield biomarkers with potential for PD diagnosis, there can be greater transparency by authors in terms of the data cleaning and processing for greater reproducibility. Different data corrections used and thresholds selected for differential expression will naturally lead to different targets reported. Publicly available datasets from some of the 79 papers analysed using tools on GEO database resulted in different sets of targets reported by the literature. Lastly, we suggest that future studies standardise the usage of UPDRS scale and analyse samples from the same PD staging to minimise confounding factors for more accurate biomarkers. We also propose future research to make use of i-omics to gain deeper understanding of PD progression via human-microbe interactions related to the proposed the gut-brain axis in PD, the clarification of which holds promise to reveal prodromal markers for the disease.

Abbreviations

8-OHdG	8-Hydroxy-2′-deoxyguanosine
AAV2-SYN	Adeno-associated virus synuclein
APOA1	Apolipoprotein A1
Arg1	Arginase 1
BCL2	B-cell lymphoma 2
CLTCL1	Clathrin Heavy Chain Like 1
COMMD6	COMM Domain Containing 6
CpG	CG Islands
CSF	Cerebral Spinal Fluid
DEGs	Differentially Expressed Genes
DLG2	Discs Large MAGUK Scaffold Protein 2
DNA	Deoxyribonucleic acid
EIF1AY	Eukaryotic translation initiation factor 1A
EV	Extracellular Vesicle
FAM47E-SCARB2	Family With Sequence Similarity 47 Member E-Scavenger receptor class B member 2
F-DOPA PET	Dopamine Positron Emission Tomography
FGG	Fibrinogen
FYN	Proto-oncogene tyrosine-protein kinase Fyn
GEO	Gene Expression Omnibus
GNS	N-acetylglucosamine-6-sulfatase
GO	Gene Ontology
HGSNAT	Heparan-Alpha-Glucosaminide N-Acetyltransferase
IGKV3-20	Immunoglobulin Kappa Variable 3–20
IL6	Interleukin 6
ITPKB	Inositol-trisphosphate 3-kinase B
KDM5D	Lysine-specific demethylase 5D
LAMP2	Lysosome-associated membrane protein 2
LRRK2	Leucine-rich repeat kinase 2
LSM 3.00	LSM3 Homolog, U6 Small Nuclear RNA And mRNA Degradation Associated
LSMEM1	Leucine Rich Single-Pass Membrane Protein 1
MANBA	Mannosidase Beta
MAPT	Tau
MCCC1	3-Methylcrotonoyl-CoA carboxylase
MHC I	Major Histocompatibility Complex I
MPP + PD	1-Methyl-4-phenylpyridinium induced Parkinson's Disease
mRNAs	Messenger Ribonucleic Acid
PARK16	Parkin
PD	Parkinson's Disease
RIT2	GTP-binding protein Rit2
ROS	Reactive Oxygen Species
SCARB2	Lysosomal integral membrane protein 2
SDPR	Serum deprivation-response protein
SNCA	Alpha-Synuclein
TCIRG1	T cell immune regulator 1
THBD	Thrombomodulin
TPP1	Tripeptidyl-peptidase 1
TRAF6	Tumour necrosis factor receptor associated factor (TRAF) protein
TTR	Transthyretin
UPDRS	Unified Parkinson's Disease Rating Scale
US FDA	United States Food and Drug Administration
VWF	Von Willebrand factor
WB	Whole Blood
XIST	X-inactivation process gene

Supplementary Information

The online version contains supplementary material available at https://doi.org/10.1186/s41231-024-00169-9.

Additional file 1: Table 1. Overall Summary. **Table 2**. Transcriptomics. **Table 3**. Proteomics. **Table 4**. Metabolomics. **Table 5**. Geo2R.

Acknowledgements
This work was supported by grant from the Singapore Ministry of Health Open Fund-Large Collaborative Grant (MOH-OFLCG18May-0002) awarded to K-L.L.

Authors' contributions
Conceptualization: T.J.W.T. and B.W.Y.W.; writing-original draft preparation: T.J.W.T., B.W.Y.W. and E.H.Y.S.; writing-review and editing: T.J.W.T., B.W.Y.W., E.K.T., W.W.B.G. and K.L.L.; visualization, T.J.W.T. and B.W.Y.W.; supervision, E.K.T., W.W.B.G. and K.L.L. All authors have read and agreed to the published version of the manuscript.

Funding
This work was supported by grant from the Singapore Ministry of Health Open Fund-Large Collaborative Grant (MOH-OFLCG18May-0002) awarded to K-L.L.

Availability of data and materials
All data generated or analysed during this study are included in this published article.

Declarations

Ethics approval and consent to participate
Not applicable.

Consent for publication
Not applicable.

Competing interests
The authors declare that they have no competing interests.

Author details
[1]Lee Kong Chian School of Medicine, Nanyang Technological University, 11 Mandalay Road, Singapore 308232, Singapore. [2]School of Biological Sciences, Nanyang Technological University, Singapore, Singapore. [3]Interdisciplinary Graduate Programme (IGP-Neuroscience), Nanyang Technological University, Singapore, Singapore. [4]School of Biomedical Sciences, Faculty of Medicine, Li Ka Shing, The University of Hong Kong, Hong Kong, China. [5]School of Chemical and Biomedical Engineering, Nanyang Technological University, Singapore, Singapore. [6]National Neuroscience Institute, Singapore, Singapore. [7]Center for Biomedical Informatics, Nanyang Technological University, Singapore, Singapore.

Received: 28 December 2023 Accepted: 17 March 2024
Published online: 23 April 2024

References

1. Jankovic J, Tan EK. Parkinson's disease: etiopathogenesis and treatment. J Neurol Neurosurg Psychiatry. 2020;91(8):795–808.
2. Bernheimer H, et al. Brain dopamine and the syndromes of Parkinson and Huntington Clinical, morphological and neurochemical correlations. J Neurol Sci. 1973;20(4):415–55.
3. Marras, C., et al., Prevalence of Parkinson's disease across North America. npj Parkinson's Disease, 2018. 4(1): p. 21.
4. Rees, R.N., et al., An early diagnosis is not the same as a timely diagnosis of Parkinson's disease. F1000Research, 2018. 7: p. F1000 Faculty Rev-1106.
5. Hustad E, Aasly JO. Clinical and Imaging Markers of Prodromal Parkinson's Disease. Front Neurol. 2020;11:395.
6. Regnault A, et al. Does the MDS-UPDRS provide the precision to assess progression in early Parkinson's disease? Learnings from the Parkinson's progression marker initiative cohort. J Neurol. 2019;266(8):1927–36.
7. Holden SK, et al. Progression of MDS-UPDRS Scores Over Five Years in De Novo Parkinson Disease from the Parkinson's Progression Markers Initiative Cohort. Movement Disorders Clinical Practice. 2018;5(1):47–53.
8. Newman EJ, et al. Accuracy of Parkinson's disease diagnosis in 610 general practice patients in the West of Scotland. Mov Disord. 2009;24(16):2379–85.
9. Beach TG, Adler CH. Importance of low diagnostic Accuracy for early Parkinson's disease. Mov Disord. 2018;33(10):1551–4.
10. Pagano G, Niccolini F, Politis M. Imaging in Parkinson's disease. Clin Med (Lond). 2016;16(4):371–5.
11. Loane C, Politis M. Positron emission tomography neuroimaging in Parkinson's disease. American journal of translational research. 2011;3(4):323–41.
12. Heim B, et al. Magnetic resonance imaging for the diagnosis of Parkinson's disease. Journal of neural transmission(Vienna Austria 1996). 2017;124(8):915–64.
13. Parnetti L, et al. CSF and blood biomarkers for Parkinson's disease. The Lancet Neurology. 2019;18(6):573–86.
14. Chang CW, et al. Plasma and Serum Alpha-Synuclein as a Biomarker of Diagnosis in Patients With Parkinson's Disease. Front Neurol. 2020;10:1388.
15. Seol W, Kim H, Son I. Urinary Biomarkers for Neurodegenerative Diseases. Experimental neurobiology. 2020;29(5):325–33.
16. Rietdijk CD, et al. Exploring Braak's Hypothesis of Parkinson's Disease. Front Neurol. 2017;8:37.
17. Parnetti L, et al. Parkinson's and Lewy body dementia CSF biomarkers. Clin Chim Acta. 2019;495:318–25.
18. Redenšek S, Dolžan V, Kunej T. From Genomics to Omics Landscapes of Parkinson's Disease: Revealing the Molecular Mechanisms. OMICS. 2018;22(1):1–16.
19. Vailati-Riboni M, Palombo V, Loor JJ. What are omics sciences? In: Periparturient diseases of dairy cows. Springer; 2017. p. 1–7.
20. Hasin Y, Seldin M, Lusis A. Multi-omics approaches to disease. Genome Biol. 2017;18(1):83.
21. Foo JN, et al. Identification of Risk Loci for Parkinson Disease in Asians and Comparison of Risk Between Asians and Europeans: A Genome-Wide Association Study. JAMA Neurol. 2020;77(6):746–54.
22. Magistrelli L, Contaldi E, Comi C. The Impact of SNCA Variations and Its Product Alpha-Synuclein on Non-Motor Features of Parkinson's Disease. Life (Basel). 2021;11(8):804.
23. Wakabayashi K, et al. The Lewy body in Parkinson's disease and related neurodegenerative disorders. Mol Neurobiol. 2013;47(2):495–508.
24. Cookson MR. LRRK2 Pathways Leading to Neurodegeneration. Curr Neurol Neurosci Rep. 2015;15(7):42–42.
25. Infante J, et al. Comparative blood transcriptome analysis in idiopathic and LRRK2 G2019S–associated Parkinson's disease. Neurobiol Aging. 2016;38:214.e1–214.e5.
26. Infante J, et al. Identification of candidate genes for Parkinson's disease through blood transcriptome analysis in LRRK2-G2019S carriers, idiopathic cases, and controls. Neurobiol Aging. 2015;36(2):1105–9.
27. Craig DW, et al. RNA sequencing of whole blood reveals early alterations in immune cells and gene expression in Parkinson's disease. Nature Aging. 2021;1(8):734–47.
28. Locascio JJ, et al. Association between α-synuclein blood transcripts and early, neuroimaging-supported Parkinson's disease. Brain. 2015;138(Pt 9):2659–71.
29. Wang C, et al. Identification of potential blood biomarkers for Parkinson's disease by gene expression and DNA methylation data integration analysis. Clin Epigenetics. 2019;11(1):24.
30. Shamir R, et al. Analysis of blood-based gene expression in idiopathic Parkinson disease. Neurology. 2017;89(16):1676–83.
31. Mutez E, et al. Transcriptional profile of Parkinson blood mononuclear cells with LRRK2 mutation. Neurobiol Aging. 2011;32(10):1839–48.
32. Mutez E, et al. Involvement of the immune system, endocytosis and EIF2 signaling in both genetically determined and sporadic forms of Parkinson's disease. Neurobiol Dis. 2014;63:165–70.
33. Scherzer CR, et al. Molecular Markers of Early Parkinson's Disease Based on Gene Expression in Blood. Proc Natl Acad Sci USA. 2007;104(3):955–60.
34. Henderson AR, et al. DNA Methylation and Expression Profiles of Whole Blood in Parkinson's Disease. Front Genet. 2021;12:640266.
35. Miki Y, et al. Alteration of autophagy-related proteins in peripheral blood mononuclear cells of patients with Parkinson's disease. Neurobiol Aging. 2018;63:33–43.
36. Calligaris R, et al. Blood transcriptomics of drug-naïve sporadic Parkinson's disease patients. BMC Genomics. 2015;16:876.
37. Li T, et al. Alterations of NURR1 and Cytokines in the Peripheral Blood Mononuclear Cells: Combined Biomarkers for Parkinson's Disease. Front Aging Neurosci. 2018;10:392.
38. Montarolo F, et al. Altered NR4A Subfamily Gene Expression Level in Peripheral Blood of Parkinson's and Alzheimer's Disease Patients. Neurotox Res. 2016;30(3):338–44.
39. Kurvits L, et al. Transcriptomic profiles in Parkinson's disease. Exp Biol Med (Maywood). 2021;246(5):584–95.
40. Jiang F, et al. Identification of potential diagnostic biomarkers for Parkinson's disease. FEBS Open Bio. 2019;9(8):1460–8.
41. Yang Z, et al. Altered Expression Levels of MicroRNA-132 and Nurr1 in Peripheral Blood of Parkinson's Disease: Potential Disease Biomarkers. ACS Chem Neurosci. 2019;10(5):2243–9.
42. DeMarshall CA, et al. Potential utility of autoantibodies as blood-based biomarkers for early detection and diagnosis of Parkinson's disease. Immunol Lett. 2015;168(1):80–8.
43. Shi M, et al. CNS tau efflux via exosomes is likely increased in Parkinson's disease but not in Alzheimer's disease. Alzheimer's Dementia. 2016;12(11):1125–31.
44. Shi M, et al. Plasma exosomal α-synuclein is likely CNS-derived and increased in Parkinson's disease. Acta Neuropathol. 2014;128(5):639–50.
45. Cerri S, et al. The Exosomal/Total α-Synuclein Ratio in Plasma Is Associated With Glucocerebrosidase Activity and Correlates With Measures of Disease Severity in PD Patients. Front Cell Neurosci. 2018;12:125–125.
46. Niu M, et al. A longitudinal study on α-synuclein in plasma neuronal exosomes as a biomarker for Parkinson's disease development and progression. Eur J Neurol. 2020;27(6):967–74.

47. Zou J, et al. Long Noncoding RNA POU3F3 and α-Synuclein in Plasma L1CAM Exosomes Combined with β-Glucocerebrosidase Activity: Potential Predictors of Parkinson's Disease. Neurotherapeutics : the journal of the American Society for Experimental NeuroTherapeutics. 2020;17(3):1104–19.
48. Stuendl A, et al. α-Synuclein in Plasma-Derived Extracellular Vesicles Is a Potential Biomarker of Parkinson's Disease. Mov Disord. 2021;36(11):2508–18.
49. Zhao Z-H, et al. Increased DJ-1 and α-Synuclein in Plasma Neural-Derived Exosomes as Potential Markers for Parkinson's Disease. Frontiers in aging neuroscience. 2019;10:438–438.
50. Leng B, et al. Plasma exosomal prion protein levels are correlated with cognitive decline in PD patients. Neurosci Lett. 2020;723: 134866.
51. Anastasi F, et al. Proteomics Profiling of Neuron-Derived Small Extracellular Vesicles from Human Plasma: Enabling Single-Subject Analysis. Int J Mol Sci. 2021;22(6):2951.
52. Kitamura Y, et al. Proteomic Profiling of Exosomal Proteins for Blood-based Biomarkers in Parkinson's Disease. Neuroscience. 2018;392:121–8.
53. Lamontagne-Proulx J, et al. Portrait of blood-derived extracellular vesicles in patients with Parkinson's disease. Neurobiol Dis. 2019;124:163–75.
54. Agliardi C, et al. Oligomeric α-Syn and SNARE complex proteins in peripheral extracellular vesicles of neural origin are biomarkers for Parkinson's disease. Neurobiol Dis. 2021;148: 105185.
55. Si X, et al. Central Nervous System-Derived Exosomal Alpha-Synuclein in Serum May Be a Biomarker in Parkinson's Disease. Neuroscience. 2019;413:308–16.
56. Picca A, et al. Mitochondrial Signatures in Circulating Extracellular Vesicles of Older Adults with Parkinson's Disease: Results from the EXosomes in PArkiNson's Disease (EXPAND) Study. J Clin Med. 2020;9(2):504.
57. Fu Y, et al. Facile Impedimetric Analysis of Neuronal Exosome Markers in Parkinson's Disease Diagnostics. Anal Chem. 2020;92(20):13647–51.
58. Dutta S, et al. α-Synuclein in blood exosomes immunoprecipitated using neuronal and oligodendroglial markers distinguishes Parkinson's disease from multiple system atrophy. Acta Neuropathol. 2021;142(3):495–511.
59. Jiang C, et al. Serum neuronal exosomes predict and differentiate Parkinson's disease from atypical parkinsonism. J Neurol Neurosurg Psychiatry. 2020;91(7):720–9.
60. Tomlinson PR, et al. Identification of distinct circulating exosomes in Parkinson's disease. Annals of clinical and translational neurology. 2015;2(4):353–61.
61. Jiang R, et al. Differential proteomic analysis of serum exosomes reveals alterations in progression of Parkinson disease. Medicine. 2019;98(41):e17478–e17478.
62. Alberio T, et al. Parkinson's disease plasma biomarkers: An automated literature analysis followed by experimental validation. J Proteomics. 2013;90:107–14.
63. Chen H-M, Lin C-Y, Wang V. Amyloid P component as a plasma marker for Parkinson's disease identified by a proteomic approach. Clin Biochem. 2011;44(5):377–85.
64. Posavi M, et al. Characterization of Parkinson's disease using blood-based biomarkers: A multicohort proteomic analysis. PLoS Med. 2019;16(10): e1002931.
65. Zhao, Y., et al., Plasma proteome profiling using tandem mass tag labeling technology reveals potential biomarkers for Parkinson's disease: a preliminary study. PROTEOMICS – Clinical Applications. n/a(n/a): p. 2100010.
66. O'Bryant SE, et al. Potential two-step proteomic signature for Parkinson's disease: Pilot analysis in the Harvard Biomarkers Study. Alzheimer's & Dementia: Diagnosis, Assessment & Disease Monitoring. 2019;11:374–82.
67. Kang J, et al. Identification of BAG2 and Cathepsin D as Plasma Biomarkers for Parkinson's Disease. Clin Transl Sci. 2021;14(2):606–16.
68. Pan C, et al. Targeted Discovery and Validation of Plasma Biomarkers of Parkinson's Disease. J Proteome Res. 2014;13(11):4535–45.
69. Lin W-C, et al. Linking Stage-Specific Plasma Biomarkers to Gray Matter Atrophy in Parkinson Disease. Am J Neuroradiol. 2021;42(8):1444–51.
70. Goldknopf IL, et al. Abnormal serum concentrations of proteins in Parkinson's disease. Biochem Biophys Res Commun. 2009;389(2):321–7.
71. Lu W, et al. Specific Changes of Serum Proteins in Parkinson's Disease Patients. PLoS ONE. 2014;9(4): e95684.
72. Calvani R, et al. A novel multi-marker discovery approach identifies new serum biomarkers for Parkinson's disease in older people: an EXosomes in PArkiNson Disease (EXPAND) ancillary study. GeroScience. 2020;42(5):1323–34.
73. Daniele S, et al. α-Synuclein Heterocomplexes with β-Amyloid Are Increased in Red Blood Cells of Parkinson's Disease Patients and Correlate with Disease Severity. Front Mol Neurosci. 2018;11:53.
74. Zhao X, et al. Proteome analysis of the sera from Chinese Parkinson's disease patients. Neurosci Lett. 2010;479(2):175–9.
75. Xicoy H, et al. Shared genetic etiology between Parkinson's disease and blood levels of specific lipids. npj Parkinson's Disease. 2021;7(1):23.
76. Bolner A, et al. Plasma and urinary HPLC-ED determination of the ratio of 8-OHdG/2-dG in Parkinson's disease. Clin Lab. 2011;57(11–12):859–66.
77. Saiki S, et al. Decreased long-chain acylcarnitines from insufficient β-oxidation as potential early diagnostic markers for Parkinson's disease. Sci Rep. 2017;7(1):7328.
78. Chang K-H, et al. Alternations of Metabolic Profile and Kynurenine Metabolism in the Plasma of Parkinson's Disease. Mol Neurobiol. 2018;55(8):6319–28.
79. Shao Y, et al. Comprehensive metabolic profiling of Parkinson's disease by liquid chromatography-mass spectrometry. Mol Neurodegener. 2021;16(1):4.
80. Klatt S, et al. A six-metabolite panel as potential blood-based biomarkers for Parkinson's disease. npj Parkinson's Disease. 2021;7(1):94.
81. Pathan M, et al. Plasma Metabolite Markers of Parkinson's Disease and Atypical Parkinsonism. Metabolites. 2021;11(12):860.
82. Stoessel D, et al. Promising Metabolite Profiles in the Plasma and CSF of Early Clinical Parkinson's Disease. Front Aging Neurosci. 2018;10:51.
83. Trupp M, et al. Metabolite and peptide levels in plasma and CSF differentiating healthy controls from patients with newly diagnosed Parkinson's disease. J Parkinsons Dis. 2014;4(3):549–60.
84. Zhao H, et al. Potential biomarkers of Parkinson's disease revealed by plasma metabolic profiling. J Chromatogr B. 2018;1081–1082:101–8.
85. Y.-F. Yao, M.-W.Q., G.-C. Li, F.-B. Zhang, H.-C. Rui, Circulating exosomal miRNAs as diagnostic biomarkers in Parkinson's disease. Eur Rev Med Pharmacol Sci, 2018. 22(16): p. 5278–5283.
86. Bogdanov M, et al. Metabolomic profiling to develop blood biomarkers for Parkinson's disease. Brain. 2008;131(Pt 2):389–96.
87. Campolo J, et al. Antioxidant and inflammatory biomarkers for the identification of prodromal Parkinson's disease. J Neurol Sci. 2016;370:167–72.
88. Wei Z, et al. Oxidative Stress in Parkinson's Disease: A Systematic Review and Meta-Analysis. Front Mol Neurosci. 2018;11:236.
89. Gonzalez-Riano C, et al. rognostic biomarkers of Parkinson's disease in the Spanish EPIC cohort: a multiplatform metabolomics approach. npj Parkinson's Disease. 2021;7(1):73.
90. Johansen KK, et al. Metabolomic profiling in LRRK2-related Parkinson's disease. PLoS ONE. 2009;4(10): e7551.
91. Plewa S, et al. The Metabolomic Approach Reveals the Alteration in Human Serum and Cerebrospinal Fluid Composition in Parkinson's Disease Patients. Pharmaceuticals (Basel). 2021;14(9):935.
92. Picca A, et al. Circulating amino acid signature in older people with Parkinson's disease: A metabolic complement to the EXosomes in PArkiNson Disease (EXPAND) study. Exp Gerontol. 2019;128: 110766.
93. Burté F, et al. metabolic profiling of Parkinson's disease and mild cognitive impairment. Mov Disord. 2017;32(6):927–32.
94. Troisi J, et al. A metabolomic signature of treated and drug-naïve patients with Parkinson's disease: a pilot study. Metabolomics. 2019;15(6):90.
95. Taku H, et al. Identification of novel biomarkers for Parkinson's disease by metabolomic technologies. J Neurol Neurosurg Psychiatry. 2016;87(3):295.
96. Ahmed SSSJ, et al. Metabolic profiling of Parkinson's disease: evidence of biomarker from gene expression analysis and rapid neural network detection. J Biomed Sci. 2009;16(1):63.
97. Roede, J.R., et al., Serum Metabolomics of Slow vs. Rapid Motor Progression Parkinson's Disease: a Pilot Study. PLOS ONE, 2013. 8(10): p. e77629.
98. Zhang J, et al. Targeted fatty acid metabolomics to discover Parkinson's disease associated metabolic alteration. J Mass Spectrom. 2021;56(10): e4781.
99. Barbagallo C, et al. Specific Signatures of Serum miRNAs as Potential Biomarkers to Discriminate Clinically Similar Neurodegenerative and Vascular-Related Diseases. Cell Mol Neurobiol. 2020;40(4):531–46.

100. Chen T, et al. Donepezil Regulates 1-Methyl-4-phenylpyridinium-Induced Microglial Polarization in Parkinson's Disease. ACS Chem Neurosci. 2015;6(10):1708–14.
101. Thome AD, et al. microRNA-155 Regulates Alpha-Synuclein-Induced Inflammatory Responses in Models of Parkinson Disease. J Neurosci. 2016;36(8):2383–90.
102. Guo S, Wang H, Yin Y. Microglia Polarization From M1 to M2 in Neurodegenerative Diseases. Front Aging Neurosci. 2022;14:815347.
103. Kantor B, et al. Downregulation of SNCA Expression by Targeted Editing of DNA Methylation: A Potential Strategy for Precision Therapy in PD. Mol Ther. 2018;26(11):2638–49.
104. Poehler AM, et al. Autophagy modulates SNCA/α-synuclein release, thereby generating a hostile microenvironment. Autophagy. 2014;10(12):2171–92.
105. Qiang JK, et al. Plasma apolipoprotein A1 as a biomarker for Parkinson disease. Ann Neurol. 2013;74(1):119–27.
106. Swanson CR, et al. Lower plasma apolipoprotein A1 levels are found in Parkinson's disease and associate with apolipoprotein A1 genotype. Movement disorders : official journal of the Movement Disorder Society. 2015;30(6):805–12.
107. Deng X, et al. Identifying clinical features and blood biomarkers associated with mild cognitive impairment in Parkinson disease using machine learning. Eur J Neurol. 2023;30(6):1658–66.
108. Sato S, Mizuno Y, Hattori N. Urinary 8-hydroxydeoxyguanosine levels as a biomarker for progression of Parkinson disease. Neurology. 2005;64(6):1081–3.
109. Kikuchi Y, et al. Urinary 8-OHdG elevations in a partial lesion rat model of Parkinson's disease correlate with behavioral symptoms and nigrostriatal dopaminergic depletion. J Cell Physiol. 2011;226(5):1390–8.
110. Goh WWB, Wong L. Dealing with Confounders in Omics Analysis. Trends Biotechnol. 2018;36(5):488–98.
111. Love MI, Huber W, Anders S. Moderated estimation of fold change and dispersion for RNA-seq data with DESeq2. Genome Biol. 2014;15(12):550.
112. Law, C.W., et al., RNA-seq analysis is easy as 1–2–3 with limma, Glimma and edgeR. F1000Research, 2016. 5: p. ISCB Comm J-1408.
113. Chandramouli K, Qian P-Y. Proteomics: challenges, techniques and possibilities to overcome biological sample complexity. Human genomics and proteomics : HGP. 2009;2009: 239204.
114. Bellei E, et al. High-abundance proteins depletion for serum proteomic analysis: concomitant removal of non-targeted proteins. Amino Acids. 2011;40(1):145–56.
115. Lista S, Faltraco F, Hampel H. Biological and methodical challenges of blood-based proteomics in the field of neurological research. Prog Neurobiol. 2013;101–102:18–34.
116. Tammen H. Specimen collection and handling. In: Clinical Proteomics. Springer; 2008. p. 35–42.
117. Timms JF, et al. Preanalytic influence of sample handling on SELDI-TOF serum protein profiles. Clin Chem. 2007;53(4):645–56.
118. Fournier ML, et al. Delayed correlation of mRNA and protein expression in rapamycin-treated cells and a role for Ggc1 in cellular sensitivity to rapamycin. Molecular & cellular proteomics : MCP. 2010;9(2):271–84.
119. Fury, W., et al. Overlapping Probabilities of Top Ranking Gene Lists, Hypergeometric Distribution, and Stringency of Gene Selection Criterion. in 2006 International Conference of the IEEE Engineering in Medicine and Biology Society. 2006.
120. Breschi A, Gingeras TR, Guigó R. Comparative transcriptomics in human and mouse. Nat Rev Genet. 2017;18(7):425–40.
121. Huang da W, Sherman BT, Lempicki RA. ystematic and integrative analysis of large gene lists using DAVID bioinformatics resources. Nat Protoc. 2009;4(1):44–57.
122. Fielding CA, et al. IL-6 regulates neutrophil trafficking during acute inflammation via STAT3. J Immunol. 2008;181(3):2189–95.
123. Peng, Z., et al., Association Between Metabolic Syndrome and Mild Parkinsonian Signs Progression in the Elderly. Frontiers in Aging Neuroscience, 2021. 13.
124. Pang, Z., et al., MetaboAnalyst 5.0: narrowing the gap between raw spectra and functional insights. Nucleic Acids Research, 2021. 49(W1): p. W388-W396.
125. Chen S-F, et al. Arginine is neuroprotective through suppressing HIF-1α/LDHA-mediated inflammatory response after cerebral ischemia/reperfusion injury. Mol Brain. 2020;13(1):63.
126. Melo HM, Santos LE, Ferreira ST. Diet-Derived Fatty Acids, Brain Inflammation, and Mental Health. Front Neurosci. 2019;13:265.
127. Smeyne M, Smeyne RJ. Glutathione metabolism and Parkinson's disease. Free Radical Biol Med. 2013;62:13–25.
128. Alam MM, et al. Alpha synuclein, the culprit in Parkinson disease, is required for normal immune function. Cell Rep. 2022;38(2): 110090.
129. Ogino K, et al. Evaluation of serum arginase I as an oxidative stress biomarker in a healthy Japanese population using a newly established ELISA. Clin Biochem. 2013;46(16–17):1717–22.
130. Halliwell B. Oxidative stress and neurodegeneration: where are we now? J Neurochem. 2006;97(6):1634–58.
131. Stone DK, et al. Innate and adaptive immunity for the pathobiology of Parkinson's disease. Antioxid Redox Signal. 2009;11(9):2151–66.
132. Dixon SJ, et al. Ferroptosis: an iron-dependent form of nonapoptotic cell death. cell. 2012;149(5):1060–72.
133. Dong-Chen X, et al. Signaling pathways in Parkinson's disease: molecular mechanisms and therapeutic interventions. Signal Transduct Target Ther. 2023;8(1):73.
134. Swanson CR, et al. Plasma apolipoprotein A1 associates with age at onset and motor severity in early Parkinson's disease patients. Mov Disord. 2015;30(12):1648–56.
135. Deng X, et al. Biomarker characterization of clinical subtypes of Parkinson Disease. NPJ Parkinsons Dis. 2022;8(1):109.
136. Dănău A, et al. Serum Uric Acid Levels in Parkinson's Disease: A Cross-Sectional Electronic Medical Record Database Study from a Tertiary Referral Centre in Romania. Medicina (Kaunas). 2022;58(2):245.
137. Del Tredici K, Braak H. Sporadic Parkinson's disease: development and distribution of α-synuclein pathology. Neuropathol Appl Neurobiol. 2016;42(1):33–50.
138. Toh TS, et al. Gut microbiome in Parkinson's disease: New insights from meta-analysis. Parkinsonism Relat Disord. 2022;94:1–9.
139. Sampson TR, et al. Gut Microbiota Regulate Motor Deficits and Neuroinflammation in a Model of Parkinson's Disease. Cell. 2016;167(6):1469–1480.e12.
140. Sender R, Fuchs S, Milo R. Revised Estimates for the Number of Human and Bacteria Cells in the Body. PLoS Biol. 2016;14(8):e1002533–e1002533.
141. Turnbaugh PJ, et al. The Human Microbiome Project. Nature. 2007;449(7164):804–10.

Publisher's Note

ESC European Society of Cardiology

European Heart Journal - Cardiovascular Imaging (2024) **00**, 1–11
https://doi.org/10.1093/ehjci/jeae260

ORIGINAL PAPER

Myocardial disarray and fibrosis across hypertrophic cardiomyopathy stages associate with ECG markers of arrhythmic risk

Z. Ashkir [1†], A.H.A. Samat[1,2†], R. Ariga[1], L.E.M. Finnigan[1], S. Jermy[3], M.A. Akhtar[1], G. Sarto[1], P. Murthy[1], B.W.Y. Wong[1], M.P. Cassar[1], N. Beyhoff[1], E.C. Wicks[4], K. Thomson[5], M. Mahmod [1], E.M. Tunnicliffe[1], S. Neubauer [1], H. Watkins[5], and B. Raman [1*]

[1]Oxford Centre for Clinical Magnetic Resonance Research (OCMR), University of Oxford, Oxford OX3 9DU, UK; [2]Faculty of Medicine, Department of Emergency Medicine, Hospital Canselor Tuanku Muhriz, Universiti Kebangsaan Malaysia, Kuala Lumpur, Malaysia; [3]Faculty of Health Sciences, Cape Universities Body Imaging Centre (CUBIC), University of Cape Town, South Africa; [4]Inherited Cardiac Conditions (ICC) Service, Oxford University Hospitals NHS Foundation Trust, Oxford, UK; and [5]Division of Cardiovascular Medicine, Radcliffe Department of Medicine, University of Oxford, Oxford, UK

Received 25 August 2024; revised 24 September 2024; accepted 26 September 2024; online publish-ahead-of-print 17 October 2024

Aims Myocardial disarray, an early feature of hypertrophic cardiomyopathy (HCM) and a substrate for ventricular arrhythmia, is poorly characterized in pre-hypertrophic sarcomeric variant carriers (SARC+LVH−). Using diffusion tensor cardiac magnetic resonance (DT-CMR) we assessed myocardial disarray and fibrosis in both SARC+LVH− and HCM patients and evaluated the relationship between microstructural alterations and electrocardiographic (ECG) parameters associated with arrhythmic risk.

Methods and results Sixty-two individuals (24 SARC+LVH−, 24 HCM, and 14 matched controls) were evaluated with multi-parametric CMR including stimulated echo acquisition mode DT-CMR, and blinded quantitative 12-lead ECG analysis. Mean diastolic fractional anisotropy (FA) was reduced in HCM compared with SARC+LVH− and controls (0.49 ± 0.05 vs. 0.52 ± 0.04 vs. 0.53 ± 0.04, $P = 0.009$), even after adjustment for differences in extracellular volume (ECV) ($P = 0.038$). Both HCM and SARC+LVH− had segments with significantly reduced diastolic FA relative to controls (54 vs. 25 vs. 0%, $P = 0.002$). Multiple repolarization parameters were prolonged in HCM and SARC+LVH−, with corrected JT interval (JTc) being most significant (354 ± 42 vs. 356 ± 26 vs. 314 ± 26 ms, $P = 0.002$). Among SARC+LVH−, JTc duration correlated negatively with mean diastolic FA ($r = -0.6$, $P = 0.002$). In HCM, the JTc interval showed a stronger association with ECV ($r = 0.6$ $P = 0.019$) than with mean diastolic FA ($r = -0.1$ $P = 0.72$). JTc discriminated SARC+LVH− from controls [area under the receiver operator curve 0.88, confidence interval 0.76–1.00, $P < 0.001$], and in HCM correlated with the European Society of Cardiology HCM sudden cardiac death risk score ($r = 0.5$, $P = 0.014$).

Conclusion Low diastolic FA, suggestive of myocardial disarray, is present in both SARC+LVH− and HCM. Low FA and raised ECV were associated with repolarization prolongation. Myocardial disarray assessment using DT-CMR and repolarization parameters such as the JTc interval demonstrate significant potential as markers of disease activity in HCM.

* Corresponding author. E-mail: betty.raman@cardiov.ox.ac.uk
† Joint first authors.

Structured Graphical Abstract

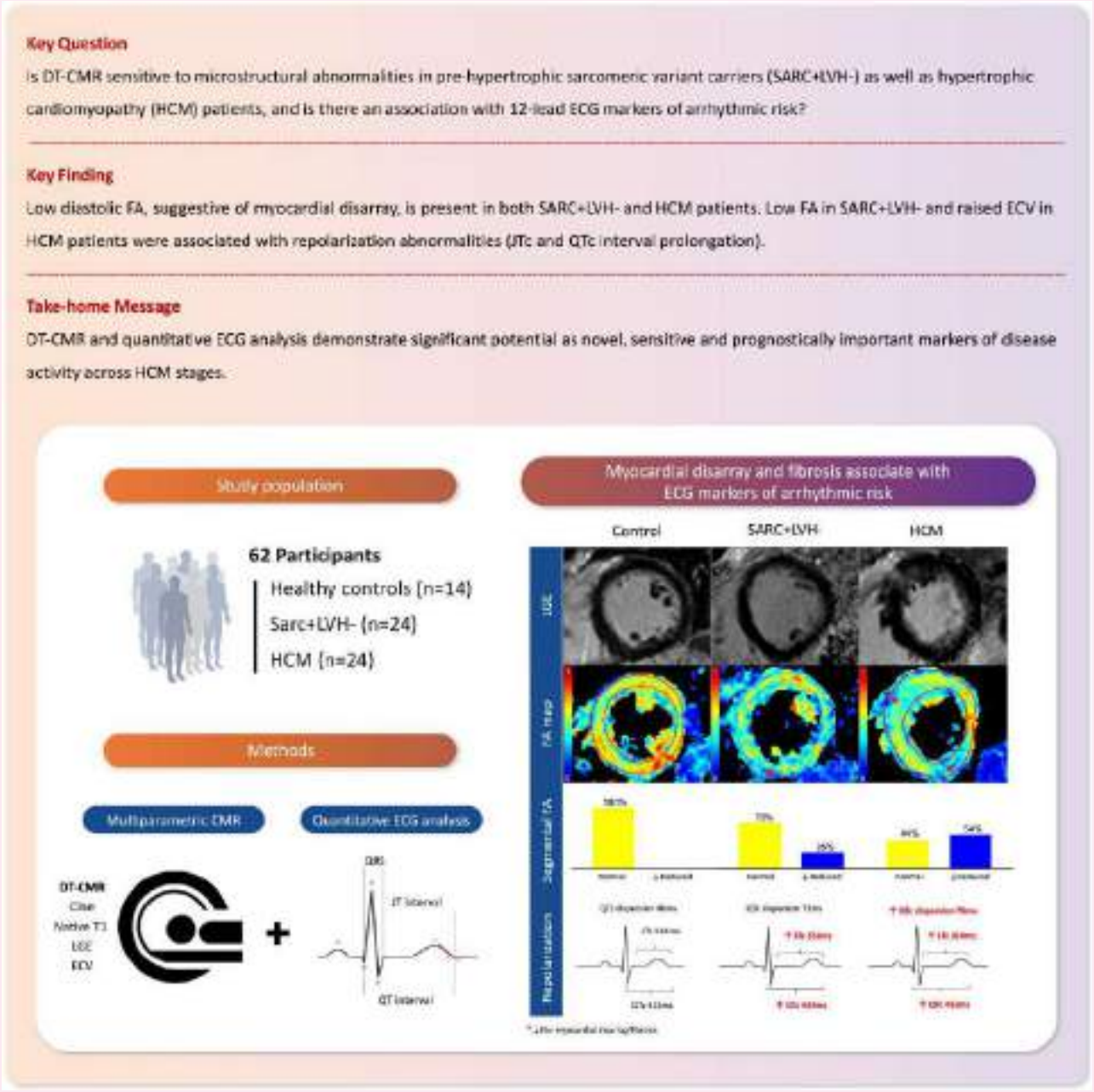

Keywords hypertrophic cardiomyopathy • sarcomere • cardiac magnetic resonance imaging • arrhythmia • sudden cardiac death • repolarization • ECG

Introduction

Myocardial disarray, a hallmark feature of hypertrophic cardiomyopathy (HCM) is an important substrate for ventricular arrhythmia. It is known that myocardial disarray can develop before the onset of hypertrophy in patients,[1,2] with emerging evidence indicating its presence even in pre-natal animal models.[3] Despite this, myocardial disarray remains poorly characterized in pre-hypertrophic sarcomeric variant carriers (SARC+LVH−), and the mechanisms by which it predisposes to ventricular arrhythmia are yet to be fully elucidated.

Several studies have explored the electrophysiological disruption caused by myocardial disarray, specifically with regards to myocardial conduction and action potential propagation.[4–6] Changes in fibre orientation and gap junction distribution are thought to lead to regional variations in conduction velocity and alterations in conduction pathways. These alterations in turn lead to myocardial repolarization heterogeneity, thereby facilitating an environment vulnerable to re-entrant arrhythmia.

Diffusion tensor cardiac magnetic resonance (DT-CMR) imaging has now made it possible to non-invasively estimate the burden of myocardial disarray. By tracking the directionality and magnitude of water

diffusion through myocardial tissue, DT-CMR enables voxel-wise assessment of myocardial microstructure. Two key DT-CMR parameters; fractional anisotropy (FA) and mean diffusivity (MD) are sensitive to microstructural alterations caused by myocardial disarray and fibrosis.[7–9] FA is a scalar value of the directionality in diffusion of water molecules (with 1 representing perfect alignment or 'isotropy', and 0 complete disorganisation or 'anisotropy'), and MD measures the magnitude of water diffusion (which increases with greater disruption of myocardial architecture). In recent years, our group and others have demonstrated that HCM patients exhibit reduced FA, even after adjustment for fibrosis and indicative of myocardial disarray.[7,10,11] We also showed that low FA independently associated with ventricular arrhythmia, suggesting a possible link between the extent of myocardial disarray and arrhythmic events.

Although DT-CMR is promising, its current status remains within the research domain, with limited clinical applicability. This is partly due to the need for complex hardware, software and expertise to interpret the data. In contrast, surface 12-lead electrocardiography (ECG) is a well-established and universally adopted clinical and diagnostic screening tool used in the management of both SARC+LVH− and overt HCM patients. Abnormalities in repolarization on ECG have long been associated with ventricular arrhythmia and sudden cardiac death (SCD) in HCM,[12–16] and as with myocardial disarray, have been shown to precede hypertrophy.[17,18] We hypothesize that myocardial disarray may influence repolarization parameter duration and heterogeneity on 12-lead ECG, including in SARC+LVH− patients. Establishing a relationship between myocardial disarray burden and ECG alterations could be of significant clinical value and provide mechanistic insight into the role of microstructural changes in HCM in arrhythmogenesis.

In this study, we aimed to characterize the extent of myocardial disarray in SARC+LVH− and HCM patients relative to healthy controls using DT-CMR. We additionally probed the relationship between myocardial disarray burden and ventricular repolarization using quantitative ECG analysis.

Methods

Study population

Twenty-four pre-hypertrophic (pathogenic or likely pathogenic) sarcomeric variant carriers (SARC+LVH−), 24 patients with HCM, and 14 age and gender-matched controls were included this study. SARC+LVH− and HCM patients were recruited from the inherited cardiac conditions service at the John Radcliffe Hospital, Oxford, UK. All SARC+LVH− and HCM patients underwent genetic testing to establish presence/absence of pathogenic and likely pathogenic sarcomeric variants (Sarc+ status) by the Oxford Medical Genetics Laboratory. Patients who tested positive for variants in genes associated with HCM phenocopies, e.g. TTR (amyloidosis) or GLA (Fabry disease) were excluded, as were cases with variants of uncertain significance. SARC+LVH− patients and healthy controls had confirmed left ventricular (LV) wall thickness < 13 mm, and HCM patients ≥ 15 mm (or ≥ 13 mm in case of positive family history/genetic test) on CMR. HCM patients with significant resting outflow tract obstruction (LV outflow tract gradient ≥ 50 mm Hg based on echocardiographic assessment) were excluded. Any participants who had past medical history of significant cardiac disease including severe hypertension (HTN), moderate/severe valvular dysfunction or ischaemic heart disease, and those with contraindications to CMR scanning were also excluded. The study was approved by the National Research Ethics Committee (REC ref 12/LO/1979). All participants provided written informed consent.

CMR protocol

CMR scans were performed using a 3T Siemens Trio scanner (Siemens Healthineers, Erlangen, Germany). The standard protocol included cine imaging, DT-CMR, pre- and post-contrast T1 mapping using a Shortened Modified Look-Locker Inversion recovery (ShMOLLI) sequence,[19] and late gadolinium enhancement (LGE) imaging.

DT-CMR was performed using a previously described stimulated echo acquisition mode (STEAM) sequence[7] to obtain a single mid-ventricular short axis slice at the diastolic pause. The same mid-ventricular slice position was used during pre- and post-contrast T1 acquisitions to obtain native T1 and extracellular volume (ECV) mapping.

CMR analysis

LV volumetric, functional, and fibrosis analysis was performed using cvi42 (Circle Cardiovascular Imaging, Calgary, Canada). Focal fibrosis was estimated from the extent of enhanced myocardial pixels (defined as signal intensity > 5 standard deviations (SDs) above a normal reference region of interest[20]). Significant LGE burden was defined as $> 15\%$ of LV mass based on increased risk of adverse clinical events.[20,21] DT-CMR data underwent rigorous quality control by two experienced observers (EMT, RA). No case required repeat MRI acquisition. DT-CMR post-processing was performed using a custom-built in-house software developed using MATLAB (MathWorks, MA, USA)[7] to obtain mean slice and segmental diastolic FA, mean slice and segmental MD, as well as helix angle gradient (HA, a measure of the helical arrangement of cardiomyocytes) and absolute diastolic sheetlet normal angles (SA, a measure of myocardial sheetlet orientation). Strain correction was not attempted due to the questionable validity of assuming that microscopic myocyte strain is accurately represented by macroscopic myocardial strain.[22] Previous work has shown that MD is strain-dependent, but that diastolic FA appears largely unaffected by strain.[23] All segmental analysis was performed using the standard American Heart Association (AHA) 16-segment model.

ECG analysis

Participants underwent standard 12-lead resting digital ECG using the CARDIOVIT FT-1 Schiller ECG system (Baar, Switzerland). Standard measurements of ECG axes, amplitudes and intervals were obtained for all leads from the ECG reports. Two independent ECG analysts (AHAS and MA), both senior physicians who were blinded to clinical data, interpreted the ECG according to the Minnesota Code of Electrocardiographic findings.[15] Specific ECG intervals were manually analysed using Adobe Acrobat Pro DC (version 2022.001.20085). Each digitized ECG was magnified to 400% for optimum resolution. Parameters measured included: the QT interval duration (ventricular depolarization and repolarization), QT dispersion (repolarization homogeneity), QTP (ventricular depolarization and repolarization), QTP dispersion (repolarization homogeneity), and JT interval duration (ventricular repolarization). The terminal end of the T wave was determined using the tangent method, defined as the intersection between the isoelectric line and the line drawn along the steepest angle of the descending arm of the T wave.[16] This technique has previously been used by our group to study associations between quantitative ECG parameters and multi-parametric CMR data.[24] Heart rate-corrected intervals were generated using the Bazett's formula [Corrected QT interval (QTc) $= QT/\sqrt{R-R}$ interval in second]. The inter-rater correlation coefficient between the two observers for corrected QT (QTc) and JT interval (JTc) were 0.88 and 0.86, respectively.

Statistical analysis

Statistical analyses were performed using SPSS Version 27.0 (IBM, Armonk, NY, USA). Normality was determined using the Kolmogorov–Smirnov test. Parametric continuous variables were presented as mean ± standard deviation (SD), and non-parametric variables as median with inter-quartile range (IQR). Categorical data were described using frequency and percentages. Difference between cohorts was assessed using either the independent Student's *t*-test or Mann–Whitney *U* test and Kruskal–Wallis test or ANOVA (with *post hoc* Bonferroni correction) as appropriate.

Associations between categorical variables were determined using the χ^2 test for independence or the Fischer's exact test. Correlation between continuous variables were analysed using Pearson's correlation coefficient (r) for parametric data and Spearman's rank correlation coefficient (rho) for non-parametric data. Linear regression using analysis of covariance (ANCOVA) with Bonferroni correction for multiple comparisons was performed to account for potential confounders. Associations between continuous variables derived from regression models were expressed as standardized β coefficients. Statistical significance was set at $P < 0.05$.

Results

Study population baseline characteristics

Demographic and clinical data are shown in Table 1. All three groups had comparable gender proportions, mean age, body mass index (BMI), and resting heart rate. The majority of HCM patients (79%) were on either beta blockers or (non-dihydropyridine) calcium channel blockers, with four patients also on concurrent low dose disopyramide. Two-thirds (18/24) of HCM patients possessed pathogenic sarcomeric variants (SARC+HCM). HCM patients had greater LV maximum wall thickness (MWT) compared with SARC+LVH− and controls, as well as greater LV ejection fraction, greater LV mass index and left atrial diameter. Pathological LGE was only present in HCM patients, where it was visually apparent in 41% of cases, however only a fraction (13%) had significant LGE burden (≥ 15% of LV mass). Native T1 was raised in HCM and SARC+LVH− patients compared with controls (1208 ± 35 vs. 1196 ± 22 vs. 1175 ± 17 ms, respectively, $P = 0.003$). ECV was also raised in HCM relative to SARC+LVH− patients and controls (30 ± 3 vs. 28 ± 2 vs. 27 ± 2%, $P = 0.039$). HCM patients with pathogenic or likely pathogenic variants (SARC+HCM) had lower LVEF and greater LGE burden than the SARC-HCM sub-group (see Supplementary data online, *Table S1*). In both SARC+HCM and SARC+LVH− patients approximately two-thirds of likely pathogenic/pathogenic variants were in the MYBPC3 gene, with the remainder involving MYH7, apart from a single Troponin I case in the SARC+HCM group.

DT-CMR parameters in SARC+LVH−, HCM, and control subjects

Mean diastolic FA was lower in HCM patients compared with both SARC+LVH− patients and healthy controls [0.49 ± 0.05 vs. 0.52 ± 0.04 vs. 0.53 ± 0.04, $P = 0.009$ (Table 1 and *Figure 1A*)], including after adjustment for ECV ($P = 0.038$). Even in patients where visible replacement fibrosis was absent (i.e. no LGE) in the myocardium, HCM patients exhibited lower mean diastolic FA relative to SARC+LVH− and healthy controls (see Supplementary data online, *Figure S1*). At a segmental level, 6/24 (25%) SARC+LVH− patients had segments with significantly reduced FA (defined as < 2 SD below control mean). A higher proportion of overt HCM 13/24 (54%) patients had abnormal

Table 1 Baseline demographic and clinical parameters

	Controls (14)	SARC+LVH (24)	HCM (24)	Sarc+LVH− vs. controls *P*-value	HCM vs. controls *P*-value	3-way comparison *P*-value
Demographics						
Male *n* (%)	11 (79)	13 (54)	18 (75)	0.132	0.803	0.187
Age	32 ± 8	32 ± 9	36 ± 11	0.859	0.234	0.322
BMI	23 ± 3	24 ± 4	26 ± 4	0.288	0.013	0.050
Hazard ratio (HR)	61 ± 13	63 ± 7	60 ± 10	0.454	0.386	0.463
HTN *n* (%)	0	0	4 (17%)		0.033	
Anti-arrhythmic therapy	0	3 (13)	19 (79)	0.283	< 0.001	< 0.001
ESC SCD risk score			3.3 ± 1.9%			
CMR findings						
LV MWT (mm)	11 ± 1	10 ± 1	22 ± 5	0.145	< 0.001	< 0.001
LV EDVI (mL/m^2)	90 ± 17	83 ± 15	81 ± 9	0.216	0.046	0.157
LV EF (%)	66 ± 6	67 ± 6	76 ± 5	0.776	< 0.001	< 0.001
LV mass index (g/m^2)	56 ± 13	51 ± 13	73 ± 20	0.289	0.010	< 0.001
LA diameter (mm)	31 ± 7	32 ± 6	37 ± 6	0.805	0.002	< 0.001
LGE present *n* (%)			10 (41)			
LGE > 15% of LV mass *n* (%)			3 (13)			
Native T1 (ms)	1175 ± 17	1197 ± 22	1208 ± 35	0.052	0.002	0.003
ECV (%)	27 ± 2	28 ± 2	30 ± 3	0.076	0.014	0.039
Mean diastolic FA	0.53 ± 0.04	0.52 ± 0.04	0.49 ± 0.05	0.535	0.009	0.009
Low segmental FA *n* (%)	0	6 (25)	13 (54)	0.041	< 0.001	0.002
Mean MD (× 10^{-3} mm^2/s)	1.20 ± 0.08	1.28 ± 0.08	1.30 ± 0.10	0.006	0.005	0.007
SA (°)	69 ± 7	59 ± 14	47 ± 10	0.031	< 0.001	< 0.001
HA (°/mm)	8 ± 2	7 ± 3	7 ± 1	0.061	0.076	0.087

Values are mean ± SD or *n* (%).
EDVI, end diastolic volume index; EF, ejection fraction; LA, left atrial; LVOT, left ventricular outflow tract.

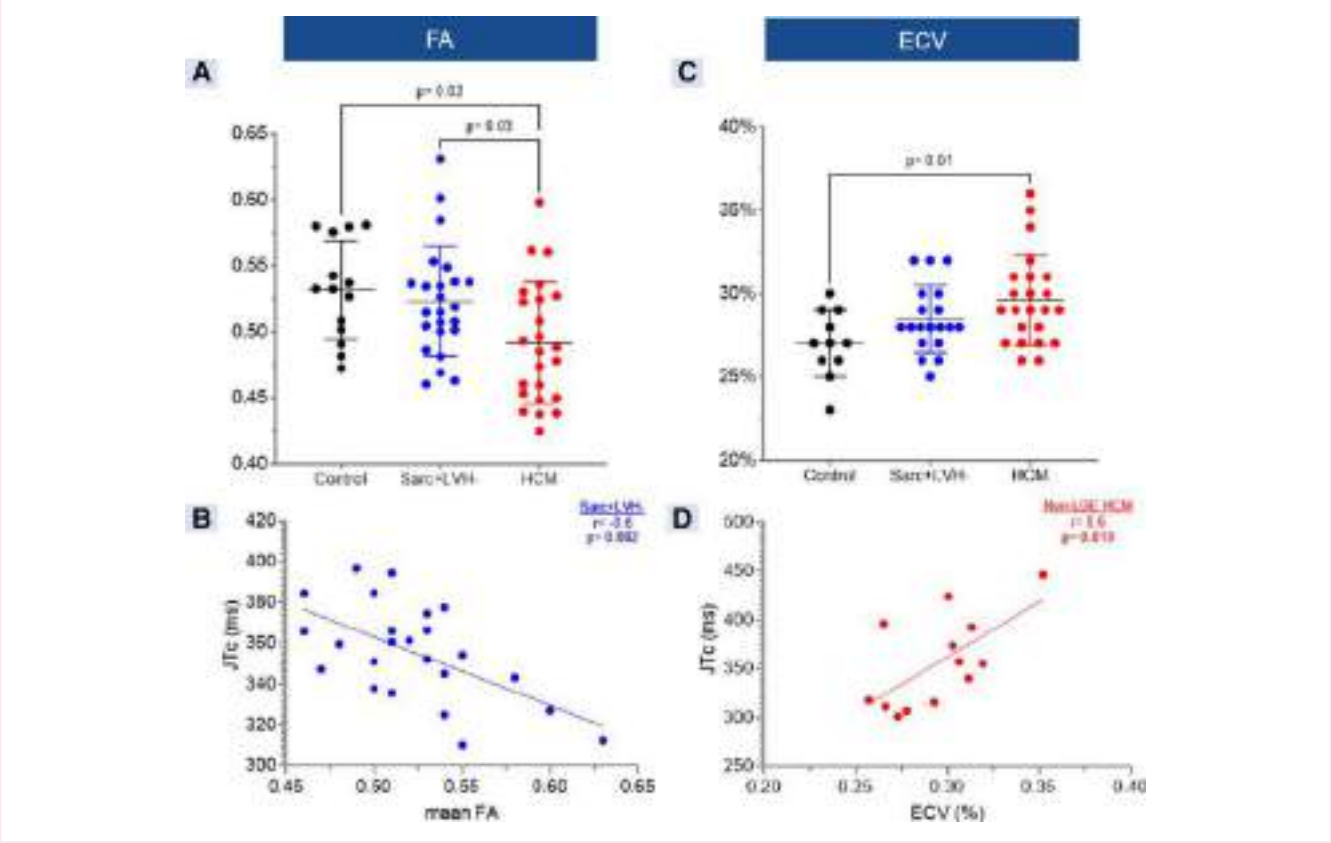

Figure 1 Mean diastolic FA and ECV correlation with JTc interval in SARC+LVH– and HCM. (*A*) Mean diastolic FA across groups. (*B*) Correlation between mean diastolic FA and JTc duration in pre-hypertrophic variant carriers. (*C*) Mean ECV across groups. (*D*) Correlation between mean ECV and JTc duration in HCM patients. ECV, extracellular volume; FA, fractional anisotropy; JTc, J point → T wave tangential line, corrected for heart rate; HCM, hypertrophic cardiomyopathy; SARC+LVH, pre-hypertrophic sarcomeric variant carriers.

segmental FA (*Figure 2*), both in patients with and without LGE (80 and 36%, respectively). There was no specific pattern in the location of low FA segments within the SARC+LVH– cohort, but in the overt HCM group abnormal segments were concentrated in the anteroseptum.

In SARC+LVH–, low segmental FA was not accompanied by raised segmental ECV in most cases (5/6 cases). In the HCM cohort, 5/13 (38%) of low FA segments did not have significantly raised ECV. There was no significant difference in mean or segmental FA in HCM patients according to sarcomeric status (see Supplementary data online, *Table S1*).

Mean MD was raised in both HCM patients (including those without LGE) and SARC+LVH– relative to healthy controls (1.30 ± 0.1 vs. 1.28 ± 0.08 vs. 1.20 ± 0.08, $P = 0.007$; Table 1. Given that impaired myocardial strain is associated with lower MD on STEAM DT-CMR,[23] we evaluated if diastolic myocardial strain was also abnormal in SARC+LVH– and HCM patients. Only HCM patients, but not SARC+LVH–, had impaired global longitudinal and circumferential diastolic strain (see Supplementary data online, *Table S2*). Despite adjusting for diastolic strain, MD was still raised in HCM patients relative to controls ($P = 0.02$).

In terms of secondary DT-CMR parameters, we noted an increase in diastolic absolute SA between HCM and controls (circular mean 47 ± 10° vs. 59 ± 14° vs. 69 ± 7°, $P < 0.001$) indicating more radially orientated sheetlet populations in the HCM patients, compared with both SARC+LVH– and controls. There was no significant difference in HA between groups. Mean diastolic FA correlated with LV wall thickness ($r = -0.352$, $P = 0.005$), LV mass ($r = -0.381$, $P = 0.002$) and LGE mass ($r = -0.497$, $P < 0.001$).

ECG parameters in SARC+LVH–, HCM, and control subjects

ECG characteristics are depicted in Table 2. PR interval and ventricular depolarization (QRS) durations were comparable between groups. In contrast, a significant higher frequency of qualitative ST/T wave abnormalities and prolongation of most repolarization parameters were observed in SARC+LVH– and overt HCM patients relative to healthy controls. In terms of quantitative parameters, QTc, QTPc, and JTc durations were prolonged in both SARC+LVH– and HCM cases relative to healthy controls, as was QTc dispersion, which was significantly longer in HCM patients compared with controls. The prolongation of these parameters was evident in SARC+LVH– and HCM patients even in the absence of regular anti-arrhythmic or QT prolonging medication use (see Supplementary data online, *Table S3*). There was no significant sex difference in any of the repolarization parameters within this cohort, and an increase in repolarization parameter durations was also observed in SARC+LVH– and HCM patients relative to healthy controls when sexes were analysed separately (see Supplementary data online, *Tables S4 and S5*). *Figure 3* shows scatter plots displaying differences in QTc interval, QTc dispersion, and JTc interval across the three groups.

Within the HCM group, patients with pathogenic sarcomeric variants tended to have longer repolarization parameters than those without. As a result, a more pronounced stepwise prolongation of repolarization parameters was evident between healthy controls, SARC+LVH– and SARC+HCM patients (Table 3). The clearest increase

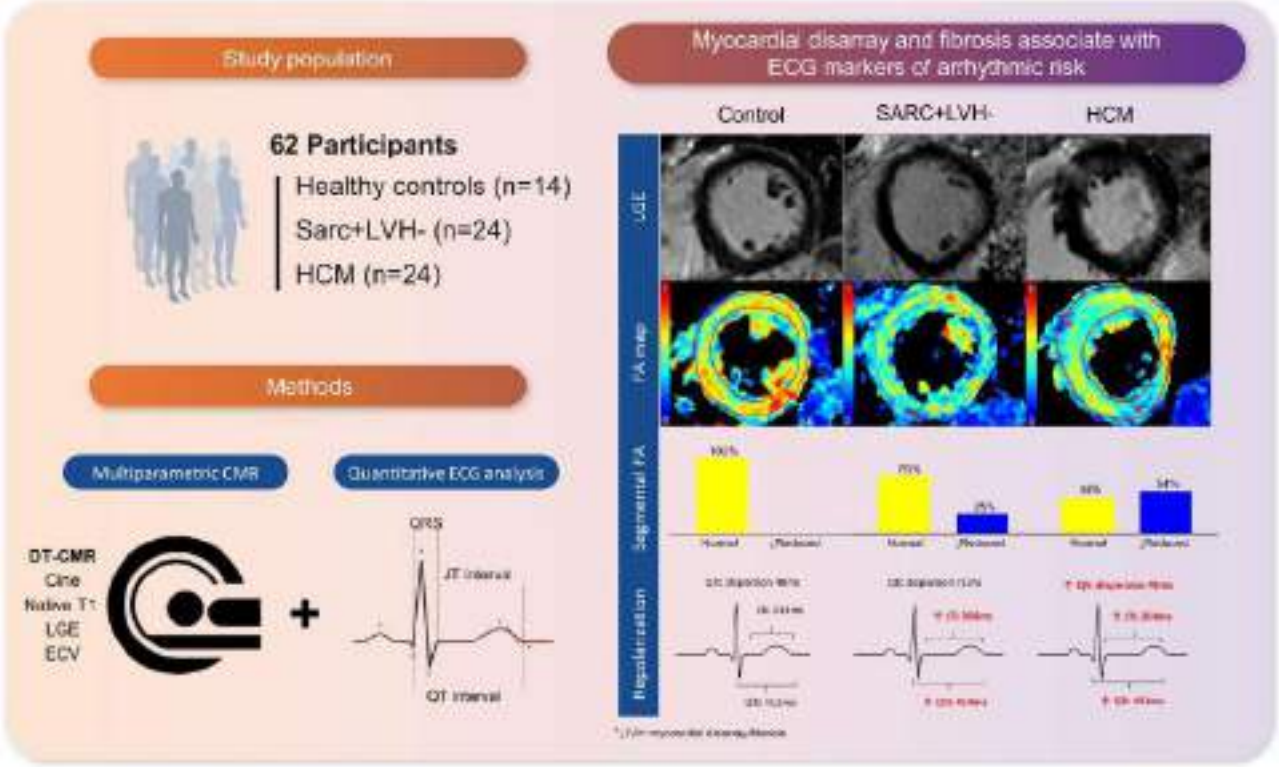

Figure 2 Microstructural abnormalities detected using DT-CMR in both SARC+LVH– and overt HCM are associated with prolongation of repolarization parameters linked to arrhythmic risk (main illustration). DT-CMR, diffusion tensor cardiac magnetic resonance imaging; HCM, hypertrophic cardiomyopathy; SARC+LVH–, pre-hypertrophic sarcomeric variant carriers.

Table 2 ECG analysis results

	Controls (14)	SARC+LVH– (24)	HCM (24)	SARC+LVH– vs. controls *P*-value	HCM vs. controls *P*-value	3-way comparison *P*-value
Qualitative ECG parameters						
Sinus rhythm	14 (100)	24 (100)	24 (100)			
Abnormal ECG	1 (2)	9 (38)	17 (63)	0.115	< 0.001	< 0.001
LVH voltage criteria	0	7 (29)	9 (38)	0.07	0.014	0.053
Pathological Q waves	0	3 (13)	5 (21)	0.536	0.088	0.220
LBBB/RBBB	0	1 (4)	2 (8)	0.99	0.303	0.541
ST/T wave abnormalities	1 (8)	5 (21)	16 (67)	0.640	< 0.001	< 0.001
Quantitative ECG parameters						
PR interval (ms)	155 ± 24	150 ± 17	165 ± 21	0.451	0.239	0.052
QRS duration (ms)	94 ± 8	91 ± 16	98 ± 13	0.652	0.328	0.258
QTc (ms)	413 ± 27	454 ± 29	451 ± 50	< 0.001	0.026	0.013
QTc dispersion (ms)	48 ± 20	71 ± 27	78 ± 41	0.017	0.027	0.033
QTPc (ms)	340 ± 24	373 ± 28	375 ± 46	0.002	0.021	0.021
QTPc dispersion (ms)	40 ± 16	66 ± 18	88 ± 81	< 0.001	0.064	0.057
JTc (ms)	314 ± 26	356 ± 26	354 ± 42	< 0.001	0.006	0.002
cTPe (ms)	89 ± 10	102 ± 15	105 ± 10	0.023	0.185	0.678

Values are mean ± SD or *n* (%).
cTPe, corrected T wave peak → T wave end; ECG, electrocardiogram; JTc, ventricular repolarization (J point → T wave tangential line); LBBB, left bundle branch abnormality PR, atrial depolarization (*P* wave → R wave); QTc, ventricular depolarization + repolarization (Q wave → T wave tangential line); QTPc, ventricular depolarization + repolarization (Q wave → T wave peak).

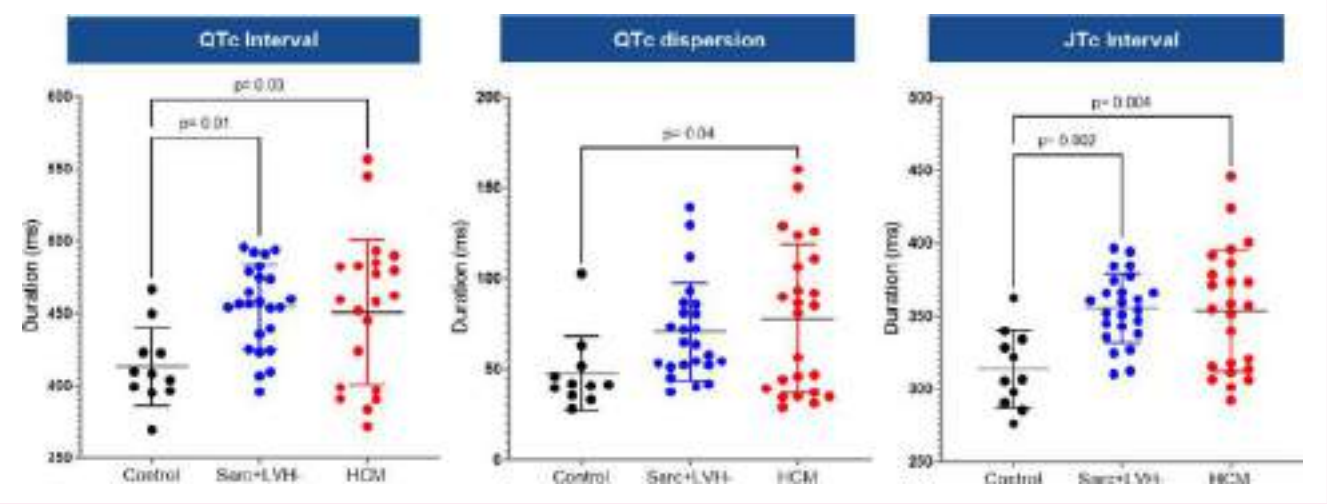

Figure 3 QTc interval, QTc dispersion, and JTc interval across groups. JTc, J point → T wave tangential line, corrected for heart rate; QTc, Q wave → T wave tangential line, corrected for heart rate.

and distinction from healthy individuals were seen with the JTc interval; this was significantly prolonged in both SARC+LVH– and overt HCM patients (354 ± 42 vs. 356 ± 26 vs. controls 314 ± 26 ms, $P = 0.002$). Both the QTc and JTc intervals showed significant correlation with the European Society of Cardiology (ESC) SCD risk score in HCM patients ($r = 0.418$, $P = 0.042$ and $r = 0.494$, $P = 0.014$, respectively). The JTc interval also demonstrated substantial diagnostic potential in discriminating SARC+LVH– from healthy controls with an area under the curve of 0.88 (95% confidence interval (CI) 0.76 – 1.00, $P < 0.001$), with a JTc interval ≥ 342 ms delivering the highest combined sensitivity (75%) and specificity (91%) (*Figure 4*). A JTc interval ≥ 342 ms had a positive predictive value of 95% and a negative predictive value of 63% for discriminating variant carriers from controls.

Relationship between DT-CMR and repolarization parameters

In SARC+LVH– patients, there was a clear negative correlation between FA and the JTc interval ($r = -0.6$, $P = 0.002$) (*Figure 1B*) and to a lesser degree the QTc interval ($r = -0.5$, $P = 0.012$). This association was not as strong in HCM patients and absent in healthy controls (see Supplementary data online, *Figure S2*). MD did not show significant associations with any repolarization parameters in the SARC+LVH– group. In the HCM group, MD was associated with longer JTc and QTc intervals, and greater QTc dispersion, even after accounting for strain in the linear regression model (JTc $\beta = 0.407$, $P = 0.04$, QTc $\beta = 0.385$, $P = 0.036$, and QTc dispersion $\beta = 0.54$, $P = 0.03$).

Relationship between markers of fibrosis and repolarization parameters

The presence of replacement fibrosis on LGE imaging did not significantly affect the duration of repolarization parameters in HCM patients. In contrast, repolarization parameters, particularly the JTc and QTc intervals demonstrated a strong positive correlation with ECV (both $r = 0.6$, $P = 0.019$), an indicator of interstitial fibrosis which was elevated in HCM (*Figure 1D*). This was also the case for QTc dispersion ($r = 0.7$, $P = 0.01$) (see Supplementary data online, *Figure S3*). This relationship between repolarization parameters and ECV was not seen in SARC+LVH– patients.

Discussion

This study assessed the sensitivity of DT-CMR in detecting microstructural changes in SARC+LVH– and HCM patients and examined whether a standard 12-lead ECG can be used to detect the presence of microstructural abnormalities in early and late phases of disease. Our findings indicate that: (i) myocardial disarray, inferred from reduced FA on DT-CMR, is detectable in one in four SARC+LVH– patients as well as the majority of HCM patients, (ii) relative to controls, SARC+LVH– patients and overt HCM patients had a higher frequency of qualitative ECG abnormalities and more prolonged repolarization intervals (i.e. QTc and JTc intervals), and (iii) the JTc interval is associated with disarray and fibrosis as a continuum in pre-hypertrophic variant carriers and HCM patients and may serve as a promising marker for risk stratification in patients.

Myocardial disarray in SARC+LVH– patients

In our study, a substantial subset of SARC+LVH– patients (25%) exhibited low segmental FA compared with healthy individuals. Our analysis showed that SARC+LVH– patients exhibited higher mean MD in contrast to controls, a measure potentially suggestive of cellular hypertrophy and early interstitial expansion. In the absence of significant fibrosis in our SARC+LVH– patients, we have interpreted the reduced FA to primarily represent localized regions of myocardial disarray. These findings are in line with published histology from post-mortem studies which have shown the presence of disarray in SARC+LVH– patients[2] and demonstrated its patchy nature within the myocardium in HCM.[25] Previous work from our group has identified low FA as a marker of myocardial disarray in overt HCM, which also correlates independently with the risk of ventricular arrhythmias.[7] Complementing our findings, a recent study by Joy *et al.* employed a spin-echo DT-CMR sequence and similarly found reduced (systolic) FA in SARC+LVH– patients.[26] Other indicators of microstructural changes, such as diffuse fibrosis, have also been observed in this group; however, the evidence remains inconsistent. For example, Ho *et al.*[27] noted an increased ECV, indicative of diffuse fibrosis, in SARC+LVH– patients, whereas Joy's study and ours did not find significant ECV differences.

Table 3 ECG analysis results (incl. only SARC+HCM)

	Controls (14)	SARC+LVH− (24)	SARC+HCM (16)	SARC+LVH− vs. controls *P*-value	SARC+HCM vs. controls *P*-value	3-way comparison *P*-value
Qualitative ECG parameters						
Sinus rhythm	14 (100)	24 (100)	16 (100)			
Abnormal ECG	0	9 (38)	10 (63)	0.115	0.004	< 0.001
LVH voltage criteria	0	7 (29)	4 (25)	0.07	0.113	0.117
Pathological Q waves	0	3 (13)	4 (25)	0.536	0.113	0.156
LBBB/RBBB	0	1 (4)	1 (6)	0.99	0.99	0.692
ST/T wave abnormalities	1 (8)	5 (21)	10 (63)	0.640	0.006	0.003
Quantitative ECG parameters						
PR interval (ms)	155± 24	150 ± 17	167 ± 22	0.451	0.208	0.043
QRS duration (ms)	94 ± 8	91 ± 16	98 ± 14	0.652	0.400	0.382
QTc (ms)	411 ± 14	454 ± 29	458 ± 44	< 0.001	0.006	0.003
QTc dispersion (ms)	48 ± 20	71 ± 27	84 ± 43	0.017	0.017	0.021
QTPc (ms)	340 ± 24	373 ± 28	379 ± 42	0.002	0.009	0.007
QTPc dispersion (ms)	40 ± 16	66 ± 18	96 ± 94	< 0.001	0.064	0.040
JTc (ms)	314 ± 26	356 ± 26	360 ± 40	< 0.001	0.002	< 0.001
cTPe (ms)	89 ± 10	102 ± 15	119 ± 88	0.023	0.284	0.315

Values are mean ± SD or *n* (%).
cTPe, corrected T wave peak → T wave end; ECG, electrocardiogram; JTc, ventricular repolarization (J point → T wave tangential line); LBBB, left bundle branch abnormality PR, atrial depolarization (*P* wave → R wave); QTc, ventricular depolarization + repolarization (Q wave → T wave tangential line); QTPc, ventricular depolarization + repolarization (Q wave → T wave peak).

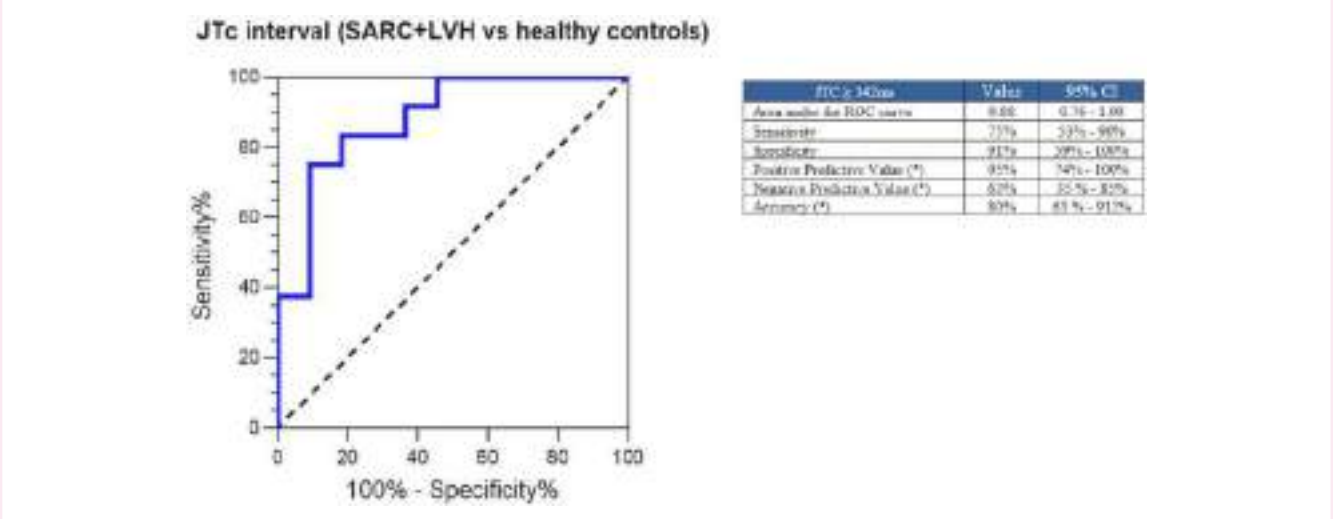

Figure 4 Receiver operator characteristic curve—diagnostic ability of JTc interval in discriminating SARC+LVH− from healthy controls. JTc, J point → T wave tangential line, corrected for heart rate; SARC+LVH−, pre-hypertrophic sarcomeric variant carriers.

Discrepancies between these studies may stem from variations in patient selection, particularly regarding the stage of disease in cohorts. Nonetheless, our findings collectively imply that DT-CMR may detect disarray before diffuse fibrosis becomes apparent, underscoring its potential as an early marker for disease progression and clinical surveillance.

Myocardial repolarization abnormalities in SARC+LVH− and HCM patients

Using quantitative ECG analysis, we were able to show that repolarization is significantly delayed (evidenced by QTc and JTc interval prolongation) and more heterogeneous (indicated by increased QTc dispersion)

in SARC+LVH− patients in comparison to controls. Importantly, none of these patients were on medications that could prolong their QT interval. Within the array of ECG parameters, JTc exhibited the highest diagnostic performance in discriminating HCM patients from controls. We also demonstrate as expected, that prolongation and heterogeneity of repolarization is more pronounced in overt HCM cases, despite most of these patients being on anti-arrhythmic medications that serve to stabilize ventricular repolarization.

In this study, we show that manual measurements on 12-lead ECG can elucidate subtle delays in these repolarization parameters prior to the onset of hypertrophy in variant carriers and demonstrate repolarization prolongation with the evolution of the HCM phenotype. Although previous studies have described ECG changes including repolarization abnormalities in HCM, they tended to focus on those with established hypertrophy, and ECG analysis has been mostly qualitative in nature with only limited quantitative ECG analysis undertaken.[17,26,28,29] Those that did focus on repolarization intervals such as the QTc interval, QTc dispersion, and JTc interval in overt HCM found, similar to us, an association between prolongation of these parameters and SCD risk.[13,15,30–32] More recently, studies using advanced automated ECG analysis techniques have demonstrated prolongation of activation time (a measure of depolarization onset) and increased duration and dispersion of repolarization parameters in both overt HCM and SARC+LVH− patients.[33–36] However, caution is needed when making direct comparisons between studies due to differences in ECG analysis approaches (e.g. use of tangent method for estimation of QTc interval in our study), including the specific parameters measured, as well as variations in group characteristics, such as the mean age of HCM cohorts. For example, in another study by Joy *et al.*,[34] which included a larger cohort (211 patients), the QRS duration was shorter in the SARC+LVH− group compared with controls, while the QTc interval remained similar—potentially suggesting subtle repolarization prolongation. Although the JTc interval was not measured, this combination of shorter QRS and unchanged QTc duration could theoretically indicate JTc prolongation, aligning with our findings. Interestingly, in their study, repolarization parameters obtained via CMR-guided electrocardiographic imaging (ECGi), such as the activation recovery interval and repolarization time, were not prolonged in SARC+LVH− patients. However, it is important to note that both parameters incorporate parts of the QRS complex, meaning they reflect a composite of both depolarization and repolarization durations, rather than repolarization alone. While complex CMR-integrated ECG mapping techniques like ECGi play an important role in probing intricate conduction abnormalities in HCM, our study used the simpler, widely available 12-lead ECG to demonstrate that parameters such as the JTc interval can potentially differentiate sub-clinical HCM (SARC+LVH−) from controls. It is also noteworthy that we identified meaningful differences in ECG parameters with a modestly sized cohort, which highlights the sensitivity of these easy-to-extract measures.

Relationship between disarray, fibrosis, and repolarization parameters

Among SARC+LVH− patients, we found a significant inverse correlation between FA and JTc interval duration, providing further evidence that myocardial disarray may be complicit in repolarization prolongation (in conjunction with other factors such as ionic remodelling and aberrations in calcium handling[6]). However, this association was less pronounced in overt HCM patients and we postulate this divergence may be due to the more prominent roles of myocyte hypertrophy, progressive interstitial fibrosis[37] and microvascular dysfunction[28]—rather than disarray—in altering repolarization in more advanced disease. This is further supported by the strong correlation seen in overt HCM patients between repolarization parameters (JTc interval and QTc dispersion) and recognized markers of interstitial fibrosis such as ECV and T1. This relationship between interstitial fibrosis and myocardial repolarization (specifically QTc dispersion) was also observed by Hurtado-de-Mendoza *et al.*[37] in their ECG and CMR study of 112 overt HCM patients. Similarly, Österberg *et al.*[28] also observed an association between an ECG risk-score incorporating QTc duration and LGE burden in early stage HCM. Most noteworthy of all and consistent with our work is a comprehensive study by Kuroda *et al.*,[12] which employed both qualitative and quantitative ECG analyses, Holter monitoring, and histological evaluations, and identified T wave alternans as indicative of a higher burden of myocardial disarray and fibrosis on histology. Recent investigations have also highlighted the potential for qualitative ECG alterations in SARC+LVH− individuals as predictors of disease progression and penetrance.[38–40] The strong correlation observed between repolarization intervals and FA in our study suggests that these intervals might serve as reliable indicators of disease severity and could potentially forecast long-term disease progression.

Clinical relevance

With the advent of disease-modifying interventions such as small molecule modulators of cardiac myosin and gene therapies, the early identification of individuals exhibiting microstructural changes—those potentially on the cusp of developing HCM—has gained paramount importance. Our study highlights the potential of myocardial disarray imaging and quantitative ECG analysis to serve as early markers of disease activity in HCM, providing measures that can contribute to more nuanced clinical surveillance of variant carriers. Traditionally, qualitative 12-lead ECG analysis has anchored the diagnostic process for HCM, serving as an essential tool for familial screenings and risk evaluations, especially for individuals considering competitive athletic sports. Our findings suggest that more granular insight into microstructural changes (both myocardial disarray and fibrosis) can be inferred from specific quantitative ECG deviations across the disease spectrum. Our observations align with established literature indicating that repolarization abnormalities are closely related to microstructural abnormalities like fibrosis,[12,28,37] and mirror documented associations with other prognostic markers including strain abnormalities[41] and arrhythmic burden.[13,31,35] Future endeavours however are needed to validate our observations in larger cohorts, with comparative analyses of other risk assessment strategies.

Limitations

Our study, albeit small and cross-sectional in nature, provided some valuable insights into the relationship between myocardial microstructure and repolarization changes in both Sarc+LVH− and HCM patients. However, these observations cannot be directly attributed to disease progression without longitudinal follow-up. For a more comprehensive understanding of causal relationships between microstructural alterations and repolarization anomalies, in-depth histological validation and electrophysiological studies are imperative. It is also worth noting that cardiac DT-CMR remains a research technique, work on standardisation of approach and improvements in acquisition and data processing are pre-requisites to future longitudinal, multi-centre clinical studies necessary for it to enter the clinical domain.

Conclusion

Low diastolic FA, suggestive of myocardial disarray, is present in both SARC+LVH− and HCM patients. Low diastolic FA in SARC+LVH− and raised ECV in HCM patients associated with prolongation of repolarization. Myocardial disarray assessment using DT-CMR and prolongation of key repolarization parameters such as the JTc interval

demonstrates significant potential as novel, sensitive, and prognostically important markers of disease activity across HCM stages. These techniques may come to support more nuanced surveillance of SARC+LVH− patients and improved risk stratification of overt HCM patients.

Acknowledgements

B.R., S.N. and H.W. acknowledge support from the Oxford British Heart Foundation Centre of Research Excellence.

Supplementary data

Supplementary data are available at *European Heart Journal - Cardiovascular Imaging* online.

Funding

Z.A. is a recipient of a British Heart Foundation Clinical Research Training Fellowship (FS/CRTF/21/24144). B.R. and S.N. report grants from NIHR Oxford Biomedical Research Centre. B.R. is a recipient of an Intermediate Clinical Transitional Research Fellowship from the BHF Centre of Research Excellence, Oxford (RE/18/3/34214). A.H.A.S. holds a doctoral scholarship funded by the Ministry of Higher Education Malaysia and Universiti Kebangsaan Malaysia (National University of Malaysia).

Conflict of interest: None declared.

Data availability

The data underlying this article will be shared on reasonable request to the corresponding author.

References

1. Finocchiaro G, Papadakis M, Robertus JL, Dhutia H, Steriotis AK, Tome M *et al.* Etiology of sudden death in sports: insights from a United Kingdom regional registry. *J Am Coll Cardiol* 2016;**67**:2108–15.
2. McKenna WJ, Stewart JT, Nihoyannopoulos P, McGinty F, Davies MJ. Hypertrophic cardiomyopathy without hypertrophy: two families with myocardial disarray in the absence of increased myocardial mass. *Br Heart J* 1990;**63**:287–90.
3. Garcia-Canadilla P, Cook AC, Mohun TJ, Oji O, Schlossarek S, Carrier L *et al.* Myoarchitectural disarray of hypertrophic cardiomyopathy begins pre-birth. *J Anat* 2019;**235**:962–76.
4. Wei D, Miyamoto N, Mashima S. A computer model of myocardial disarray in simulating ECG features of hypertrophic cardiomyopathy. *Jpn Heart J* 1999;**40**:819–26.
5. Saumarez RC. Electrophysiological investigation of patients with hypertrophic cardiomyopathy. *Br Heart J* 1994;**72**(Suppl. 6):19–23.
6. Finocchiaro G, Sheikh N, Leone O, Westaby J, Mazzarotto F, Pantazis A *et al.* Arrhythmogenic potential of myocardial disarray in hypertrophic cardiomyopathy: genetic basis, functional consequences and relation to sudden cardiac death. *Europace* 2021;**23**:985–95.
7. Ariga R, Tunnicliffe EM, Manohar SG, Mahmod M, Raman B, Piechnik SK *et al.* Identification of myocardial disarray in patients with hypertrophic cardiomyopathy and ventricular arrhythmias. *J Am Coll Cardiol* 2019;**73**:2493–502.
8. Nguyen C, Lu M, Fan Z, Bi X, Kellman P, Zhao S, *et al.* Contrast-free detection of myocardial fibrosis in hypertrophic cardiomyopathy patients with diffusion-weighted cardiovascular magnetic resonance. *J Cardiovasc Magn Reson* 2015;**17**:107.
9. Abdullah OM, Drakos SG, Diakos NA, Wever-Pinzon O, Kfoury AG, Stehlik J *et al.* Characterization of diffuse fibrosis in the failing human heart via diffusion tensor imaging and quantitative histological validation. *NMR Biomed* 2014;**27**:1378–86.
10. Khalique Z, Scott AD, Ferreira PF, Nielles-Vallespin S, Firmin DN, Pennell DJ. Diffusion tensor cardiovascular magnetic resonance in hypertrophic cardiomyopathy: a comparison of motion-compensated spin echo and stimulated echo techniques. *MAGMA* 2020;**33**:331–42.
11. Das A, Kelly C, Teh I, Nguyen C, Brown LAE, Chowdhary A *et al.* Phenotyping hypertrophic cardiomyopathy using cardiac diffusion magnetic resonance imaging: the relationship between microvascular dysfunction and microstructural changes. *Eur Heart J Cardiovasc Imaging* 2022;**23**:352–62.
12. Kuroda N, Ohnishi Y, Yoshida A, Kimura A, Yokoyama M. Clinical significance of T-wave alternans in hypertrophic cardiomyopathy. *Circ J* 2002;**66**:457–62.
13. Magri D, Santolamazza C, Limite L, Mastromarino V, Casenghi M, Orlando P *et al.* QT spatial dispersion and sudden cardiac death in hypertrophic cardiomyopathy: time for reappraisal. *J Cardiol* 2017;**70**:310–5.
14. Yi G, Poloniecki J, Dickie S, Elliott PM, Malik M, McKenna WJ. Is QT dispersion associated with sudden cardiac death in patients with hypertrophic cardiomyopathy? *Ann Noninvasive Electrocardiol* 2001;**6**:209–15.
15. Buja G, Miorelli M, Turrini P, Melacini P, Nava A. Comparison of QT dispersion in hypertrophic cardiomyopathy between patients with and without ventricular arrhythmias and sudden death. *Am J Cardiol* 1993;**72**:973–6.
16. Marian AJ, Mares A, Kelly DP, Yu QT, Abchee AB, Hill R *et al.* Sudden cardiac death in hypertrophic cardiomyopathy. *Eur Heart J* 1995;**16**:368–76.
17. Konno T, Shimizu M, Ino H, Fujino N, Hayashi K, Uchiyama K *et al.* Differences in diagnostic value of four electrocardiographic voltage criteria for hypertrophic cardiomyopathy in a genotyped population. *Am J Cardiol* 2005;**96**:1308–12.
18. al-Mahdawi S, Chamberlain S, Chojnowska L, Michalak E, Nihoyannopoulos P, Ryan M *et al.* The electrocardiogram is a more sensitive indicator than echocardiography of hypertrophic cardiomyopathy in families with a mutation in the MYH7 gene. *Br Heart J* 1994;**72**:105–11.
19. Piechnik SK, Ferreira VM, Dall'Armellina E, Cochlin LE, Greiser A, Neubauer S *et al.* Shortened Modified Look-Locker Inversion recovery (ShMOLLI) for clinical myocardial T1-mapping at 1.5 and 3 T within a 9 heartbeat breathhold. *J Cardiovasc Magn Reson* 2010;**12**:69.
20. Raman B, Ariga R, Spartera M, Sivalokanathan S, Chan K, Dass S *et al.* Progression of myocardial fibrosis in hypertrophic cardiomyopathy: mechanisms and clinical implications. *Eur Heart J Cardiovasc Imaging* 2019;**20**:157–67.
21. Chan RH, Maron BJ, Olivotto I, Pencina MJ, Assenza GE, Haas T *et al.* Prognostic value of quantitative contrast-enhanced cardiovascular magnetic resonance for the evaluation of sudden death risk in patients with hypertrophic cardiomyopathy. *Circulation* 2014;**130**:484–95.
22. Ferreira PF, Nielles-Vallespin S, Scott AD, de Silva R, Kilner PJ, Ennis DB *et al.* Evaluation of the impact of strain correction on the orientation of cardiac diffusion tensors with in vivo and ex vivo porcine hearts. *Magn Reson Med* 2018;**79**:2205–15.
23. Stoeck CT, Kalinowska A, von Deuster C, Harmer J, Chan RW, Niemann M *et al.* Dual-phase cardiac diffusion tensor imaging with strain correction. *PLoS One* 2014;**9**:e107159.
24. Samat AHA, Cassar MP, Akhtar AM, McCracken C, Ashkir ZM, Mills R *et al.* Diagnostic utility of electrocardiogram for screening of cardiac injury on cardiac magnetic resonance in post-hospitalised COVID-19 patients: a prospective multicenter study. *Int J Cardiol* 2024;**415**:132415.
25. Varnava AM, Elliott PM, Mahon N, Davies MJ, McKenna WJ. Relation between myocyte disarray and outcome in hypertrophic cardiomyopathy. *Am J Cardiol* 2001;**88**:275–9.
26. Joy G, Kelly CI, Webber M, Pierce I, Teh I, McGrath L *et al.* Microstructural and microvascular phenotype of sarcomere mutation carriers and overt hypertrophic cardiomyopathy. *Circulation* 2023;**148**:808–18.
27. Ho CY, Abbasi SA, Neilan TG, Shah RV, Chen Y, Heydari B *et al.* T1 measurements identify extracellular volume expansion in hypertrophic cardiomyopathy sarcomere mutation carriers with and without left ventricular hypertrophy. *Circ Cardiovasc Imaging* 2013;**6**:415–22.
28. Osterberg AW, Ostman-Smith I, Jablonowski R, Carlsson M, Green H, Gunnarsson C *et al.* High ECG risk-scores predict late gadolinium enhancement on magnetic resonance imaging in HCM in the young. *Pediatr Cardiol* 2021;**42**:492–500.
29. Ostman-Smith I, Wisten A, Nylander E, Bratt EL, Granelli A, Oulhaj A *et al.* Electrocardiographic amplitudes: a new risk factor for sudden death in hypertrophic cardiomyopathy. *Eur Heart J* 2010;**31**:439–49.
30. Yi G, Poloniecki J, Dickie S, Elliott PM, Malik M, McKenna WJ. Can the assessment of dynamic QT dispersion on exercise electrocardiogram predict sudden cardiac death in hypertrophic cardiomyopathy? *Pacing Clin Electrophysiol* 2000;**23**(11 Pt 2):1953–6.
31. Patel SI, Ackerman MJ, Shamoun FE, Geske JB, Ommen SR, Love WT *et al.* QT prolongation and sudden cardiac death risk in hypertrophic cardiomyopathy. *Acta Cardiol* 2019;**74**:53–8.
32. Biagini E, Pazzi C, Olivotto I, Musumeci B, Limongelli G, Boriani G *et al.* Usefulness of electrocardiographic patterns at presentation to predict long-term risk of cardiac death in patients with hypertrophic cardiomyopathy. *Am J Cardiol* 2016;**118**:432–9.
33. Chow J-J, Leong KMW, Shun-Shin M, Jones S, Guttmann OP, Mohiddin SA *et al.* The arrhythmic substrate of hypertrophic cardiomyopathy using ECG imaging. *Front Physiol* 2024;**15**:1428709.
34. Joy G, Lopes LR, Webber M, Ardissino AM, Wilson J, Chan F *et al.* Electrophysiological characterization of subclinical and overt hypertrophic cardiomyopathy by magnetic resonance imaging-guided electrocardiography. *J Am Coll Cardiol* 2024;**83**:1042–55.
35. Suszko AM, Chakraborty P, Viswanathan K, Barichello S, Sapp J, Talajic M *et al.* Automated quantification of abnormal QRS peaks from high-resolution ECGs predicts late ventricular arrhythmias in hypertrophic cardiomyopathy: a 5-year prospective multicenter study. *J Am Heart Assoc* 2022;**11**:e026025.
36. Domain G, Chouquet C, Réant P, Bongard V, Vedis T, Rollin A *et al.* Relationships between left ventricular mass and QRS duration in diverse types of left ventricular hypertrophy. *Eur Heart J Cardiovasc Imaging* 2022;**23**:560–8.
37. Hurtado-De-Mendoza D, Corona-Villalobos CP, Pozios I, Gonzales J, Soleimanifard Y, Sivalokanathan S *et al.* Diffuse interstitial fibrosis assessed by cardiac magnetic resonance is associated with dispersion of ventricular repolarization in patients with hypertrophic cardiomyopathy. *J Arrhythm* 2017;**33**:201–7.

38. Lorenzini M, Norrish G, Field E, Ochoa JP, Cicerchia M, Akhtar MM *et al.* Penetrance of hypertrophic cardiomyopathy in sarcomere protein mutation carriers. *J Am Coll Cardiol* 2020;**76**:550–9.
39. Anvekar P, Stephens P Jr, Calderon-Anyosa RJC, Kauffman HL, Burstein DS, Ritter AL *et al.* Electrocardiographic findings in genotype-positive and non-sarcomeric children with definite hypertrophic cardiomyopathy and subclinical variant carriers. *Pediatr Cardiol* 2023;**45**:1784–97.
40. Gruner C, Ivanov J, Care M, Williams L, Moravsky G, Yang H *et al.* Toronto hypertrophic cardiomyopathy genotype score for prediction of a positive genotype in hypertrophic cardiomyopathy. *Circ Cardiovasc Genet* 2013;**6**:19–26.
41. Badran HM, Elnoamany MF, Soltan G, Ezat M, Elsedi M, Abdelfatah RA *et al.* Relationship of mechanical dyssynchrony to QT interval prolongation in hypertrophic cardiomyopathy. *Eur Heart J Cardiovasc Imaging* 2012;**13**:423–32.

Translational Neurodegeneration

REVIEW

Open Access

LRRK2, *GBA* and their interaction in the regulation of autophagy: implications on therapeutics in Parkinson's disease

Shirley Yin-Yu Pang[1], Rachel Cheuk Nam Lo[1], Philip Wing-Lok Ho[1], Hui-Fang Liu[1], Eunice Eun Seo Chang[1], Chi-Ting Leung[1], Yasine Malki[1], Zoe Yuen-Kiu Choi[1], Wing Yan Wong[2], Michelle Hiu-Wai Kung[1], David Boyer Ramsden[3] and Shu-Leong Ho[1*]

Abstract

Mutations in leucine-rich repeat kinase 2 (*LRRK2*) and glucocerebrosidase (*GBA*) represent two most common genetic causes of Parkinson's disease (PD). Both genes are important in the autophagic-lysosomal pathway (ALP), defects of which are associated with α-synuclein (α-syn) accumulation. LRRK2 regulates macroautophagy *via* activation of the mitogen activated protein kinase/extracellular signal regulated protein kinase (MAPK/ERK) kinase (MEK) and the calcium-dependent adenosine monophosphate (AMP)-activated protein kinase (AMPK) pathways. Phosphorylation of Rab GTPases by LRRK2 regulates lysosomal homeostasis and endosomal trafficking. Mutant LRRK2 impairs chaperone-mediated autophagy, resulting in α-syn binding and oligomerization on lysosomal membranes. Mutations in *GBA* reduce glucocerebrosidase (GCase) activity, leading to glucosylceramide accumulation, α-syn aggregation and broad autophagic abnormalities. *LRRK2* and *GBA* influence each other: GCase activity is reduced in *LRRK2* mutant cells, and LRRK2 kinase inhibition can alter GCase activity in *GBA* mutant cells. Clinically, *LRRK2* G2019S mutation seems to modify the effects of *GBA* mutation, resulting in milder symptoms than those resulting from *GBA* mutation alone. However, dual mutation carriers have an increased risk of PD and earlier age of onset compared with single mutation carriers, suggesting an additive deleterious effect on the initiation of PD pathogenic processes. Crosstalk between *LRRK2* and *GBA* in PD exists, but its exact mechanism is unclear. Drugs that inhibit LRRK2 kinase or activate GCase are showing efficacy in pre-clinical models. Since LRRK2 kinase and GCase activities are also altered in idiopathic PD (iPD), it remains to be seen if these drugs will be useful in disease modification of iPD.

Keywords: Parkinson's disease, Interaction, LRRK2, GBA, GCase, Mutation, Autophagy, α-Synuclein

Background

Autophagy is a degradation process to remove proteins and dysfunctional organelles from cells to prevent subsequent toxicity and cell death. There are three forms of autophagy: (1) macroautophagy, which involves sequestration of portions of the cytosol into double-membrane vesicles or autophagic vacuoles (AV) that then fuse with lysosomes [1]; (2) chaperone-mediated autophagy (CMA), which involves the direct transport of cytosolic soluble proteins across the lysosomal membrane in a selective fashion [2]; and (3) microautophagy, which involves sequestration of cytosolic contents directly by lysosomes through membrane invagination [3]. Parkinson's disease (PD), the second most common neurodegenerative disease after Alzheimer's disease, is characterized pathologically by loss of dopaminergic neurons in the substantia nigra pars

*Correspondence: slho@hku.hk
[1] Division of Neurology, Department of Medicine, Queen Mary Hospital, University of Hong Kong, Hong Kong, China
Full list of author information is available at the end of the article

compacta and intraneuronal inclusions called Lewy bodies (LB) that consist of aggregated α-synuclein (α-syn) [4, 5]. In postmortem PD brains, reduction of lysosomal markers is apparent in nigral neurons that contain α-syn inclusions [6]. Furthermore, lysosomal depletion has been shown to precede dopaminergic cell death in a PD mouse model [7]. Since α-syn is degraded in lysosomes, impairment of the autophagic-lysosomal pathway (ALP) could lead to impaired α-syn clearance. Aggregation of α-syn into toxic oligomers then further aggravates the impairment in autophagic and lysosomal functions, forming a vicious cycle [6–8].

Genetic studies have indicated that malfunctioning degradation pathways contribute to the pathogenesis of PD. Only 5%–10% of PD patients have familial forms of the disease [8], and PD has traditionally been considered as a largely sporadic disease. However, advancements in our understanding of the genetic basis of PD suggest that genetic factors can cause or increase the susceptibility to PD to a much larger extent than previously thought: the heritability of PD has been estimated to be at least 27% and up to 60% in large genome-wide association studies (GWAS) (reviewed in [9]). Genes and genetic loci identified in familial and sporadic PD are strongly enriched for autosomal/lysosomal functions: among the 24 loci identified by GWAS to be associated with PD [10], at least 11 genes are implicated in the ALP [9, 11]. In particular, mutations in *LRRK2* (encoding leucine-rich repeat kinase 2, LRRK2) and *GBA* (encoding glucocerebrosidase, GCase) are now recognized as two most common genetic causes of PD worldwide [9]. Recent evidence in experimental models of PD suggests that *LRRK2* and *GBA* are closely related to the regulation of ALP [12–14]. Importantly, enzymatic activities of LRRK2 and GCase have also been shown to be altered in idiopathic PD (iPD) [15–17].

Dopaminergic neuronal loss in late-onset PD starts 20–30 years before first motor symptoms of rest tremor, rigidity and bradykinesia appear, by which time there is already 50% striatal dopamine (DA) reduction [18]. There is a long prodromal or pre-motor period during which non-motor symptoms such as hyposmia and rapid eye movement sleep behavior disorder (RBD) already start to emerge [19]. It is hypothesized that during different stages of the disease, α-syn aggregates into oligomeric species, which then seed further aggregation and spread within the nervous system in a prion-like fashion [20, 21]. The long prodromal period represents a window of opportunity to modify disease progression. Understanding the roles *LRRK2* and *GBA* play in autophagy and α-syn aggregation will help elucidate the pathogenesis of PD and formulate rational therapeutic strategies.

LRRK2 and autophagy

LRRK2 mutations in PD

Mutations in *LRRK2*, located in the *PARK8* locus, are the most common mutations in familial autosomal-dominant PD [22, 23], and *LRRK2* polymorphisms are associated with increased PD risk in GWAS [24], suggesting a role of *LRRK2* in both sporadic and familial PD. Pleomorphic pathology including tauopathy or pure nigral degeneration has been reported in rare cases. Nevertheless, most *LRRK2*-PD cases have clinical and pathological features indistinguishable from iPD with late-onset disease, dopaminergic neuron degeneration in the substantia nigra and intracytoplasmic LB aggregates with positive staining for α-syn [23].

The LRRK2 protein is ubiquitously expressed, with highest levels in kidney, lung and brain (reviewed in [25]). It consists of multiple domains: armadillo repeats, ankyrin repeats, leucine-rich repeats, Ras of complex (Roc) with GTPase activity, C-terminal of Roc (COR), kinase, and WD40 domains [26]. The two most common mutations, G2019S located in the kinase domain of *LRRK2* and R1441C/G/H located in the GTPase domain, account for up to 10% and 2.5% of sporadic iPD cases, respectively [27]. Structural analyses of LRRK2 showed that the kinase and GTPase domains are in close proximity and can influence each other [28]. All known pathogenic *LRRK2* mutations, including G2019S and R1441C/G/H, can lead to increased kinase activity [29–32], suggesting that the increased phosphorylation of LRRK2 kinase substrates may result in toxicity to dopaminergic neurons.

LRRK2 and regulation of macroautophagy

Under normal conditions, autophagy occurs at a basal level to maintain homeostasis. When cells are under stress, autophagy promotes cell survival against apoptosis, but in some settings it can also cause cell death [33]. There is evidence that *LRRK2* plays a role in the regulation of macroautophagy. Accumulation of AV, shortened neurite length and reduced neuronal survival have been noted in rat neurons overexpressing PD-associated *LRRK2* mutant proteins in a LRRK2 kinase-dependent manner [34]. These abnormalities are not seen in cells that overexpress wild-type (WT) *LRRK2* or the kinase-dead *LRRK2* K1906M mutant, suggesting that the increased LRRK2 kinase activity is responsible for the abnormalities observed. Accumulation of AV has also been identified in dopaminergic neurons in the substantia nigra of iPD patients [35]. The increased amount of AV may be due to the increased induction of macroautophagy, reduced clearance of autophagosomes, or both. Fibroblasts from PD patients with *LRRK2* G2019S mutation have increased basal macroautophagy

as evidenced by increased numbers of autophagosomes and autolysosomes, increased protein degradation, and increased cell death [36]. Induction of macroautophagy by rapamycin in human neuroblastoma cells overexpressing *LRRK2* G2019S exacerbates autophagosome accumulation and neurite shortening, confirming that excessive macroautophagy induction can cause stress in susceptible cells [37]. Furthermore, these abnormalities can be reversed by inhibition of the mitogen activated protein kinase/extracellular signal regulated protein kinase (MAPK/ERK) kinase (MEK), suggesting that the increased LRRK2 kinase activity leads to activation of the MEK/ERK pathway, excessive macroautophagic induction and cell death [36, 37]. Another pathway implicated in autophagosome accumulation in *LRRK2* mutant cells is the Ca^{2+}-dependent activation of the CaMKK/adenosine monophosphate (AMP)-activated protein kinase (AMPK) pathway, which can be blocked by calcium chelation or by treatment with a specific antagonist of the Ca^{2+}-mobilizing messenger nicotinic acid adenine dinucleotide phosphate (NAADP), suggesting that NAADP receptors may be targets for regulation by *LRRK2* [38].

Cellular stress, such as starvation, can induce macroautophagy by inhibiting the mammalian target of rapamycin (mTOR) [39]. Interestingly, while rapamycin as an inhibitor of mTOR induces macroautophagy similar to that occurring in cells overexpressing *LRRK2* G2019S, the macroautophagy inhibitor 3-methyladenine reverses autophagosome accumulation induced by rapamycin but not by *LRRK2* mutation. This suggests a mechanistic difference between the mTOR- and *LRRK2*-mediated macroautophagy induction [38]. When cells are further stressed with a proteasome inhibitor, cell death is markedly increased in *LRRK2* mutant cells, which can be rescued by rapamycin that increases autophagic flux through the mTOR pathway.

Collectively, these studies show that the mutant LRRK2 protein with increased kinase activity causes excessive induction of basal macroautophagy, AV accumulation and cell death. Conversely, following proteasomal inhibition, cells with mutant LRRK2 show reduced degradative capacity and survival, which can be rescued by macroautophagy induction via the mTOR pathway. These observations suggest that *LRRK2* plays an important regulatory role in autophagic balance under different cellular conditions, disturbance of which may lead to reduced cell survival.

LRRK2 and lysosomal function

In addition to autophagosome induction, *LRRK2* mutation also compromises the maturation of autophagosomes into autolysosomes as shown by reduced co-localization of light chain 3 (LC3; an autophagosome marker) with lysosome-associated membrane protein 1 (LAMP1) [40]. Furthermore, lysosomes are abnormal with increased alkalinization and reduced protein degradation in a *LRRK2* R1441C transgenic mouse model and in SH-SY5Y cells overexpressing *LRRK2* G2019S, highlighting the role of *LRRK2* in lysosomal biology [41, 42]. Lysosomal dysfunction in *LRRK2* mutant cells is associated with increased detergent-insoluble α-syn, accumulation of phosphorylated α-syn at serine 129 (pS129-α-syn), and increased neuronal release of α-syn, all of which can be reversed by pharmacologic inhibition of LRRK2 kinase [14, 42, 43]. Interestingly, in WT cells, the same phenotype of abnormal lysosomal morphology and increased insoluble α-syn can be induced by treatment with lysosomal inhibitors, indicating that lysosomal inhibition can increase insoluble α-syn in WT cells similarly to that seen in *LRRK2* mutant cells, thereby confirming the importance of functional lysosomes in α-syn degradation [42].

LRRK2 may regulate lysosomal function through its kinase activity on a subset of Rab GTPases, which have been shown to be bona fide substrates of LRRK2 [31]. Upon lysosomal stress, LRRK2 is recruited by Rab7L1 (also called Rab29) from the cytoplasm onto enlarged lysosomes [44]. Furthermore, Rab8a and Rab10 accumulate in LRRK2-positive enlarged lysosomes in a LRRK2 kinase-dependent manner. Collectively, the sequential recruitment of Rab7L1, LRRK2, phosphorylated Rab8a and Rab10 onto lysosomes under stress suppresses lysosomal enlargement and promotes release of lysosomal content, illustrating the role of the Rab7L1-LRRK2 pathway in lysosome homeostasis. LRRK2 and Rab7L1 are also involved in retromer function which is required for retrograde transport of selective cargos between endosome and Golgi [45]. Disruption of the retromer function by *LRRK2* mutation leads to impairment in recruitment of lysosomal hydrolases, and lysosomal deficits. Another LRRK2 substrate, Rab35, is increased and colocalized with α-syn on enlarged endosomes in transgenic mice overexpressing α-syn [46]. Treatment with LRRK2 kinase inhibitor reduces Rab35 levels and its co-localization with α-syn, normalizes the size of enlarged endosomes and increases co-localization of α-syn with cathepsin, indicating increased trafficking of α-syn to lysosome for degradation. Collectively, this series of studies suggests that LRRK2 regulates lysosomal function through its kinase activity on a subset of Rab GTPases.

LRRK2 and CMA

There is evidence that CMA is perturbed in PD: lysosome-associated membrane protein 2A (LAMP2A), which multimerizes to form a translocation complex on lysosomal membranes essential for CMA, is reduced in

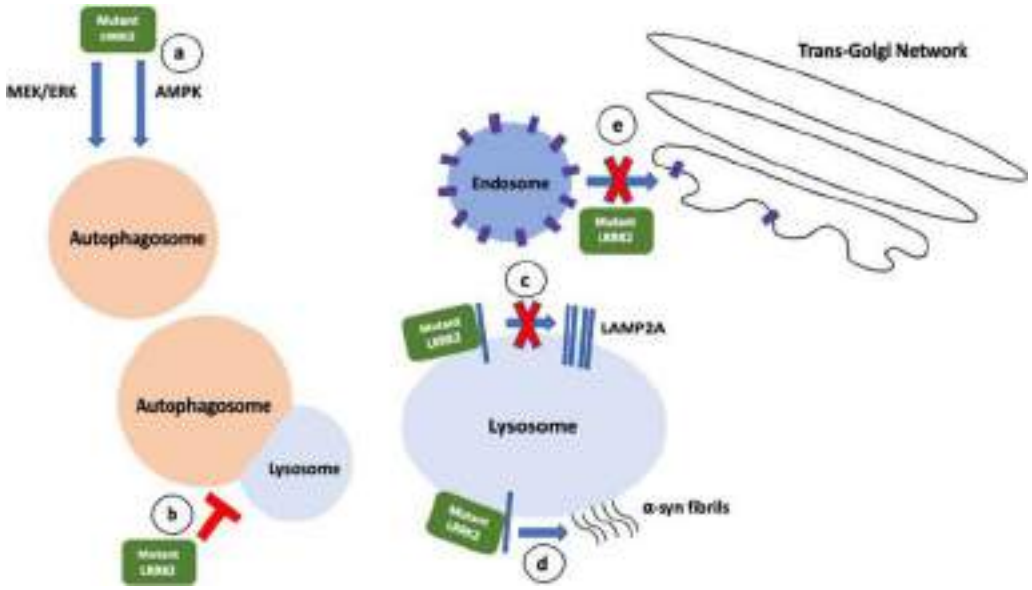

Fig. 1 Defects in autophagy associated with LRRK2 mutations. **a** Mutant LRRK2 induces autophagosome formation by activating the MEK/ERK pathway and the Ca^{2+}-dependent AMPK pathway. **b** Fusion of autophagosome with lysosome is blocked, exacerbating autophagosome accumulation. **c** Mutant LRRK2 binds to LAMP2A and prevents its multimerization to form the translocation complex required for transport of CMA substrates into lysosome for degradation. **d** Mutant LRRK2 promotes binding of α-syn onto lysosomal membranes where they form oligomers. **e** Impaired protein trafficking from endosome to trans-Golgi network due to retromer dysfunction leads to hydrolase deficiencies in lysosome

the substantia nigra of postmortem PD brain samples [47]. Notably, α-syn and LRRK2 are both substrates of CMA and their paths may converge in the lysosome [48, 49]. Mutant LRRK2 binds to lysosomal membranes less efficiently than WT LRRK2, but once bound, its binding to LAMP2A is more stable and it seems to prevent LAMP2A multimerization to form the translocation complex, leading to impaired degradation of other CMA substrates including α-syn [49]. Furthermore, rather than competing with α-syn for binding to LAMP2A, mutant LRRK2 actually enhances binding of monomeric α-syn to lysosomal membranes. Since LAMP2A multimerization is blocked by mutant LRRK2, α-syn bound to lysosomal membrane would not be translocated into the lysosome, resulting in a marked increase of the formation of α-syn oligomers at the surface of lysosomes. Based on observations in induced pluripotent stem cell (iPSC)-derived DA neurons from PD patients with *LRRK2* mutation, alterations in CMA appear to be an early event, detectable before impaired macroautophagy and overt neurodegeneration [40, 49]. In light of these findings, CMA activation has been explored as a therapeutic strategy. Our study using a *LRRK2* R1441G-knockin mouse model of PD has shown an age-dependent accumulation of oligomeric α-syn, increased LAMP2A levels, and impaired CMA and lysosomal activity [50]. Treatment of cells with a CMA activator increases lysosomal activity and reduces intra- and extra-cellular α-syn oligomers in primary cortical neurons back to the levels comparable to WT, suggesting that activation of CMA may be a viable therapeutic strategy to reduce α-syn accumulation and release.

In summary, the PD-associated pathogenic *LRRK2* mutations increase phosphorylation of LRRK2 kinase substrates *in vivo* [31] and are associated with: (1) alterations in the regulation of macroautophagy under different cellular conditions, (2) impaired lysosomal function with abnormal lysosomal morphology and increased alkalinization, (3) altered endolysosomal trafficking mediated by increased phosphorylation of a subset of Rab GTPases, and (4) impaired CMA by enhanced binding to LAMP2A and blockage of degradation of other CMA substrates including α-syn. These abnormalities likely contribute to α-syn accumulation and oligomerization in *LRRK2*-PD (Fig. 1).

GBA and autophagy

GBA mutations in PD

GBA encodes the lysosomal enzyme GCase, which cleaves the glucose moiety from glucosylceramide (GlcCer). Homozygous mutations of *GBA*, resulting in GCase enzymatic deficiency, cause Gaucher disease (GD) in which affected cells are engorged with abnormal lysosomes containing the GCase substrate, GlcCer (reviewed in [51–53]). *GBA* is located on chromosome

1q21. At least 495 mutations, including missense, frameshift, splice-site mutations and null alleles resulting from recombination with the homologous *GBA* pseudogene have been described in GD [53]. The prevalence of different *GBA* mutations varies with ethnicity. N370S is the most common mutation among Ashkenazi Jews, while L444P is more prevalent in Asians and Caucasians with non-Ashkenazi Jew ancestry [51, 52]. The earliest clues of *GBA* involvement in PD came from observations that GD patients and their relatives had increased incidence of PD compared with the general population [54, 55]. Heterozygous *GBA* mutation carriers have a 10%–30% probability of developing PD at the age of 80 (a 20-fold rise compared to non-mutation carriers) (reviewed in [56]). Moreover, *GBA* mutations occur in 5%–10% of PD patients, making *GBA* mutations the most significant genetic risk factor for PD [55, 57]. The most common *GBA* mutations in PD patients worldwide are N370S and L444P [52]. The pathogenicity of *GBA* mutations in PD is thought to be related to reduced GCase activity (i.e. loss-of-function) as severe *GBA* mutations appear to be correlated with a higher risk of PD development and significantly worse motor and non-motor symptoms compared with mild mutations [58, 59]. Patients with *GBA*-associated PD (*GBA*-PD) have similar motor symptoms as iPD, but may have earlier age of onset and increased prevalence of cognitive impairment [60, 61]. *GBA*-PD is also shown to have similar brain pathology in terms of Lewy-type synucleinopathy to non-*GBA* PD subjects [61]. GCase activity has been found to be reduced in the caudate and substantia nigra of iPD patients [17, 62], suggesting that GCase dysfunction is a common pathogenic mechanism in iPD. However, in addition to GCase enzymatic deficiency, it is likely that other pathogenic mechanisms are also involved. Not all GD patients, even those with severe *GBA* mutations, develop PD and some variants, notably E326K and T369M, confer increased risk of PD but do not cause GD [56, 63]. Although no mechanisms have been established for the pathogenicity of the latter variants, a gain-of-function mechanism is possible where mutated and misfolded GCase protein accumulates in the endoplasmic reticulum (ER), leading to ER stress, ER-associated degradation and cell death (reviewed in [53, 56]). Moreover, GCase has been shown to be present in LBs [64]. Overall, mutations in *GBA* represent a genetic risk factor for PD as penetrance is incomplete, and both loss-of-function and gain-of-function mechanisms have been proposed. Regardless of the degree of GCase deficiency, *GBA*-PD is characterized by increased α-syn aggregation, the mechanisms of which will be discussed below.

GBA and lysosomal function

GCase is synthesized in the ER and transported by lysosomal integral membrane protein 2 (LIMP2) to the lysosome. Upon reaching the lysosomal lumen, GCase becomes active and hydrolyzes GlcCer to ceramide and glucose (reviewed in [11, 56]). The link between GCase deficiency and synucleinopathy was first reported in neuropathological studies of GD patients with parkinsonism, which revealed the presence of LBs and α-syn aggregation in the hippocampus [65, 66]. Since GCase is a lysosomal enzyme, GCase deficiency may perceivably alter lysosomal function, leading to defective protein degradation and synucleinopathy. Indeed, knockdown of *GBA* in primary cortical neurons results in reduced GCase activity, increased accumulation of its substrate GlcCer, reduced rate of lysosomal proteolysis, accumulation of enlarged lysosomes, and increased α-syn without increasing its mRNA (suggesting that the increased α-syn is due to reduced degradation) [67]. Neuroblastoma cells with *GBA* knockout have increased accumulation of lysosomal substrates p62 and polyubiquinated proteins, increased Lysotracker staining indicative of reduced breakdown of acidic organelles, increased abnormal accumulation of enlarged autophagic vesicles and increased insoluble α-syn as well as α-syn release, further illustrating the critical role of GCase activity in maintaining normal lysosomal function and α-syn homeostasis [68]. DA neurons derived from iPSCs of *GBA*-PD patients carrying heterozygous *GBA* mutations show reduced GCase activity and increased accumulation of GlcCer and α-syn compared with control DA neurons [69]. Defects in ALP are evident due to the following alterations: (1) increased LAMP1-positive puncta suggesting accumulation of lysosomes, (2) reduced activity of other lysosomal enzymes, (3) increased LC3-positive vesicles, and (4) reduced co-localization between LC3 and LAMP1 vesicles, indicating impaired autophagosome-lysosome fusion. Importantly, these abnormalities are rescued by correction of the *GBA* mutations. Furthermore, control neurons treated with a GCase inhibitor show increased α-syn levels similar to *GBA*-mutant neurons. Collectively, these studies suggest that GCase deficiency causes numerous abnormalities in the ALP: accumulation of lysosomes, reduced activity of lysosomal enzymes, autophagosome accumulation with impaired maturation, accumulation of the GCase substrate GlcCer, and increased insoluble α-syn and α-syn release.

Lysosome biogenesis and recycling are important for cellular homeostasis. Lysosomal proteins are transported to the lysosome *via* the endosomal system, where early endosomes mature to late endosomes, which then fuse with the lysosome, delivering their cargo [70]. There is evidence that GCase deficiency impairs lysosome

biogenesis *via* autophagic lysosome reformation [71]. Normally, after degradation of autolysosomal products, mTOR is activated to terminate autophagy and phosphorylates its substrate p70S6Kinase (phopho-S6K). This leads to formation of proto-lysosomal tubules in the autolysosomes; these tubules are ultimately excluded from autolysosomes to mature into functional lysosomes *via* the endosomal system [70]. Mouse embryonic fibroblasts with *GBA* knockout or heterozygous *GBA* mutation have reduced levels of phopho-S6K, which can be reversed by recombinant GCase enzyme replacement, confirming the direct relationship between loss of GCase activity and loss of mTOR activity [71]. Furthermore, these cells exhibit increased levels of Rab7 (a marker of late endosomes) and increased co-localization of Rab7 with the lysosomal enzyme cathepsin D, suggesting slower dissociation of proto-lysosomes from autolysosomes and slower lysosome maturation and recycling. Over time, with repeated cycles of autophagy followed by autophagic lysosome reformation, this would conceivably result in fewer functional lysosomes, contributing to lysosomal dysfunction in *GBA*-mutant cells.

GCase and α-syn: a bi-directional loop?

Knockdown of GCase in neurons causes accumulation of GlcCer, reduced rate of proteolysis, accumulation and enlargement of lysosomal compartment, and increased levels of soluble monomeric, oligomeric and insoluble α-syn [67]. When these cells over-express WT or A53T α-syn, there is a significant decline in cell viability compared with cells with normal GCase; interestingly, cell viability is not reduced if the cells with GCase knockdown over-express an artificially generated fibrillation-incompetent α-syn mutant, suggesting that GCase knockdown promotes accumulation and neurotoxicity of α-syn through polymerization-dependent mechanisms. Intriguingly, the effect of lysosomal dysfunction in GCase deficiency seems to preferentially affect α-syn, since the levels of other aggregation-prone proteins such as tau and huntingtin are not increased in GCase-knockdown cells. Furthermore, treatment with the lysosomal inhibitor leupeptin results in increased total insoluble proteins but does not increase levels of soluble oligomeric α-syn, while knockdown of GCase results in increased levels of soluble oligomeric α-syn but not total insoluble proteins. This suggests that GCase deficiency preferentially affects the solubility of α-syn and that this effect is due to alteration of the GlcCer pathway rather than a result of general lysosomal inhibition. In vitro data have shown that increasing the concentrations of GlcCer can stabilize the formation of a soluble assembly-competent intermediate α-syn species and promote α-syn fibril formation, thus offering a potential mechanism by which GlcCer accumulation in GCase deficiency may promote synucleinopathy. These observations are corroborated in GD mouse brain showing reduced GCase activity, accumulation of GlcCer, and degeneration of neurons in substantia nigra and cortex, with increased soluble oligomeric and insoluble α-syn [67].

Decreased GCase activity has also been noted in postmortem brain samples of iPD patients; furthermore, the decrease in GCase activity in the substantia nigra of PD patients correlates with increased α-syn levels [16, 17, 65, 72]. In SH-SY5Y cells, over-expression of α-syn reduces GCase activity in a dose-dependent manner, suggesting that α-syn accumulation can lead to reduced activity of WT GCase in cells with no *GBA* mutations. A study on postmortem brain samples of early-stage iPD patients has shown reduced GCase activity selectively in brain regions that accumulate α-syn [16]. Furthermore, even though there is no change in constituent lysosomal membrane proteins (indicating no overt loss or accumulation of lysosomes), there is evidence of impaired CMA with reduced LAMP2A levels that correlates with increased α-syn and reduced GCase activity, suggesting that these are early events in the clinical course of PD.

α-Syn accumulation likely causes reduced GCase activity by interfering with the trafficking of GCase [66]. Normally, GCase binds the lysosomal transporter LIMP2 in the ER and is transported *via* the Golgi apparatus to lysosomes. In neurons overexpressing α-syn, LIMP2 fails to bind GCase and there is increased trapping of GCase in the ER, with concomitant reduction of GCase activity in lysosomes [17, 67]. The mechanism underlying this is unclear since LIMP2 does not appear to bind α-syn. Interestingly, this effect is not observed if mutant α-syn lacking amino acids 71–82 (i.e. fibrillation-incompetent α-syn) is overexpressed, again suggesting that the impairment in ER-to-lysosome trafficking of GCase is dependent on polymerization of α-syn [67]. Retention of GCase in ER may induce ER stress, as shown by activation of the unfolded protein response in DA neurons differentiated from iPSC of *GBA*-PD patients, together with numerous defects in autophagy: increased autophagosomes, impaired lysosomal protein degradation, increased number of lysosomes and increased α-syn release [73].

In summary, *GBA* mutations likely increase PD risk by the following proposed mechanisms: (1) gain-of-function mechanism where mutant and misfolded GCase accumulates in ER, causing ER stress, (2) loss-of-function mechanism where GCase deficiency causes accumulation of its substrate GlcCer, which stabilizes and promotes α-syn aggregation, and (3) a bi-directional loop where oligomeric α-syn interferes with GCase trafficking, further exacerbating GCase deficiency, leading to more α-syn

aggregation. These changes are associated with broad abnormalities in the ALP (Fig. 2).

Crosstalk between *LRRK2* and *GBA*

Both *LRRK2* and *GBA* play critical roles in the ALP. Mutations in either gene cause similar dysfunction in macroautophagy, lysosomal biology and CMA, resulting in the aggregation and propagation of α-syn, raising the possibility that *LRRK2* and *GBA* mutations may contribute to PD pathogenesis through a common biological pathway. Dissecting how the two genes interact and regulate autophagy may identify potential therapeutic targets for disease modification in PD.

Crosstalk between *LRRK2* and *GBA* can been seen in DA neurons with *LRRK2* R1441C, R1441G or G2019S mutation, which show reduced GCase activity [14]. GCase activity can be restored by treatment with LRRK2 kinase inhibitor, indicating that *LRRK2* mutations reduce GCase activity in a kinase-dependent manner. Rab10 is a key mediator of GCase activity and is regulated by *LRRK2*: phosphorylation of Rab10 by LRRK2 reduces GCase activity. Notably, treatment with LRRK2 kinase inhibitor also increases GCase activity in DA neurons derived from healthy controls and from PD patients with heterozygous *GBA* mutation, suggesting that LRRK2 kinase regulates GCase activity irrespective of the mutation status or the disease state [14]. The increase in GCase activity after treatment with LRRK2 kinase inhibitor in *LRRK2*-mutant and in *GBA*-mutant neurons is accompanied by the reduction of pS129-α-syn, the predominant form of α-syn found in LBs [5, 74].

Neurons with heterozygous-null *GBA* mutation with apparent normal LRRK2 kinase activity show broad lysosomal impairment and increased α-syn accumulation and release [12]. Despite having normal intrinsic LRRK2 kinase activity, treatment of these *GBA*-mutant neurons with LRRK2 kinase inhibitor results in near complete rescue of lysosomal deficits, supporting a functional link between the two proteins in the regulation of lysosomal function [12]. Similarly, *GBA*-mutant astrocytes do not have elevated intrinsic LRRK2 kinase activity but show impaired basal and evoked cytokine production, which can be reversed with LRRK2 kinase inhibitor, indicating the possibility of a broader effect on immune response exerted by *GBA*–*LRRK2* crosstalk [13]. Collectively, these studies indicate that *LRRK2* and *GBA* influence each other in the regulation of lysosomal function and that LRRK2 kinase inhibitor may be a potential treatment strategy to correct defects in lysosome and cytokine response in not only *LRRK2*-PD but also *GBA*-PD or perhaps even iPD.

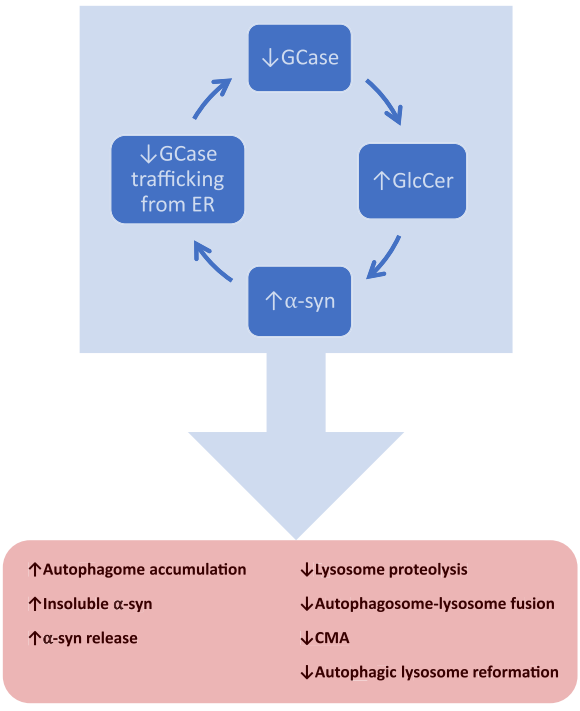

Fig. 2 Vicious cycle of GCase deficiency and α-syn accumulation is associated with multiple defects in autophagic-lysosomal pathway. Reduced GCase activity leads to accumulation of its substrate GlcCer, which acts as a scaffold for α-syn fibril formation. α-Syn aggregation impairs the transport of GCase from ER to lysosome, further reducing lysosomal GCase activity

Dual *LRRK2-GBA* mutations in PD patients

Since *LRRK2* and *GBA* mutations are two most common genetic causes of PD, patients with mutations in either gene or in both genes are increasingly reported, with an opportunity to study the effects of these mutations on phenotype. Two studies, which include 503 *LRRK2*-PD patients, the majority (89%) being G2019S mutation carriers, show that the motor phenotypes of *LRRK2*-PD are generally indistinguishable from iPD [27, 75]. Studies of non-motor features in 485 *LRRK2*-PD patients (480 or 99% being G2019S carriers) show conflicting results. Some report higher rates of depression in *LRRK2* G2019S patients [76], while others show no significant difference in depression and anxiety in *LRRK2* G2019S carriers compared with non-carriers [77, 78]. Cognitive function is similar in *LRRK2* G2019S carriers and non-carriers in some studies [79, 80], while others show better cognitive function with lower rates of dementia in *LRRK2* G2019S carriers [27, 81]. *GBA* carriers have been observed to have a more rapid motor decline and a higher burden of nonmotor features, specifically dementia, depression and anxiety, than iPD patients [82–87]. In particular, severe *GBA* mutations (e.g. L444P) are associated with a higher risk of PD, earlier age of onset, more rapid progression

and worse cognitive functions than mild mutations (e.g. N370S) [59, 88, 89]. The age of onset is comparable between *LRRK2* carriers and iPD, but is significantly earlier in *GBA*-PD [77, 78, 90, 91]. In PD patients with *GBA* mutations, the age of onset in those with severe *GBA* mutations is up to 8 years earlier than patients with iPD, while mild *GBA* mutation carriers have similar age of onset as iPD patients [91, 92]. Overall, *GBA*-PD patients seem to have worse motor and non-motor symptoms than iPD while *LRRK2*-PD patients are more similar to iPD. However, current evidence is not sufficient to distinguish *GBA*- or *LRRK2*-PD from iPD by clinical features alone.

A study of 12 *LRRK2-GBA* dual mutation carriers (all with *LRRK2* G2019S; 9 with *GBA* N370S, 2 with E326K and 1 with R496H) among 556 PD patients reports no significant differences in clinical motor scores, motor fluctuations, freezing of gait, and number of patients reaching Hoehn & Yahr stage 3 compared with carriers of single-mutation or non-carriers [93]. However, *GBA*-PD patients (N370S being the most common) show higher rates of dementia, RBD and psychosis while dual mutation carriers have the least RBD and psychosis, suggesting that *LRRK2* G2019S may exert a protective effect among patients with *GBA* mutations. In a larger study, 27 dual mutation patients (all with *LRRK2* G2019S and a majority with mild *GBA* mutations) have significantly better motor function, lower rates of dementia and slower cognitive decline than both mild and severe *GBA* mutation carriers, again implying a modifying role of *LRRK2* on motor and nonmotor phenotypes of patients with *GBA* mutations [94]. Combining data from multiple studies, Ortega and colleagues showed that *GBA*-PD (containing similar proportions of patients with mild and severe *GBA* mutation to the dual mutation group) have the fastest motor and cognitive decline compared with *LRRK2*-PD, PD with dual mutations and iPD, while the latter three groups are similar on this aspect [95]. Data concerning the age of onset of *LRRK2-GBA* dual mutation carriers are conflicting. Two studies reported that PD patients with *LRRK2-GBA* dual mutations were younger at first motor symptom onset than single mutation carriers [93, 96], while no such differences were found in two other studies [94, 95].

Collectively, these studies show that *LRRK2-GBA* dual mutation carriers have similar motor and non-motor symptoms to *LRRK2* carriers, which are milder than those seen in *GBA*-PD. Furthermore, dual mutation carriers have milder clinical features even when compared with *GBA*-PD patients carrying the mild *GBA* N370S mutation, suggesting that the consistently worst phenotype in *GBA*-PD is not driven by those carrying severe *GBA* mutations [94]. There are limitations to these studies: (1) the numbers of dual mutation carriers in most studies are small, and (2) most studies included only one *LRRK2* mutation (G2019S) and hence it is not clear if other *LRRK2* mutations have the same effect. Nevertheless, the observations from these studies challenge the notion of an additive deleterious effect of dual mutations suggested by (1) the findings of increased risk of PD and earlier age of onset in dual mutation carriers compared with single mutation carriers [93, 96] and (2) the finding in cell models of improved GCase activity after treatment with LRRK2 kinase inhibitor [12–14]. Furthermore, increased GCase activity has been found in dried blood spots of *LRRK2* G2019S PD patients, again suggesting a protective effect of LRRK2 leading to compensatory increase in GCase activity, although it is not known whether GCase activity in blood reflects its activity in the brain [97]. Clearly, the interaction between *LRRK2* and *GBA* is complex. Given that both *LRRK2* and *GBA* mutations have incomplete penetrance in PD, other unknown factors are likely to affect the overall risk and clinical progression of PD. Further studies are needed to clarify how the two genes interact to affect the phenotype and whether this interaction represents an opportunity for disease modification.

Therapeutic strategies targeting *GBA* and *LRRK2*

The ALP is regulated by *LRRK2* and *GBA* along with several other PD-associated genes. Its disturbance is a key mechanism in the pathogenesis of PD (reviewed in [11]). Since there is strong evidence linking lysosomal dysfunction with α-syn aggregation and propagation, therapeutic strategies to enhance autophagy and improve lysosomal dysfunction are being employed in disease modification of PD. GBA is well studied for its role in maintaining normal lysosomal function. Its bi-directional relationship with α-syn metabolism suggests that enhancement of GCase activity will be beneficial not only in *GBA* mutation carriers but in iPD as well. Strategies to mitigate the effects of reduced GCase activity are mainly headed in two directions: (1) small molecule chaperones to facilitate transit of GCase to the lysosome and (2) substrate reduction therapy to inhibit biosynthesis of GlcCer (reviewed in [98]).

Ambroxol, which is widely used as a mucolytic agent, has been shown to increase GCase activity in fibroblasts from healthy controls, *GBA* carriers (with or without PD) and iPD patients [99, 100] with associated improvement in functional lysosomal mass and proteolytic activity. Transgenic mice overexpressing α-syn have reduced GCase activity compared with WT control mice, confirming that elevated α-syn can lead to reduced WT GCase activity [101]. Ambroxol treatment of these mice increases GCase activity and reduces α-syn and

pS129-α-syn levels in brain. Another study employing a rat model of PD with unilateral intrastriatal injection of 6-hydroxydopamine (6-OHDA) shows that ambroxol treatment initiated 4 weeks after 6-OHDA injection (when motor symptoms have fully developed and nigral cell loss has reached maximal levels) results in restoration of GCase activity, restoration of the dopaminergic system measured by tyrosine hydroxylase and DA transporter levels, reduction in α-syn pathology, and recovery of behavioral symptoms [102], suggesting disease-modifying effects in PD. Ambroxol has also been tested in human subjects. A single-center, open-label noncontrolled clinical trial with *GBA*-PD and iPD patients (ClinicalTrials.gov Identifier NCT02941822) shows that ambroxol achieves good cerebrospinal fluid penetration and improves motor symptom scores [103]. A phase II placebo-controlled clinical trial (ClinicalTrials.gov Identifier NCT02914366) is currently recruiting PD patients with mild-to-moderate dementia to study the disease-modifying effects of ambroxol. Another approach to mitigate the effects of reduced GCase activity is to inhibit the synthesis of GlcCer. In mouse models of PD, treatment with a GlcCer synthase inhibitor has been shown to reduce GlcCer in the brain, slow the accumulation of hippocampal α-syn aggregates, and improve memory deficits [104]. Another GlcCer synthase inhibitor has been shown to reduce GlcCer levels in *GBA* mutant mouse brain and to rescue lysosomal deficits, reduce α-syn pathology and DA neuronal cell loss in mouse neurons [105]. In humans, Venglustat (an oral GlcCer synthase inhibitor) has been shown in a phase I study to be well tolerated and a phase II trial has recently completed recruitment (ClinicalTrials.gov Identifier NCT02906020) [106].

Increased kinase function in *LRRK2* mutations represents a toxic "gain-of-function" mechanism causing autophagic dysfunction, and is an attractive target for pharmacologic intervention. In cell and transgenic animal models overexpressing mutant *LRRK2*, LRRK2 kinase inhibition has been shown to reduce pS129-α-syn accumulation, oligomeric α-syn levels and α-syn release [14, 42, 43], and attenuate neurite shortening and DA neuronal death (reviewed in [107]). Going forward, mouse models with *LRRK2* knockin mutation incorporate genetic susceptibility and aging to model PD pathogenesis and can be very useful in the study of the *in vivo* effects of LRRK2 kinase inhibition [108, 109]. An important consideration of using LRRK2 inhibition as a treatment strategy of PD is its safety profile. Since *LRRK2* is expressed not only in the brain but also in kidney, lung and immune cells, long-term LRRK2 kinase inhibition could potentially affect these tissues. Mice and non-human primates do not exhibit any renal toxicity after receiving LRRK2 kinase inhibitor treatment [107, 110, 111]. In contrast, abnormal cytoplasmic accumulation of lysosome-related lamellar bodies in type II pneumocytes has been noted in the lungs of rodents and non-human primates after LRRK2 kinase inhibition [111, 112]. These abnormalities appear to be reversible on drug withdrawal and, more importantly, lower doses of LRRK2 kinase inhibitor which can achieve substantial brain LRRK2 kinase inhibition do not induce lung pathology [113], indicating a safety margin where brain LRRK2 kinase is inhibited without adverse effects on the lungs. It is of much interest to know whether LRRK2 kinase inhibition can be a viable treatment strategy beyond *LRRK2* mutation carriers. In particular, *LRRK2* and *GBA* mutations show substantial biological overlap in their effects on ALP impairment and α-syn pathology. LRRK2 reduces GCase activity by phosphorylating Rab10 [14]. In cell models, LRRK kinase inhibition has been shown to increase GCase activity and reduce pS129-α-syn levels in neurons carrying *LRRK2* or *GBA* mutations. In addition, variants in regions around the *LRRK2* locus have been identified in GWAS of sporadic PD patients [24]. Hence, it is conceivable that LRRK2 inhibition may be useful in *GBA*-PD and a subset of sporadic PD patients. One LRRK2 kinase inhibitor, DNL201, is in phase I clinical trial that has just completed recruitment of PD patients with and without *LRRK2* mutation (ClinicalTrials.gov Identifier NCT03710707).

Apart from directly modulating enzymatic activities of LRRK2 kinase and GCase, the general abnormalities in ALP as revealed in postmortem PD brain samples as well as cell and animal models suggest that modulation of pathways to enhance autophagy may also be viable therapeutic options. For example, farnesyltransferase inhibitors have been shown to enhance GCase activity, reduce α-syn aggregation and improve neuronal viability in PD patient-derived iPSC-midbrain neurons expressing A53T mutant α-syn by promoting hydrolase trafficking to the lysosome [11, 114]. Inhibition of mTOR promotes macroautophagy and ALP, and induces nuclear translocation of transcription factor B (TFEB), thus activating transcription of autophagic and lysosomal proteins [11, 115]. Hence, inhibitors of mTOR, such as rapamycin, represent another treatment strategy. Activation of CMA may improve α-syn degradation. Treatment of cells and mice with CMA activators has been shown to reduce α-syn accumulation and release [11, 50, 116]. Nilotinib, a tyrosine kinase inhibitor which activates autophagy through the AMPK pathway, has been shown to reduce α-syn levels, suppress DA neuronal loss and improve motor deficits in mice [117]. However, results in a human clinical trial recently published have been disappointing. Nilotinib achieved low CSF penetrance with no improvement

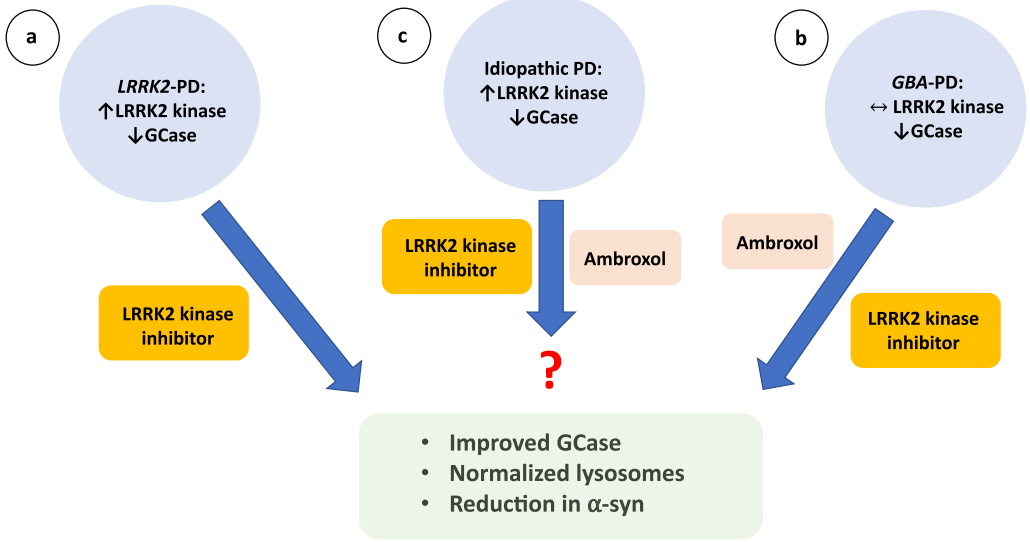

Fig. 3 Treatment targeting LRRK2 kinase and GCase activities in PD. **a** In *LRRK2*-PD, LRRK2 kinase activity is increased and GCase activity is reduced. Treatment with LRRK2 kinase inhibitor has been shown to improve GCase activity, normalize lysosome function and reduce α-syn. **b** In *GBA*-PD, GCase activity is reduced while LRRK2 kinase activity is normal. Both ambroxol and LRRK2 kinase inhibitor have been shown to improve GCase activity, lysosomal function and reduce α-syn. **c** Idiopathic PD has been shown to have increased LRRK2 kinase and reduced GCase activities; it remains to be seen whether treatment with ambroxol or LRRK2 kinase inhibitor will be useful

in clinical motor scores in patients with moderately advanced PD [118]. Further advancements in our understanding of the regulation of ALP will hopefully lead to new therapeutic targets in the disease modification of PD.

Conclusions and future directions

The identification of *LRRK2* and *GBA* mutations in familial and sporadic PD has led to major advancement in the past 10 years in our understanding of the regulation of ALP. The lysosome has emerged to be a critical player in maintaining α-syn homeostasis and is also where the effects of *LRRK2* and *GBA* mutations converge. Impairment of lysosomal function causes broad abnormalities in autophagy that ultimately lead to accumulation of toxic oligomeric α-syn, which further impairs autophagy, forming a vicious cycle. Mitochondrial dysfunction and impaired mitophagy have also been described in *LRRK2* and *GBA* mutations, which are likely linked to reduced efficiency of ALP [119, 120]. Specifically, in a mouse model with heterozygous *GBA* L444P mutation and another mouse model with *LRRK2* R1441C homozygous knockin mutation, accumulation of mitochondria with abnormal morphology, increased oxidative stress, reduced ATP production, increased accumulation of autophagosomes with reduced rate of mitophagy has been described [119, 120]. These abnormalities are consistent with mitochondrial dysfunction observed in PD, with impaired electron transport chain function, impaired calcium buffering and abnormal mitochondrial morphology and dynamics (reviewed in [121, 122]). Furthermore, *LRRK2* and *GBA* have also been implicated in immune response, indicating their multi-faceted functions [123]. There are still huge gaps in our knowledge. It is unclear at present why LRRK2 kinase activity is increased in iPD or how α-syn impairs trafficking of GCase from ER to the lysosome. Furthermore, in the majority of PD patients who have no known mutations, it is unclear what triggers the pathogenic cascade leading to lysosomal dysfunction and α-syn accumulation. Nevertheless, altered LRRK2 and GCase activities and their associated autophagic defects have been observed in iPD, potentially extending the application of drugs that modulate their functions to the wider PD population (Fig. 3). For example, ambroxol and LRRK2 kinase inhibitors have both been shown to increase GCase activity in WT cells, and LRRK2 kinase inhibitors correct lysosomal defects in *GBA* mutant cells. Clinical trials of some of these drugs are underway and their results, particularly in iPD patients, will be eagerly awaited.

Abbreviations

ALP: Autophagic-lysosomal pathway; AMPK: Adenosine monophosphate (AMP)-activated protein kinase; AV: Autophagic vacuoles; CMA: Chaperone-mediated autophagy; DA: Dopamine; ER: Endoplasmic reticulum; ERK: Extracellular signal regulated protein kinase; GBA: Glucocerebrosidase; GCase: Glucocerebrosidase; GD: Gaucher disease; GlcCer: Glucosylceramide; GWAS:

Genome-wide association study; iPD: Idiopathic Parkinson's disease; iPSC: Induced pluripotent stem cells; LAMP1: Lysosome-associated membrane protein 1; LAMP2A: Lysosome-associated membrane protein 2A; LB: Lewy bodies; LC3: Light chain 3; LIMP2: Lysosomal integral membrane protein 2; LRRK2: Leucine-rich repeat kinase 2; MEK: Mitogen activated protein kinase/extracellular signal regulated protein kinase (MAPK/ERK) kinase; mTOR: Mammalian target of rapamycin; NAADP: Nicotinic acid adenine dinucleotide phosphate; PD: Parkinson's disease; RBD: Rapid eye movement sleep behavior disorder.

Acknowledgements
We thank the Tai Hung Fai Charitable Foundation - Edwin S H Leong Research Programme for Parkinson's Disease, Henry G. Leong Endowed Professorship in Neurology (SLH), and the Donation Fund for Neurology Research for their support. We also thank the Department of Medicine, the University of Hong Kong, for technical and administrative support.

Authors' contributions
SP, RL: Reviewing the literature, drafting and revising the manuscript; All other authors: critically revising the manuscript. All authors read and approved the final manuscript.

Funding
Tai Hung Fai Charitable Foundation—Edwin S H Leong Research Programme for Parkinson's Disease; The Henry G. Leong Endowed Professorship in Neurology; The Donation Fund for Neurology Research.

Availability of data and materials
Not applicable.

Declarations

Ethics approval and consent to participate
Not applicable.

Consent for publication
Not applicable.

Competing interests
The authors declare that they have no competing interests.

Author details
[1]Division of Neurology, Department of Medicine, Queen Mary Hospital, University of Hong Kong, Hong Kong, China. [2]School of Biomedical Sciences, Li Ka Shing Faculty of Medicine, University of Hong Kong, Hong Kong, China. [3]Institute of Metabolism and Systems Research, University of Birmingham, Birmingham, UK.

Received: 11 October 2021 Accepted: 12 January 2022
Published online: 31 January 2022

References

1. Mizushima N, Levine B, Cuervo A, Klionsky D. Autophagy fights disease through cellular self-digestion. Nature. 2008;451:1069–75.
2. Orenstein SJ, Cuervo AM. Chaperone-mediated autophagy: molecular mechanisms and physiological relevance. Semin Cell Dev Biol. 2010;21:719–26.
3. Mijaljica D, Prescrott M, Devenish RJ. Microautophagy in mammalian cells: revisiting a 40-year-old conundrum. Autophagy. 2011;7:673–82.
4. Baba M, Nakajo S, Tu PH, Tomita T, Nakaya K, Lee VM, et al. Aggregation of α-synculein in Lewy bodies of sporadic Parkinson's disease and dementia with Lewy bodies. Am J Pathol. 1998;152:879–84.
5. Fujiwara H, Hasegawa M, Dohmae N, Kawashima A, Masliah E, Goldberg MS, et al. α-Synuclein is phosphorylated in synucleinopathy lesions. Nat Cell Biol. 2002;4:160–4.
6. Chu Y, Dodiya H, Aebischer P, Olanow CW, Kordlower JH. Alterations in lysosomal and proteasomal markers in Parkinson's disease: relationship to alpha-synuclein inclusions. Neurobiol Dis. 2009;35:385–98.
7. Dehay B, Bove J, Rodriguez-Muela N, Perier C, Recasens A, Boya P, et al. Pathogenic lysosomal depletion in Parkinson's disease. J Neurosci. 2010;30:12535–44.
8. Hou X, Watzlawik JO, Fiesel FC, Springer W. Autophagy in Parkinson's disease. J Mol Biol. 2020;432:2651–72.
9. Gan-Or Z, Dion PA, Rouleau GA. Genetic perspective on the role of the autophagy-lysosome pathway in Parkinson disease. Autophagy. 2015;11:1443–57.
10. Nalls MA, Pankratz N, Lill CM, Do CB, Hernandez DG, Saad M, et al. Large-scale meta-analysis of genome-wide association data identifies six new risk loci for Parkinson disease. Nat Genet. 2014;46:989–93.
11. Abe T, Kuwahara T. Targeting of lysosomal pathway genes for Parkinson's disease modification: insights from cellular and animal models. Front Neurol. 2021;12:681369.
12. Sanyal A, Novis HS, Gasser E, Lin S, LaVoie MJ. LRRK2 kinase inhibition rescues deficits in lysosome function due to heterozygous GBA1 expression in human iPSC-derived neurons. Front Neurosci. 2020;14:442.
13. Sanyal A, DeAndrade MP, Novis HS, Lin S, Chang J, Lengacher N, et al. Lysosome and inflammatory defects in GBA1-mutant astrocytes are normalized by LRRK2 inhibition. Mov Disord. 2020;35:760–73.
14. Ysselstein D, Nguyen M, Young TJ, Severino A, Schwake M, Merchant K, et al. LRRK2 kinase activity regulates lysosomal glucocerebrosidase in neurons derived from Parkinson's disease patients. Nat Comm. 2019;10:5570.
15. Di Maio R, Hoffman EK, Rocha EM, Keeney MT, Sanders LH, De Miranda BR, et al. LRRK2 activation in idiopathic Parkinson's disease. Sci Transl Med. 2018;10:eaar5429.
16. Murphy KE, Gysbers AM, Abbott SK, Tayebi N, Kim WS, Sidransky E, et al. Reduced glucocerebrosidase is associated with increased α-synuclein in sporadic Parkinson's disease. Brain. 2014;137:834–48.
17. Gegg ME, Burke D, Heales SJR, Cooper JM, Hardy J, Wood NW, et al. Glucocerebrosidase deficiency in substantia nigra of Parkinson disease brains. Ann Neurol. 2012;72:455–63.
18. Scherman D, Desnos C, Darchen F, Pollak P, Javoy-Agid F, Agid Y. Striatal dopamine deficiency in Parkinson's disease: role of aging. Ann Neurol. 1989;26:551–7.
19. Chen H. The changing landscape of Parkinson epidemiologic research. J Parkinson Dis. 2018;8:1–12.
20. Braak H, Del Tredici K, Rub U, de Vos RAI, Jansen Steur ENG, Braak E. Staging of brain pathology related to sporadic Parkinson's disease. Neurobiol Aging. 2003;24:197–211.
21. Goedert M. Alzheimer's and Parkinson's diseases: the prion concept in relation to assembled Aβ, tau, and α-synuclein. Science. 2015;349:1255555.
22. Paisan-Ruiz C, Jain S, Evans EW, Gilks WP, Simon J, van der Brug M, et al. Cloning of the gene containing mutations that cause PARK8-linked Parkinson's disease. Neuron. 2004;44:595–600.
23. Zimprich A, Biskup S, Leitner P, Lichtner P, Ferrer M, Lincoln S, et al. Mutations in LRRK2 cause autosomal-dominant parkinsonism with pleomorphic pathology. Neuron. 2004;44:601–7.
24. Nalls MA, Pankratz N, Lill CM, Do CB, Hernandez DG, Saad M, et al. Large-scale meta-analysis of genome-wide association data identifies six new risk loci for Parkinson's disease. Nat Genet. 2014;46:989–93.
25. Madureira M, Conor-Robson N, Wade-Martins R. LRRK2: autophagy and lysosomal activity. Front Neurosci. 2020;14:498.
26. Guaitoli G, Gilsbach BK, Raimondi F, Gloeckner CJ. First model of dimeric LRRK2: the challenge of unrevealing the structure of a multidomain Parkinson's-associated protein. Biochem Soc Trans. 2016;44:1635–41.
27. Healy DG, Falchi M, O'Sullivan SS, Bonifati V, Durr A, Bressman S, et al. Phenotype, genotype, and worldwide genetic penetrance of LRRK2-associated Parkinson's disease: a case-control study. Lancet Neurol. 2008;7:583–90.
28. Deniston CK, Salgogiannis J, Mathea S, Snead DM, Lahiri I, Matyszewski M, et al. Structure of LRRK2 in Parkinson's disease and model for microtubule interaction. Nature. 2020;588:344–9.
29. Sheng Z, Zhang S, Bustos D, Kleinheinz T, Le Pichon CE, Dominguez SL, et al. Ser1292 autophosphorylation is an indicator of LRRK2 kinase activity and contributes to the cellular effects of PD mutations. Sci Transl Med. 2012;4:164ral.

30. Greggio E, Jain S, Kingsbury A, Bandopadhyay R, Lewis P, Kaganovich A, et al. Kinase activity is required for the toxic effects of mutant LRRK2/dardarin. Neurobiol Dis. 2006;23:329–41.
31. West AB, Moore DJ, Biskup S, Bugayenko A, Smith WW, Ross CA, et al. Parkinson's disease-associated mutations in leucine-rich repeat kinase 2 augment kinase activity. Proc Natl Acad Sci U S A. 2005;102:16842–7.
32. Steger M, Tonelli F, Ito G, Davies P, Trost M, Vetter M, et al. Phosphoproteomics reveals that Parkinson's disease kinase LRRK2 regulates a subset of Rab GTPases. Elife. 2016;5:e12813.
33. Maiuri M, Zalckvar E, Kimchi A, Kroemer G. Self-eating and self-killing: crosstalk between autophagy and apoptosis. Nat Rev Mol Cell Biol. 2007;8:741–52.
34. MacLeod D, Dowman J, Hammond R, Leete T, Inoue K, Abeliovich A. The familial Parkinsonism gene *LRRK2* regulates neurite process morphology. Neuron. 2006;52:587–93.
35. Anglade P, Vyas S, Javoy-Agid F, Herrero MT, Michel PP, Marquex J, et al. Apoptosis and autophagy in nigral neurons of patients with Parkinson's disease. Histol Histopathol. 1997;12:25–31.
36. Bravo-San Pedro JM, Niso-Santano M, Gomez-Sanchez R, Pizarro-Estrella E, Aiastui-Pujana A, Gorostidi A, et al. The LRRK2 G2019S mutant exacerbates basal autophagy through activation of the MEK/ERK pathway. Cell Mol Life Sci. 2013;70:121–36.
37. Plowey ED, Cherra SJ, Liu YJ, Chu CT. Role of autophagy in G2019S-LRRK2-associated neurite shortening in differentiated SH-SY5Y cells. J Neurochem. 2008;105:1048–56.
38. Gomez-Suaga P, Luzon-Toro B, Churamani D, Zhang L, Bloor-Young D, Patel S, et al. Leucine-rich repeat kinase 2 regulates autophagy through a calcium-dependent pathway involving NAADP. Hum Mol Genet. 2012;21:511–25.
39. Kim J, Kundu M, Viollet B, Guan KL. AMPK and mTOR regulate autophagy through direct phosphorylation of Ulk1. Nat Cell Biol. 2011;13:132–41.
40. Sanchez-Danes A, Richaud-Patin Y, Carballo-Carbajal I, Jimenez-Delgado S, Caig C, Mora S, et al. Disease-specific phenotypes in dopamine neurons from human iPSC-based models of genetic and sporadic Parkinson's disease. EMBO Mol Med. 2012;4:380–95.
41. Wallings R, Connor-Robson N, Wade-Martins R. LRRK2 interacts with the vacuolar-type H^+-ATPase pump a1 subunit to regulate lysosomal function. Hum Mol Genet. 2019;28:2696–710.
42. Schapansky J, Khasnavis S, DeAndrade MP, Nardozzi JD, Falkson SR, Boyd JD, et al. Familial knockin mutation of LRRK2 causes lysosomal dysfunction and accumulation of endogenous insoluble α-synuclein in neurons. Neurobiol Dis. 2018;111:26–35.
43. Obergasteiger J, Frapporti G, Lamonaca G, Pizzi S, Picard A, Lavdas AA, et al. Kinase inhibition of G2019S-LRRK2 enhances autolysosome formation and function to reduce endogenous alpha-synuclein intracellular inclusions. Cell Death Discov. 2020;6:45.
44. Eguchi T, Kuwahara T, Sakurai M, Komori T, Fujimoto T, Ito G, et al. LRRK2 and its substrate Rab GTPases are sequentially targeted onto stressed lysosomes and maintain their homeostasis. Proc Natl Acad Sci U S A. 2018;115:E9115–24.
45. MacLeod DA, Rhinn H, Kuwahara T, Zolin A, Di Paolo G, McCabe BD, et al. RAB7L1 interacts with LRRK2 to modify intraneuronal protein sorting and Parkinson's disease risk. Neuron. 2013;77:425–39.
46. Bae EJ, Kim DK, Kim C, Mante M, Adame A, Rockenstein E, et al. LRRK2 kinase regulates α-synuclein propagation *via* RAB35 phosphorylation. Nat Comm. 2018;9:3465.
47. Alvarez-Erviti L, Rodriguez-Oroz MC, Cooper JM, Caballero C, Ferrer I, Obesso JA, et al. Chaperone-mediated autophagy markers in Parkinson disease brains. Arch Neurol. 2010;67:1464–72.
48. Curevo AM, Stefanis L, Fredenburg R, Lansburry PT, Sulzer D. Impaired degradation of mutant alpha-synuclein by chaperone-mediated autophagy. Science. 2004;305:1292–5.
49. Orenstein SJ, Kuo SH, Tasset I, Arias E, Koga H, Fernandez-Carasa I, et al. Interplay of LRRK2 with chaperone-mediated autophagy. Nat Neurosci. 2013;16:394–406.
50. Ho PW, Leung CT, Liu H, Pang SY, Lam CS, Xian J, et al. Age-dependent accumulation of oligomeric SNCA/α-synuclein from impaired degradation in mutant LRRK2 knockin mouse model of Parkinson disease: role for therapeutic activation of chaperone-mediated autophagy. Autophagy. 2020;16:347–70.
51. Sidransky E, Lopez G. The link between the GBA gene and parkinsonism. Lancet Neurol. 2012;11:986–98.
52. Riboldi G, Di Fonzo AB. GBA, Gaucher disease, and Parkinson's disease: from genetic to clinic to new therapeutic approaches. Cells. 2019;8:364.
53. Do J, NcKinney C, Sharma P, Sidransky E. Glucocerebrosidase and its relevance to Parkinson disease. Mol Neurodegener. 2019;14:36.
54. Tayebi N, Walker J, Stubblefield B, Orvisky E, LaMarca M, Wong K, et al. Gaucher disease with parkinsonian manifestations: dose glucocerebrosidase deficiency contribute to a vulnerability to parkinsonism? Mol Genet Metab. 2003;79:104–9.
55. Halperin A, Elstein D, Zimran A. Increased incidence of Parkinson disease among relatives of patients with Gaucher disease. Blood Cells Mol Dis. 2006;36:426–8.
56. Behl T, Kaur G, Fratila O, Buhas C, Judea-Pusta CT, Negrut N, et al. Cross-talks among GBA mutations, glucocerebrosidase, and α-synuclein in GBA-associated Parkinson's disease and their targeted therapeutic approaches: a comprehensive review. Transl Neurodegener. 2021;10:4.
57. Rosenbloom B, Balwani M, Bronstein JM, Kolodny E, Sathe S, Gwosdow AR, et al. The incidence of parkinsonism in patients with type 1 Gaucher disease: data from the ICGG Gaucher registry. Blood Cells Mol Dis. 2011;46:95–102.
58. Gan-Or Z, Giladi N, Rozovski U, Shifrin C, Rosner S, Gurevich T, et al. Genotype-phenotype correlations between GBA mutations and Parkinson disease risk and onset. Neurology. 2008;70:2277–83.
59. Thaler A, Guervich T, Shira AB, Weisz MG, Ash E, Shiner T, et al. A "dose" effect of mutations in the GBA gene on Parkinson's disease phenotype. Parkinsonism Relat Disord. 2017;36:47–51.
60. Alcalay RN, Caccappolo E, Mejia-Santana H, Tang MX, Rosado L, Orbe Reilly M, et al. Cognitive performance of GBA mutation carriers with early-onset PD: the CORE-PD study. Neurology. 2012;78:1434–40.
61. Nichols WC, Pankratz N, Marek DK, Pauciulo MW, Elsaesser VE, Halter CA, et al. Mutations in GBA are associated with familial Parkinson disease susceptibility and age of onset. Neurology. 2008;72:310–6.
62. Adler CH, Beach TG, Shill HA, Caviness JN, Driver-Dunckley E, Sabbagh MN, et al. GBA mutations in Parkinson disease: earlier death but similar neuropathological features. Eur J Neurol. 2017;24:1363–8.
63. Horowitz M, Paskmanik-Chor M, Ron I, Kolodny EH. The enigma of the E326K mutation in acid β-glucocerebrosidase. Mol Genet Metab. 2011;104:35–8.
64. Goker-Alpan O, Stubblefield BK, Giasson BI, Sidransky E. Glucerebrosidase is present in alpha-synuclein inclusions in Lewy body disorders. Acta Neuropathol. 2010;120:641–9.
65. Chiasserini D, Paciotti S, Eusebi P, Persichetti E, Tasegian A, Kurzawa-Akanbi M, et al. Selective loss of glucocerebrosidase activity in sporadic Parkinson's disease and dementia with Lewy bodies. Mol Neurodegener. 2015;10:15.
66. Wong K, Sidransky E, Verma A, Mixon T, Sandberg GD, Wakefield LK, et al. Neuropathology provides clues to the pathophysiology of Gaucher disease. Mol Genet Metab. 2004;82:192–207.
67. Mazzulli JR, Xu YH, Sun Y, Knight AL, McLean PJ, Caldwell G, et al. Gaucher disease glucocerebrosidase and α-synuclein form a bidirectional pathogenic loop in synucleinopathies. Cell. 2011;146:37–52.
68. Bae EJ, Yang NY, Lee C, Lee HJ, Kim S, Sardi SP, et al. Loss of glucocerebrosidase 1 activity causes lysosomal dysfunction and α-synuclein aggregation. Exp Mol Med. 2015;47:e153.
69. Schondorf DC, Aureli M, McAllister FE, Hindley CJ, Mayer F, Schmid B, et al. iPCS-derived neurons from GBA1-associated Parkinson's disease patients show autophagic defects and impaired calcium homeostasis. Nat Comm. 2014;5:4028.
70. Yu L, McPhee CK, Zheng L, Mardones GA, Rong Y, Peng J, et al. Termination of autophagy and reformation of lysosomes regulated by mTOR. Nature. 2010;465:942–6.
71. Magalhaes J, Gegg ME, Migdalska-Richards A, Doherty MK, Whitfield PD, Schapira AH. Autophagic lysosome reformation dysfunction in glucocerebrosidase deficient cells: relevance to Parkinson disease. Hum Mol Genet. 2016;16:3432–45.
72. Gunder AL, Duran-Pacheco G, Zimmermann S, Ruf I, Moors T, Bauman K, et al. Path mediation analysis reveals GBA impacts Lewy body disease status by increasing alpha-synuclein levels. Neurobiol Dis. 2019;121:205–13.

73. Fernandes HJ, Hartfield EM, Christian HC, Emmanoulidou E, Zheng Y, Booth H, et al. ER stress and autophagic perturbations lead to elevated extracellular α-synuclein in GBA-N370S Parkinson's iPSC-derived dopamine neurons. Stem Cell Rep. 2016;6:342–56.
74. Anderson JP, Walker DE, Goldstein JM, de Laat R, Banducci K, Caccavello RJ, et al. Phosphorylation of Ser-129 is the dominant pathological modification of alpha-synuclein in familial and sporadic Lewy body disease. J Biol Chem. 2006;281:29739–52.
75. Nabli F, Ben Sassi S, Amouri R, Duda JE, Farrer MJ, Hentati F. Motor phenotype of LRRK2-associated Parkinson's disease: a Tunisian longitudinal study. Mov Disord. 2015;30:253–8.
76. Belarbi S, Hecham N, Lesage S, Kediha MI, Smail N, Benhassine T, et al. LRRK2 G2019S mutation in Parkinson's disease: A neuropsychological and neuropsychiatric study in a large Algerian cohort. Parkinsonism Relat Disord. 2010;16:676–9.
77. Alcalay RN, Mirelman A, Saunders-Pullman R, Tang MX, Mejia Santana H, Raymond D, et al. Parkinson disease phenotype in Ashkenazi Jews with and without LRRK2 G2019S mutations. Mov Disord. 2013;28:1966-1971.c.
78. Marras C, Schüle B, Munhoz RP, Rogaeva E, Langston JW, Kasten M, et al. Phenotype in parkinsonian and nonparkinsonian LRRK2 G2019S mutation carriers. Neurology. 2011;77:325–33.
79. Ben Sassi S, Nabli F, Hentati E, Nahdi H, Trabelsi M, Ben Ayed H, et al. Cognitive dysfunction in Tunisian LRRK2 associated Parkinson's disease. Parkinsonism Relat Disord. 2012;18:243–6.
80. Trinh J, Amouri R, Duda JE, Morley JF, Read M, Donald A, et al. Comparative study of Parkinson's disease and leucine-rich repeat kinase 2 p.G2019S parkinsonism. Neurobiol Aging. 2014;35:1125–31.
81. Srivatsal S, Cholerton B, Leverenz JB, Wszolek ZK, Uitti RJ, Dickson DW, et al. Cognitive profile of LRRK2-related Parkinson's disease. Mov Disord. 2015;30:728–33.
82. Brockmann K, Srulijes K, Pflederer S, Hauser AK, Schulte C, Maetzler W, et al. GBA-associated Parkinson's disease: reduced survival and more rapid progression in a prospective longitudinal study. Mov Disord. 2015;30:407–11.
83. McNeill A, Duran R, Hughes DA, Mehta A, Schapira AHV. A clinical and family history study of Parkinson's disease in heterozygous glucocerebrosidase mutation carriers. J Neurol Neurosurg Psychiatry. 2012;83:853–4.
84. Brockmann K, Srulijes K, Hauser AK, Schulte C, Csoti I, Gasser T, et al. GBA-associated PD presents with nonmotor characteristics. Neurology. 2011;77:276–80.
85. Oeda T, Umemura A, Mori Y, Tomita S, Kohsaka M, Park K, et al. Impact of glucocerebrosidase mutations on motor and nonmotor complications in Parkinson's disease. Neurobiol Aging. 2015;36:3306–13.
86. Stoker TB, Camacho M, Winder-Rhodes S, Liu G, Scherzer CR, Foltynie T, et al. Impact of GBA1 variants on long-term clinical progression and mortality in incident Parkinson's disease. J Neurol Neurosurg Psychiatry. 2020;91:695–702.
87. Swan M, Doan N, Ortega RA, Barrett M, Nichols W, Ozelius L, et al. Neuropsychiatric characteristics of GBA-associated Parkinson disease. J Neurol Sci. 2016;370:63–9.
88. Cilia R, Tunesi S, Marotta G, Cereda E, Siri C, Tesei S, et al. Survival and dementia in GBA-associated Parkinson's disease: the mutation matters. Ann Neurol. 2016;80:662–73.
89. Liu G, Boot B, Locascio JJ, Jansen IE, Winder-Rhodes S, Eberly S, et al. Specifically neuropathic Gaucher's mutations accelerate cognitive decline in Parkinson's. Ann Neurol. 2016;80:674–85.
90. Wang C, Cai Y, Gu Z, Ma J, Zheng Z, Tang BS, et al. Clinical profiles of Parkinson's disease associated with common leucine-rich repeat kinase 2 and glucocerebrosidase genetic variants in Chinese individuals. Neurobiol Aging. 2014;35(725):e1-6.
91. da Silva CP, de Abreu MG, Cabello Acero PH, Campos M, Pereira JS, de Ramos ASR, et al. Clinical profiles associated with LRRK2 and GBA mutations in Brazilians with Parkinson's disease. J Neurol Sci. 2017;381:160–4.
92. Gan-Or Z, Amshalom I, Kilarski LL, Bar-Shira A, Gana-Weisz M, Mirelman A, et al. Differential effects of severe vs mild GBA mutations on Parkinson disease. Neurology. 2015;84:880–7.
93. Yahalom G, Greenbaum L, Israeli-Korn S, Fay-Karmon T, Livneh V, Ruskey JA, et al. Carriers of both GBA and LRRK2 mutations, compared to carriers of either, in Parkinson's disease: risk estimates and genotype-phenotype correlations. Parkinsonism Relat Disord. 2019;62:179–84.
94. Omer N, Giladi N, Gurevich T, Bar-Shira A, Gana-Weisz M, Goldstein O, et al. A possible modifying effect of the G2019S mutation in the LRRK2 gene on GBA Parkinson's disease. Mov Disord. 2020;35:1249–53.
95. Ortega RA, Wang C, Raymond D, Bryant N, Scherzer CR, Thaler A, et al. Association of dual LRRK2 G2019S and GBA variations with Parkinson disease progression. JAMA Netw Open. 2021;4:e215845.
96. Goldstein O, Gana-Weisz M, Cohen-Avinoam D, Shiner T, Thaler A, Cedarbaum JM, et al. Revisiting the non-Gaucher-GBA-E326K carrier state: Is it sufficient to increase Parkinson's disease risk? Mol Genet Metab. 2019;128:470–5.
97. Alcalay RN, Levy OA, Waters CC, Fahn S, Ford B, Kuo SH, et al. Glucocerebrosidase activity in Parkinson's disease with and without GBA mutations. Brain. 2015;138:2648–58.
98. Schneider SA, Alcalay RN. Precision medicine in Parkinson's disease: emerging treatments for genetic Parkinson's disease. J Neurol. 2020;267:860–9.
99. McNeill A, Magalhaes J, Shen C, Chau KY, Hughes D, Mehta A, et al. Ambroxol improves lysosomal biochemistry in glucocerebrosidase mutation-linked Parkinson disease cells. Brain. 2014;137:1481–95.
100. Ambrosi G, Ghezzi C, Zangaglia R, Levandis G, Pacchetti C, Blandini F. Ambroxol-induced rescue of defective glucocerebrosidase is associated with increased LIMP-2 and saposin C levels in GBA1 mutant Parkinson's disease cells. Neurobiol Dis. 2015;82:235–42.
101. Migdalska-Richards A, Daly L, Bezard E, Schapira AH. Ambroxol effects in glucocerebrosidase and α-synuclein transgenic mice. Ann Neurol. 2016;80:766–75.
102. Mishra A, Krishnamurthy S. Neurorestorative effects of sub-chronic administration of ambroxol in rodent model of Parkinson's disease. Naunyn Schmeidebergs Arch Pharmacol. 2020;393:429–44.
103. Mullin S, Smith L, Lee K, D'Souza G, Woodgate P, Elflein J, et al. Ambroxol for the treatment of patients with Parkinson disease with and without glucocerebrosidase gene mutations. JAMA Neurol. 2020;77:427–34.
104. Sardi SP, Viel C, Clarke J, Treleaven CM, Richards AM, Park H, et al. Glucosylceramide synthase inhibition alleviates aberrations in synucleinopathy models. Proc Natl Acad Sci U S A. 2017;114:2699–704.
105. Cosden M, Jinn S, Yao L, Gretzula CA, Kandebo M, Toolan D, et al. A novel glucosylceramide synthase inhibitor attenuates alpha synuclein pathology and lysosomal dysfunction in preclinical models of synucleinopathy. Neurobiol Dis. 2021;159:105507.
106. Peterschmitt M, Crawford N, Gaemers S, Ji A, Sharma J, Pham T. Pharmacokinetics, pharmacodynamics, safety and tolerability of oral venglustat in healthy volunteers. Clin Pharmacol Drug Dev. 2021;10:86–98.
107. Zhao Y, Dzamko N. Recent developments in LRRK2-targeted therapy for Parkinson's disease. Drugs. 2019;79:1937–51.
108. Liu HF, Ho PW, Leung GC, Lam CS, Pang SY, Li L, et al. Combined LRRK2 mutation, aging and chronic low dose oral rotenone as a model of Parkinson's disease. Sci Rep. 2017;7:40887.
109. Liu HT, Lu S, Ho PW, Tse HM, Pang SY, Kung MH, et al. LRRK2 R1441G mice are more liable to dopamine depletion and locomotor inactivity. Ann Clin Transl Neurol. 2014;1:199–208.
110. Fell MJ, Mirescu C, Basu K, Cheewatrakoolpong B, DeMong DE, Ellis JM, et al. MLi-2, a potent, selective, and centrally active compound for exploring the therapeutic potential and safety of LRRK2 kinase inhibition. J Pharmacol Exp Ther. 2015;355:397–409.
111. Fuji RN, Flagella M, Baca M, Baptista MA, Brodbeck J, Chan BK, et al. Effect of selective LRRK2 kinase inhibition on nonhuman primate lung. Sci Transl Med. 2015;7:273ra15.
112. Herzig MC, Kolly C, Persohn E, Theil D, Schweizer T, Hafner T, et al. LRRK2 protein levels are determined by kinase function and are crucial for kidney and lung homeostasis in mice. Hum Mol Genet. 2011;20:4209–23.
113. Baptista M, Merchant K, Barrett T, Bhargava S, Bryce DK, Ellis JM, et al. LRRK2 inhibitors induce reversible changes in nonhuman primate lungs without measurable pulmonary deficits. Sci Transl Med. 2020;12:eaav0820.
114. Cuddy LK, Wani WY, Morella ML, Pitcairn C, Tsutsumi K, Fredriksen K, et al. Stress-induced cellular clearance is mediated by the SNARE protein ykt6 and disrupted by α-synuclein. Neuron. 2019;104:869-84.e11.

115. Settembre C, Di Malta C, Polito VA, Garcia Arencibia M, Vetrini F, Erdin S, et al. TFEB links autophagy to lysosomal biogenesis. Science. 2011;332:1429–33.
116. Su C, Yang X, Lou J. Geniposide reduces α-synuclein by blocking microRNA-21/lysosome-associated membrane protein 2A interaction in Parkinson disease models. Brain Res. 2016;1644:98–106.
117. Hebron ML, Lonskaya I, Moussa CE. Nilotinib reverses loss of dopamine neurons and improves motor behavior *via* autophagic degradation of α-synuclein in Parkinson's disease models. Hum Mol Genet. 2013;22:3315–28.
118. Simuni T, Fiske B, Merchant K, Coffey CS, Klingner E, Caspell-Garcia C, et al. Efficacy of Nilotinib in patients with moderately advanced Parkinson disease: a randomized clinical trial. JAMA Neurol. 2021;78:312–20.
119. Li H, Ham A, Ma TC, Kuo SH, Kanter E, Kim D, et al. Mitochondrial dysfunction and mitophagy defect triggered by heterozygous GBA mutations. Autophagy. 2019;15:113–30.
120. Liu H, Ho PW, Leung CT, Pang SY, Chang E, Choi Z, et al. Aberrant mitochondrial morphology and function associated with impaired mitophagy and DNM1L-MAPK/ERK signaling are found in aged mutant Parkinsonian LRRK2^{R1441G} mice. Autophagy. 2020;10:1–25.
121. Ryan BJ, Hoek S, Fon EA, Wade-Martins R. Mitochondrial dysfunction and mitophagy in Parkinson's: from familial to sporadic disease. Trends Biochem Sci. 2015;40:200–10.
122. Malpartida AB, Williamson M, Narendra DP, Wade-Martins RBJ. Mitochondrial dysfunction and mitophagy in Parkinson's disease: from mechanism to therapy. Trends Biochem Sci. 2021;46:329–43.
123. Kozina E, Sadasivan S, Jiao Y, Dou Y, Ma Z, Tan H, et al. Mutant LRRK2 mediates peripheral and central immune responses leading to neurodegeneration in vivo. Brain. 2018;141:1753–69.